ACS OMEGA

Open Access

http://pubs.acs.org/journal/acsodf

Review

Advancements in Glass Fiber Separator Technology for Lithium-Sulfur Batteries: The Role of Transport, Material Properties, and Modifications

Razieh Fazaeli,* Hamid Aliyan, Zhe Huang, Yonglin Wang, and Yuning Li*

Cite This: *ACS Omega* 2025, 10, 3228−3261

Read Online

ACCESS | Metrics & More | Article Recommendations

ABSTRACT: Lithium-sulfur batteries (LSBs) are widely regarded as a promising next-generation energy storage technology due to their exceptional theoretical capacity and energy density. However, their commercialization has been hindered by challenges such as the polysulfide shuttle effect and poor reaction kinetics, which limit efficiency and cycle life. This review delves into the critical aspects of LSB technology, beginning with an overview of the fundamental mechanisms and challenges. The role of transport in porous media is analyzed, particularly in relation to its impact on ion mobility, sulfur utilization, and overall battery performance. Key criteria for separator design are then explored, emphasizing the importance of multifunctional separators in mitigating polysulfide diffusion, enhancing electrochemical stability, and prolonging cycle life. Glass fiber (GF) separators are highlighted for their intrinsic properties, including thermal stability and electrolyte wettability, which make them ideal candidates for modification. Various modification techniques are reviewed, demonstrating how functional coatings and advanced materials can transform GF separators into highly efficient components of Li-S batteries. By integrating novel approaches to separator modification, significant improvements in performance and cycling stability are achieved. The outlook and future directions in this research field are also given.

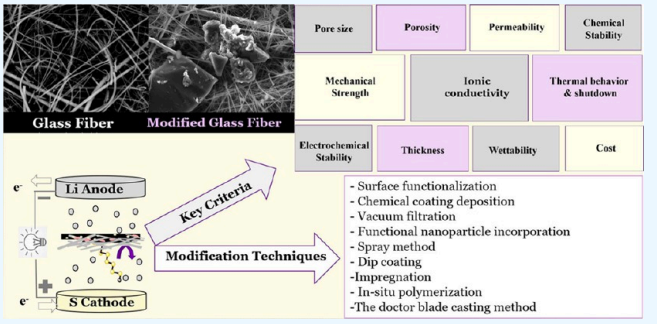

1. OVERVIEW OF LI-SULFUR BATTERY TECHNOLOGY

Lithium sulfur batteries (LSBs) have garnered significant attention as next-generation energy storage systems due to their high theoretical energy density, abundance of sulfur, and relatively low cost. A key advantage of LSBs lies in their high theoretical specific capacity of 1675 mAh/g and energy density of 2600 Wh/kg, which surpass traditional lithium-ion batteries.[1] These characteristics make LSBs a promising solution for applications requiring lightweight, high-capacity power sources, such as electric vehicles (EVs) and renewable energy storage.[2] Lithium-sulfur (Li-S) batteries operate through a redox reaction between lithium and sulfur during charging and discharging. In the discharge cycle, lithium ions migrate from the lithium metal anode to the sulfur cathode, forming lithium polysulfides (e.g., Li_2S_6 and Li_2S_4) and eventually lithium sulfide (Li_2S).[3] During charging, the reaction reverses, converting lithium sulfide back to sulfur. This reaction provides a high theoretical energy density and specific capacity, making LSBs a promising energy storage solution due to sulfur's abundance and low cost.[4]

However, several challenges limit the commercialization of Li-S batteries. The polysulfide shuttle effect causes the migration of intermediate polysulfides from the cathode to the anode, leading to active material loss and capacity fading. Volume expansion during the sulfur-to-lithium-sulfide transition (up to 80%) destabilizes the electrode structure, while sulfur's poor conductivity reduces electrochemical performance. Additionally, lithium dendrite formation in the lithium metal anode presents safety risks, as dendrites can cause short circuits and battery failure.[5,6]

Recent innovations in lithium-sulfur (Li-S) batteries, including the development of novel cathode composite materials such as 3D hierarchical nanosheets,[7,8] sulfur-carbon composites,[9] metal-organic frameworks,[10] functional binders,[11−13] along with advanced electrolyte formulations like solid-state electrolytes[14] and ionic liquids,[15] have significantly improved their performance and stability. These advancements address key challenges, such as the polysulfide shuttle effect and lithium dendrite formation, enhancing the efficiency,

Received: August 1, 2024
Revised: September 29, 2024
Accepted: January 9, 2025
Published: January 21, 2025

Table 1. Factors Affecting Transport in Porous Media

Factor (Definition)	Impact on Transport	Theory, Modeling or Technique
1. **Porosity**: The fraction of the total volume of a material that is occupied by pores or voids.	**Ionic Conductivity**: Higher porosity generally increases ionic conductivity by providing more pathways for ion movement. However, excessive porosity can reduce mechanical stability and decrease the electrode's energy density.[22]	- Physical displacement[24]
	Electrolyte Uptake: Increased porosity allows for better electrolyte uptake, ensuring that the electrolyte fills the pores completely, which is essential for efficient ion transport.[23]	- Gas pycnometry[25]
		- Buoyancy principle[26]
2. **Capillarity**: The movement of a liquid within the small pores of a porous medium due to surface tension. It occurs when the adhesive forces between the liquid (electrolyte) and the solid (porous medium) are stronger than the cohesive forces within the liquid.	**Electrolyte Distribution and Wettability**: Capillary action ensures effective electrolyte penetration and uniform distribution within porous electrodes and separators, maintaining good contact with active materials and preventing dry spots that could reduce ionic conductivity and battery efficiency.[27]	- Capillary rise method[29]
	Improved Ion Transport: Capillarity facilitates ion access throughout the electrode and rapidly replenishes electrolyte at reaction sites, ensuring consistent reaction kinetics and preventing concentration polarization.[28]	- Washburn equation (Mercury Intrusion Porosimetry (MIP))[30]
		- Liquid absorption method[31]
		- Dynamic contact angle measurement[32]
		- Porosimetry with optical techniques[33]
		- Optical microscopy and digital image analysis[34]
3. **Phase Saturation**: The ratio of the volume of a particular phase (liquid or gas) within the porous structure to the total pore volume of the material.	**Ionic and Molecular Transport**: High saturation increases the availability of the conducting phase (e.g., electrolyte) for ionic transport, enhancing conductivity and reaction kinetics.[35]	- Gravimetric method[39]
	Capillary Action: Saturation levels influence the capillary forces and liquid distribution within the pores.[36]	- Nuclear magnetic resonance (NMR)[40]
	Thermal Conductivity: Phase distribution affects thermal conductivity since different phases (liquid or gas) have different thermal conductivities.[37]	- X-ray computed tomography (CT)[41]
	Mechanical Properties: Saturation effects influences the mechanical strength and stability of the porous material. Excessive saturation can lead to material deformation or failure.[38]	- Capillary pressure methods[42]
		- Optical imaging techniques[43]
4. **Surface Area**: The total area available for electrochemical reactions within the porous structure.	**Reaction Kinetics**: A larger surface area provides more active sites for electrochemical reactions, enhancing reaction rates. However, this requires efficient ion and electron transport to avoid concentration gradients.[44]	- Brunauer-Emmett-Teller (bet) method
	Capacity Enhancement: When more active material is available for reactions due to the larger surface area, the battery can store more energy, thereby enhancing its capacity.[45]	- Langmuir adsorption method
		- Gas sorption method
		- Surface area by porosimetry (mercury intrusion porosimetry (MIP))[46]
		- Scanning probe microscopy (SPM) and atomic force microscopy (AFM)
		- Contact angle measurement
5. **Tortuosity**: A measure of the complexity of the pathways that ions must travel through the porous medium.	**Ion Transport Resistance**: High tortuosity increases the effective path length for ion transport, leading to higher resistance and slower transport rates. Optimizing tortuosity is critical for balancing ion transport and minimizing energy losses.[47]	- Image Analysis Techniques[49]
	Effect on Performance: Lower tortuosity enhances the transport of ions, improving the overall power density and rate capability of the battery.[48]	- Tracer Studies[50]
		- Computational Modeling[51]
6. **Connectivity**: The degree to which pores or channels within a porous material are interconnected.	**Fluid and Gas Flow**: High connectivity facilitates efficient flow of fluids or gases through the porous network by providing a more continuous and open network of pathways.[52]	- Percolation Theory[58]
	Permeability: High connectivity generally leads to higher permeability as more interconnected pathways allow for easier passage of fluids or gases through the material.[53]	- Network Modeling[59]
	Diffusion Rates: High connectivity enhances diffusion rates as molecules or ions can move more freely through a well-connected network of pores.[54]	- Imaging Techniques[60]
	Capillary Action: High connectivity Improves capillary action by ensuring that liquid can be transported	

https://doi.org/10.1021/acsomega.4c07070
ACS Omega 2025, 10, 3228−3261

Table 1. continued

Factor (Definition)	Impact on Transport	Theory, Modeling or Technique
	efficiently through interconnected pores, leading to better wetting and distribution.[55]	
	Mechanical Properties: High connectivity often contributes to better mechanical strength and stability as the material is more uniformly connected, leading to more effective stress distribution.[56]	
	Reactivity and Efficiency: High connectivity enhances reactivity and process efficiency in applications such as catalysis or filtration by providing more surface area and better contact between reactants or particles.[57]	
7. **Coordination number**: The number of nearest neighbors or adjacent pores to a given pore or particle within a porous material.	-**Flow Connectivity**: Higher coordination number implies a greater number of direct pathways for fluids or ions, enhancing connectivity and facilitating smoother flow.[61]	- Image Analysis
	-**Permeability**: Higher coordination number typically corresponds to increased permeability, as the interconnected network of pores allows for easier passage of fluids or gases through the material.[62]	- Computational Modeling
	-**Diffusion Rates**: Higher coordination number facilitates higher diffusion rates since the more connected network allows for more efficient transport of molecules or ions.[63]	- X-ray Diffraction (XRD) and Neutron Diffraction
	-**Mechanical Properties:** Higher coordination number generally contributes to more robust mechanical stability, as the material is more uniformly connected, distributing mechanical stresses more evenly.[64]	
	-**Reactivity and Efficiency**: Higher coordination number often improves reactivity and efficiency in applications such as catalysis or energy storage, where efficient contact between reactants or electrolytes is crucial.[65]	
8. **Domain Size (Pore and Throat)**: The size of the pores or channels within the porous media.	**Diffusivity**: Smaller domain sizes can restrict ion movement, reducing diffusivity. Larger domains facilitate easier ion transport but may reduce the electrode's mechanical strength.[66]	- Mercury Intrusion Porosimetry
	Selective Transport: The domain size must be optimized to allow the desired ions (e.g., Li^+) to pass through while blocking unwanted species (e.g., polysulfides in Li-S batteries).[67]	- Gas Adsorption (e.g., Nitrogen Adsorption)
		- Small-Angle X-ray Scattering (SAXS) and Small-Angle Neutron Scattering (SANS)
		- Optical Microscopy
		- Image Analysis Techniques
		- X-ray Computed Tomography (CT)
		- Porosimetry and Capillary Pressure Methods
9. **Solute Properties**: Solute properties include the nature, concentration, and mobility of ions or molecules dissolved in the electrolyte, such as diffusion coefficients, solubility, and partition coefficients.	**Ion Mobility**: Solute properties, such as ionic size and charge, influence their mobility through the porous medium. Smaller, highly charged ions generally move faster, whereas larger ions or those with complex hydration shells may move more slowly.[68]	**For diffusion coefficients**:
	Electrolyte Conductivity: The concentration and type of solute affect the overall conductivity of the electrolyte, impacting the rate of ion transport and battery efficiency.[69]	- Pulsed-Field Gradient Nuclear Magnetic Resonance (PFG-NMR)
	Solubility and Interaction: The interaction of solutes with the porous medium can lead to adsorption or precipitation, affecting ion availability and transport efficiency.[69]	- Tracer Diffusion Experiments
		- Electrochemical Impedance Spectroscopy (EIS)
		- Electrokinetic methods
		- Electrophoresis
		- Zeta Potential Measurements
		For solubility:
		- Gravimetric Method
		- Spectrophotometric Method
		- Turbidimetric Method
		For partition coefficient:
		- Shake Flask Method
		- Chromatographic Methods
10. **Hierarchical Media**: Media with multiple levels of pore sizes, ranging from nanometer to micrometer scales, creating a network of interconnected pores.	- **Improved Ion and Electron Transport**: Different pore sizes provide multiple pathways for ions and electrons, enhancing conductivity and facilitating faster transport across the electrode.[70]	- Gas Adsorption (e.g., BET Analysis)
	- **Optimized Reaction Kinetics**: The combination of large pores for rapid ion diffusion and small pores for increased surface area improves reaction rates and energy density.[71]	- Mercury Intrusion Porosimetry

https://doi.org/10.1021/acsomega.4c07070
ACS Omega 2025, 10, 3228−3261

Table 1. continued

Factor (Definition)	Impact on Transport	Theory, Modeling or Technique
		- X-ray Computed Tomography (X-ray CT) - Scanning Electron Microscopy (SEM) and Transmission Electron Microscopy (TEM) - Nuclear Magnetic Resonance (NMR) Cryoporometry - Small-Angle X-ray Scattering (SAXS) and Small-Angle Neutron Scattering (SANS)
11. **Fractals**: Structures with self-similar patterns at different scales, often found in natural and synthetic porous materials.	**Enhanced Surface Area**: Fractal structures maximize surface area for electrochemical reactions while maintaining connectivity, boosting capacity and reaction kinetics.[72]	- Scanning Probe Microscopy (SPM) and Atomic Force Microscopy (AFM)
	Efficient Transport Pathways: The self-similar, repeating patterns create efficient pathways for ion and electrolyte movement, reducing resistance and improving charge/discharge rates.[73]	- Small-Angle X-ray Scattering (SAXS) and Small-Angle Neutron Scattering (SANS) - Mercury Intrusion Porosimetry - Box-Counting Method (Digital Image Analysis) - Fractal Analysis from Electrochemical Impedance Spectroscopy (EIS)

safety, and cycle life of Li-S batteries. Researchers have also explored modified cathode architectures, electrolyte designs, and separator modifications to further mitigate these issues. For instance, coating separators with materials like covalent organic frameworks (COFs)[16] or metal oxides[17] helps reduce polysulfide migration, while protecting the lithium anode with coatings or solid electrolytes can prevent dendrite formation. The mechanical strength and integrity of separator materials must be adequate to endure the stresses and strains experienced during battery assembly, cycling, and operation. Physical damage to weak or fragile separators could jeopardize the battery's structural integrity and cause thermal runaway or short circuits. Polysulfide retention in the cathode, ion transport, and electrolyte infiltration are all made possible by the tortuosity and pore structure of the separator. Ion transit can be hampered by poor pore structure or too tortuosity, which raises the battery's internal resistance.[18] To avoid deterioration or chemical reactions that could jeopardize the safety or performance of the battery, separator materials must be compatible with the electrolyte used in the Li-S battery system. Interactions between the electrolyte components and separator material may give rise to incompatibility problems. For commercial Li-S battery applications, scalability, affordability, and ease of production are crucial factors to consider while selecting separator materials. Separator materials need to be able to be produced in large quantities while yet meeting requirements for dependability and performance.[19] The creation of innovative separator materials with better mechanical robustness, superior ion transport properties, higher electrochemical stability, and improved polysulfide trapping capabilities is necessary to meet these problems. To further fulfill the changing needs of high-performance energy storage applications, a thorough understanding of the fundamental mechanisms and interactions within the Li-S battery system is essential for the logical design and optimization of separators.[20] While these advancements highlight the potential of Li-S batteries, their overall performance and longevity are deeply influenced by factors such as ion transport within porous materials and the design of effective separators. In the following sections, we will explore how transport properties in porous media and the specific requirements for separators play critical roles in optimizing battery efficiency and addressing the challenges inherent in Li-S technology.

2. THE ROLE OF TRANSPORT IN POROUS MEDIA IN BATTERIES

Batteries rely on the efficient transport of ions, electrons, and reactants to achieve optimal performance. Porous media, such as separators and electrodes, play a critical role in facilitating this transport. Porous media in batteries serve as pathways for ion and electron transport and provide surfaces for electrochemical reactions.[21] Their properties dictate how effectively ions move through the electrolyte, how reactions occur at the electrode surfaces, and how the overall battery performs. Balancing porosity, surface area, tortuosity, and domain size is key to optimizing transport.[14] High porosity and surface area enhance ionic movement and reaction rates, while controlled tortuosity and domain size ensure efficient ion pathways without compromising mechanical stability or selectivity.[14] Table 1 summarized the factors affecting transport in porous media.

3. KEY CRITERIA FOR SEPARATOR DESIGN

Separators in lithium batteries must meet several critical requirements to ensure optimal performance and safety.[74] A few key requirements that will be discussed separately are categorized in Figure 1.

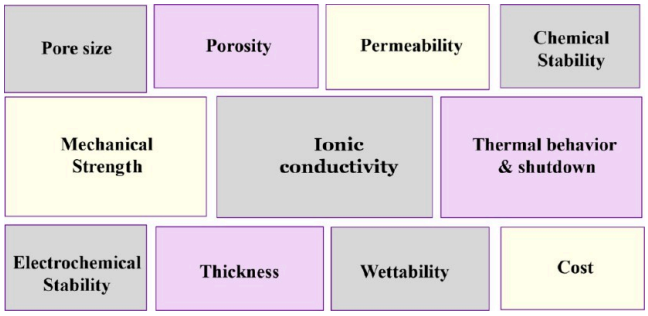

Figure 1. Some key criteria for separators in Li batteries.

3.1. Porosity and Pore Size. Porosity, in the context of battery separators, is a crucial parameter that defines the volume of pores within the separator material relative to its total volume. This ratio directly impacts the performance and safety of the battery. Porosity is generally expressed as a percentage and calculated by[75]

https://doi.org/10.1021/acsomega.4c07070
ACS Omega 2025, 10, 3228−3261

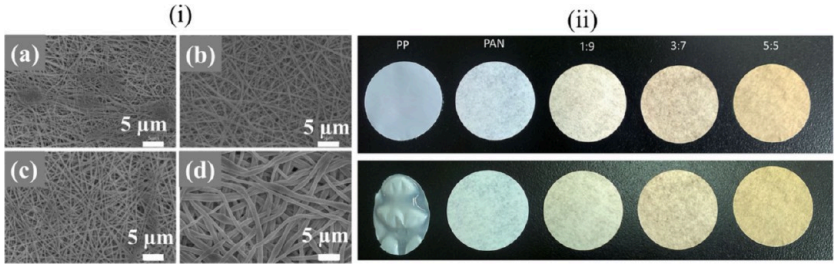

Figure 2. (i) SEM images of membranes with different lignin/PAN weight ratio. (a) PAN, (b) 1:9, (c) 3:7, (d) 5:5. (ii) Photographs of the separators before and after thermal exposure at 150 °C for 15 min.[83] Reprinted with permission from ref 83. Copyright 2015 The Royal Society of Chemistry.

$$\text{Porosity } (\%) = \left(1 - \frac{\rho_M}{\rho_P}\right) \times 100$$

where ρ_M and ρ_P represent the density of the separator and the polymer (or other material), respectively.

Porosity determines the ability of the separator to allow gases to pass through and retain the liquid electrolyte within its structure. This directly affects the battery's capacity and cycle life. A suitable porosity ensures that there is enough space within the separator to accommodate the liquid electrolyte, facilitating sufficient ionic conductivity for the battery's operation. If the porosity is too low, there will not be enough liquid electrolyte between the electrodes, leading to increased internal resistance within the battery. This resistance hampers the efficient flow of ions, affecting the battery's performance. On the other hand, excessive porosity can compromise the mechanical strength of the separator, potentially jeopardizing the safety of the battery. High porosity separators may shrink with temperature variations, which can affect the overall stability of the battery. Moreover, a decrease in mechanical strength due to high porosity increases the risk of separator damage during handling or operation. It is important to note that uneven distribution of pore channels within the separator leads to nonuniform current density across the battery electrodes. This nonuniformity reduces the activity of the electrode, impacting the overall efficiency and performance of the battery. Rechargeable battery polyolefin separator porosity typically ranges from 40% to 50%.[76] The techniques used to manage the porosity of separators often involve the following: vacuum impregnation, soaking media, microscopic analysis, direct weighing, and floating.[77,78] The soaking medium and direct weighing are the two most often utilized ones among them.

In practical applications, controlling and measuring the porosity of separators is essential and the porosity is determined by weighing the separator before and after absorbing the liquid electrolytes by

$$\text{Porosity } (\%) = \left(\frac{W - W_0}{\rho_L V_0}\right) \times 100$$

where W_0 and W are the separators weights before and after adsorbing the liquid electrolyte, ρ_L is the density of the liquid electrolyte, and V_0 is the separator volume. Methods such as direct weighing and soaking medium absorption are commonly used. These methods allow for precise determination of porosity, ensuring that it falls within the optimal range for battery performance. The uniformity of pore size directly influences the flow of ions within the battery. Rechargeable battery separators typically have submicron pore sizes with uniform distribution to ensure consistent current density at the interface between the electrode and electrolyte. When the pore sizes are uniform, ions can move through the separator more evenly, leading to stable and efficient battery operation. Larger pore sizes in the separator reduce the resistance to the migration of metal ions. This means that ions can move more freely through the separator, enhancing the battery's overall conductivity. However, excessively large pore sizes can lead to problems such as indirect contact between electrodes, increasing the risk of short-circuiting the battery. During battery operation, variations in pore size distribution can lead to uneven distribution of current.[79] This can result in localized areas of high current density, impacting the battery's performance and potentially leading to degradation or failure over time. Pore size is closely related to porosity, which is the volume fraction of pores in the separator material. Commercial membranes typically have pore sizes ranging between 0.03 and 0.12 μm, with a narrow and uniform distribution. Maintaining a consistent pore size distribution is critical for ensuring optimal battery performance. The difference between the maximum and average pore size distribution should be minimal, typically no more than 0.01 μm. This level of control ensures that there are no significant variations in pore size throughout the separator, minimizing the risk of performance issues or safety hazards.[80]

The tortuosity (s) of the electrolyte membrane conduction pathways (pores), e.g., the ratio between the thickness sample and the effective pore length, was determined by the relation[16]

$$\tau = \sqrt{\frac{\sigma_0 \phi}{\sigma_i}}$$

where σ_0 is the conductivity of the liquid electrolyte and σ_i and ϕ represent the conductivity and the porosity of the membrane, respectively.

Sousa et al.[81] developed polymer electrolyte membranes based on the P(VdF-HFP) copolymer with various polymer/DMF ratios, demonstrating promising properties for lithium battery separators. These membranes achieve optimal porosity and tortuosity when the solvent content is 90% or higher. They can retain up to 77% liquid and exhibit conductivities above 10^{-3} S cm^{-1} at room temperature, aiming to enhance rate capability by improving pore distribution and interconnection. Further investigations into the effect of separator thickness and porosity on the performance of Lithium Iron Phosphate batteries were conducted.[82] The study found that the porosity of the separator significantly influences cell performance, with higher porosity separators leading to lower performance. Four different separators were tested: a polypropylene (PP)

https://doi.org/10.1021/acsomega.4c07070
ACS Omega 2025, 10, 3228−3261

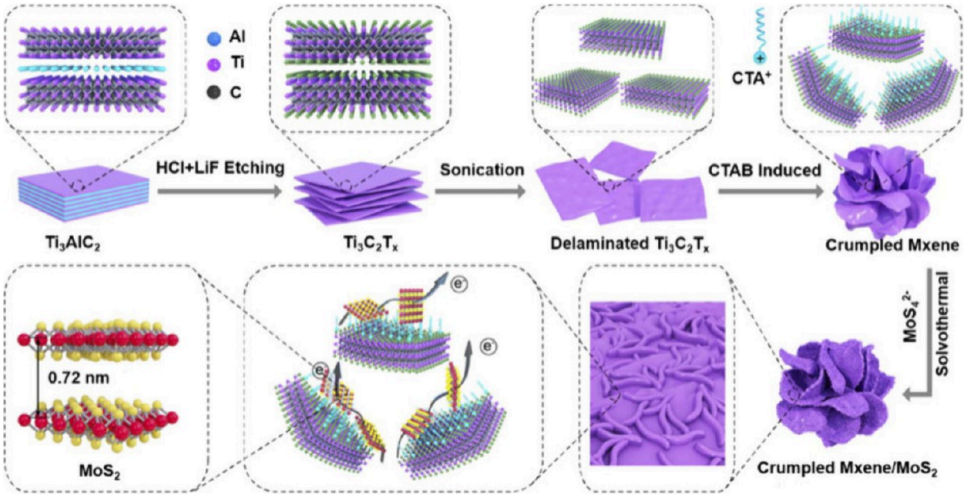

Figure 3. Schematic illustration of the synthesis of a 3D hierarchical crumpled MXene/MoS_2 heterostructure.[86] Reprinted with permission from ref 86. Copyright 2022 Royal Society of Chemistry.

monolayer and a polypropylene/polyethylene/polypropylene (PP/PE/PP) trilayer, each with thicknesses of 20 and 25 μm, and porosities of 41%, 45%, 48%, and 50%. It was determined that the PP separator with 41% porosity and the PP/PE/PP separator with 45% porosity performed better than the others. Additionally, lignin/polyacrylonitrile composite fiber-based nonwoven membranes (L-PANs) were fabricated through electrospinning by incorporating varying amounts of lignin into polyacrylonitrile (PAN) solutions (Figure 2(i)).[83] The L-PANs achieved a porosity of 74%, significantly higher than the 42% porosity of the commercial PP separator. When exposed to 150 °C for 15 min, the L-PANs maintained their dimensions without wrinkling (Figure 2(ii)), whereas the commercial PP separator shrank by 32%.

3.2. Permeability. Permeability refers to the ability of a material, in this case, the separator in a battery, to allow the flow of gases or liquids through it. In the context of battery separators, permeability is a crucial property that influences several aspects of battery performance. Permeability directly affects the efficiency of the battery by controlling the movement of electrolyte ions between the electrodes. A separator with higher permeability allows ions to pass through more easily, facilitating faster charging and discharging processes. This results in improved battery efficiency and performance. The permeability of the separator is influenced by factors such as thickness, porosity, pore size, and distribution.[74] Permeability is often quantified using the Gurley value, which is measured according to ASTM standards such as D7264 and D737.[74,84] This value indicates the time it takes for a certain volume of air to pass through a given area of the separator under specific conditions. Gurley values for separators in rechargeable batteries are typically less than 0.025 $s\mu m^{-1}$, indicating high permeability. The tortuosity of the pores, which refers to the convoluted path that ions must take through the separator, also influences permeability. Higher tortuosity increases the effective path length, resulting in lower permeability. Additionally, thickness plays a role in determining permeability, with thinner separators generally exhibiting higher permeability due to reduced resistance to ion flow. A separator with inadequate permeability can lead to performance issues such as increased internal resistance, slower charging and discharging rates, and reduced overall battery efficiency. Therefore, ensuring optimal permeability is essential for maximizing the performance and longevity of rechargeable batteries. The importance of separators in nonaqueous systems is highlighted by the need for continued exploration and optimization of ion exchange membranes, as commonly used aqueous membranes do not maintain their performance in nonaqueous environments. Research shows that polymer design strategies for aqueous systems may not directly transfer to nonaqueous systems. For instance, phenoxyaniline trisulfonate- poly(phenylene oxide) membranes, (POATS-PPO), achieved higher ionic conductivity than traditional membranes used in nonaqueous redox flow batteries, indicating the potential for significant performance improvements by modifying polymers specifically for nonaqueous conditions.[85] This underscores the critical role of tailored separator materials in enhancing battery performance. Jiang et al. developed a high-throughput screening permeability separator with high catalytic conversion kinetics specifically designed for Li-S batteries. They utilized a hierarchical crumpled MXene/MoS_2 (CM/MoS_2) heterostructure (Figure 3) as an efficient ion-selective membrane on a polypropylene (PP) separator. This innovative membrane achieves multiple objectives: it effectively immobilizes lithium polysulfides (LiPS), enhances catalytic conversion kinetics, and facilitates lithium-ion diffusion. Experimental and theoretical results confirm that the MXene/MoS_2 heterostructure immobilizes LiPSs chemically through a combination of Lewis acid-base interactions and sulfur-chain catenation. Additionally, it catalytically converts LiPSs into lithium disulfide (Li_2S_2) and lithium sulfide (Li_2S) by lowering the diffusion barrier for lithium atoms. This dual functionality significantly improves the overall performance of the Li-S batteries.[86]

3.3. Thickness. The thickness of the separator in a battery is crucial because it directly impacts several key aspects of battery performance and safety. A thinner separator allows for quicker passage of lithium ions between the cathode and anode, reducing internal resistance. This low internal resistance enables the battery to deliver power more efficiently, resulting in higher power density. In simpler terms, thinner separators facilitate faster charging and discharging ofU8 the battery. Furthermore, thinner separators enable higher energy density because they allow for more active material (such as lithium

https://doi.org/10.1021/acsomega.4c07070
ACS Omega 2025, 10, 3228−3261

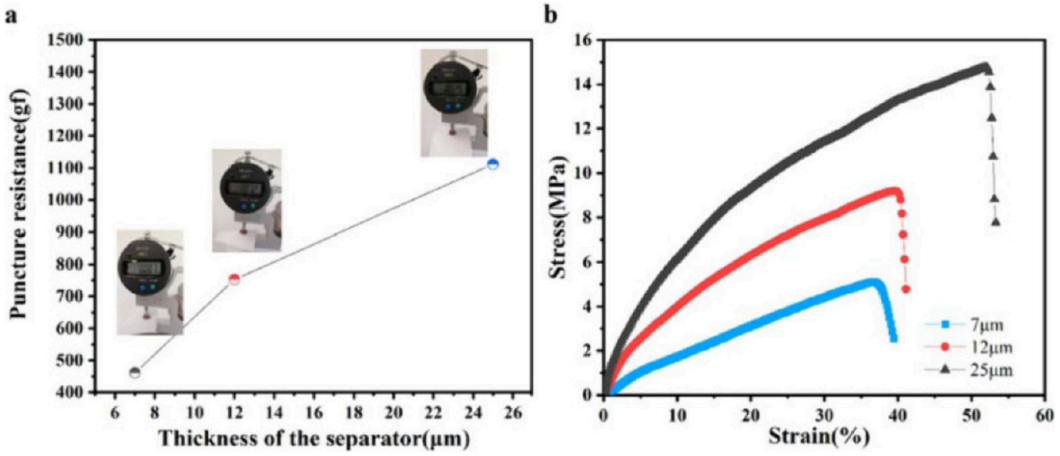

Figure 4. Performance of the separator with thicknesses of 25 μm, 12 μm, and 7 μm. (a) Tensile strength, (b) puncture resistance.[88] Reprinted with permission from ref 88. Copyright 2021 Published on behalf of The Electrochemical Society by IOP Publishing Limited.

ions) to be packed into the same volume of the battery. This means that for a given size, a battery with a thinner separator can store more energy.[22] However, if the separator becomes too thin, it may struggle to retain the electrolyte (liquid component of the battery) effectively. Additionally, a thin separator might compromise its ability to provide electronic insulation between the cathode and anode. Both of these factors are critical for the safe and efficient operation of the battery. Additionally, thicker separators generally offer better mechanical strength, which is important for maintaining the structural integrity of the battery. If the separator is too thin, it may be prone to tearing or puncturing, which can lead to short circuits and potentially dangerous situations. It is worth to mention that a uniform separator thickness is essential for ensuring stable performance and long cycle life of the battery. Variations in thickness can lead to uneven distribution of lithium ions during charging and discharging cycles, which may result in capacity loss or degradation over time.[87] Improving the energy density of the conventional battery requires a significant reduction in separator thickness. The safety and electrical performance of the battery are significantly impacted by the mechanical and thermal stability of the conventional separator as its thickness decreases (Figure 4).[88] There is no doubt that the mechanical qualities decrease as the separator thickness decreases. To attain a balance between its mechanical qualities and Li-ion transport properties, the separator needs to be the right thickness.[89] The selection of mechanical qualities and thermal stability of superior separator material is therefore crucial, in addition to the requirement for ongoing optimization in the separator structure design, process, and equipment.

Horváth et al.[90] investigated the impact of separator thickness on the rate performance of $LiNi_{0.5}Mn_{0.3}Co_{0.2}O_2$ (NMC)-nanotube composite batteries. They found that the characteristic charge/discharge time increased linearly with separator thickness up to approximately 100 μm, beyond which the increase in time plateaued. Their analysis revealed that the primary rate-limiting factor was the electrolyte resistance within the separator, rather than ion diffusion. This finding suggests that the electrolyte's resistance to ion flow through the separator is the critical factor affecting the battery's charge and discharge rates. The study also highlights that this method of analysis can be applied to examine how other separator characteristics, such as tortuosity (the complexity of the pathway through the separator), porosity (the volume fraction of the separator that is void space), and pore size, influence the rate capability of batteries. This approach provides a valuable framework for optimizing separator design to improve battery performance.

3.4. Chemical Stability. In the realm of battery technology, the chemical stability of separators plays a pivotal role in ensuring the efficient and safe operation of batteries. Separators serve as the physical barrier between the positive and negative electrodes in a battery cell, preventing short circuits while allowing the flow of ions during the charge and discharge cycles. However, beyond mere physical integrity, separators must exhibit high chemical stability to withstand the harsh conditions within the battery environment, including exposure to reactive lithium,[91] corrosive electrolytes,[92] and elevated temperatures. These conditions can cause thermal stress, degradation, or failure if the separator is not robust enough.[85]

One crucial aspect of chemical stability is the ability of separators to endure the charge and discharge processes without undergoing chemical reactions that could compromise their structural integrity or introduce impurities into the battery system. Impurities can detrimentally affect the performance and lifespan of batteries, leading to reduced efficiency and potential safety hazards. To evaluate the chemical stability of separators, various tests are conducted to assess their resistance to corrosion and their tendency to expand or contract when exposed to the battery's electrolyte. Typically, these tests involve immersing the separators in the electrolyte solution under controlled conditions, such as elevated temperatures (e.g., 50 °C), for a specific duration, usually ranging from 4 to 6 h. During these immersion tests, any adverse reactions between the separator material and the electrolyte are monitored. The absence of corrosion or degradation of the separator material indicates its high chemical stability. Additionally, the expansion and contraction rate of the separator, which could potentially lead to mechanical failure or compromise its ability to maintain electrode separation, are carefully observed. A chemically stable separator ensures the long-term performance and reliability of batteries by preserving the integrity of the battery system and preventing the introduction of impurities that could degrade its function. Moreover, by maintaining structural integrity under various operating conditions, chemically stable

https://doi.org/10.1021/acsomega.4c07070
ACS Omega 2025, 10, 3228−3261

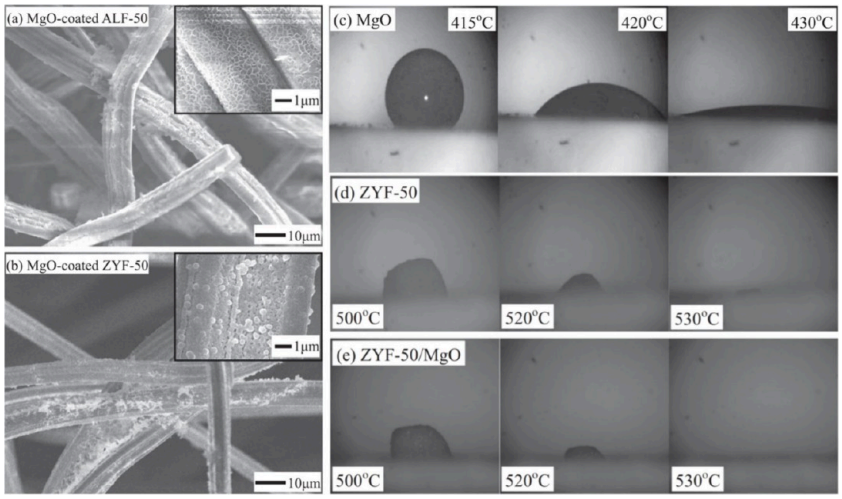

Figure 5. SEM images of the MgO-coated (a) ALF-50 and (b) ZYF-50 ceramic felts. The images at high magnification are shown in the inset. (c) Images for the wetting behavior of the LiCl-KCl electrolyte on the MgO pellets as a function of temperature. (d, e) Infiltration behavior of the LiF-LiCl-LiBr electrolyte on the ZYF-50 and MgO coated ZYF-50 felt as a function of temperature, respectively.[94] Reprinted with permission from ref 94. Copyright 2016 Elsevier.

separators contribute to the safety of battery systems, reducing the risk of thermal runaway or other catastrophic failures.[93] The use of a thermally and chemically stable ceramic felt separator in thermal batteries is expected to improve reliability by preventing sudden electrolyte failure upon shock. The separator should retain sufficient molten electrolyte to avoid physical contact between the cathode and anode and maintain chemical stability in a reactive molten Li-salt electrolyte environment for high ionic conductivity and reliability. To enhance thermal battery reliability, three types of ceramic felt separators (two types of Al_2O_3 with different porosities and one ZrO_2) were tested, with and without MgO coating.[94] Figures 5a and 5b present SEM images of MgO-coated ALF-50 and ZYF-50 felts, prepared by repeatedly dipping the fibers in Mg-nitrate solution followed by pyrolysis at 400 °C. Despite differing coating morphologies, both felts are well-coated with MgO, confirmed by XRD and EDS analyses. Figure 5c shows that the LiCl-KCl electrolyte forms a hemisphere upon melting at 415 °C due to its high surface tension (123 dyn cm^{-1}), which is much greater than that of water. Figures 5d and 5e depict the infiltration behavior of the LiF-LiCl-LiBr electrolyte on ZYF-50 and MgO-coated ZYF-50 felts, suggesting that MgO coating may not be necessary for wetting and infiltration. The chemical stability of the MgO-coated felts in a molten electrolyte environment, confirmed by analyzing the compounds formed at high temperatures, indicates that all types of ceramic felts remain stable.

The felts exhibited good wetting and infiltration behaviors with molten LiCl-KCl and LiF-LiCl-LiBr electrolytes, achieving full wetting at temperatures above the electrolytes' melting points. The felts' electrolyte loading exceeded 85%, with leakage under 25%, suitable for practical use. Chemical stability was confirmed, as the felts formed low melting point compounds without reducing ionic conductivity. The study found no significant barriers to using these ceramic felts as separators, even without MgO coating.

3.5. Mechanical Strength. Mechanical strength is a critical aspect of separator performance in batteries, as it ensures the structural integrity of the separator under various conditions encountered during battery operation. The mechanical strength of separators is typically evaluated in terms of tensile strength and puncture strength in the machine direction (MD) and the transverse direction (TD).[95] Tensile strength measures the ability of the separator to withstand stretching forces, while puncture strength assesses its resistance to penetration. These properties are crucial for maintaining the structural integrity of the separator during battery assembly and operation. Batteries are often assembled by winding the separator and electrode layers under tension. A separator with adequate tensile strength can withstand this winding process without significant elongation or deformation. This ensures that the separator maintains its dimensional stability and does not shrink excessively in width, which could lead to internal short circuits within the battery. The minimum tensile strength measured for a separator with a thickness of 25 μm is 98.06 MPa, in accordance with ASTM D882 and D638.[96] Currently, the mechanical properties of the single-layer polyolefin PP separator made via uniaxial stretching are anisotropic. Merely 5 N is the strength in the vertical stretching direction, however it is approximately one tenth of the longitudinal tensile strength. The strength of the polyolefin separator created by biaxial stretching is essentially the same in both the vertical and extended directions. Separator strength can vary depending on the direction of stretching during manufacturing. Anisotropic separators, where the strength differs between the machine direction (MD) and transverse direction (TD), may exhibit uneven performance when subjected to mechanical stress. To ensure uniform performance, especially during winding and assembly, separators should ideally have consistent strength in all directions. The separator must also possess puncture resistance to prevent penetration by rough electrode surfaces, which could lead to short circuits within the battery. Puncture strength is particularly important given the presence of active material and carbon black on the electrode surface, which can increase the risk of puncture. Standards such as ASTM D882, D638, and D3763 provide guidelines for evaluating the mechanical strength of separators. These tests ensure that separators meet minimum strength requirements necessary for safe and reliable battery operation.[93] The PE/glass fiber (GF)$Mg(OH)_2$/PE composite (PGMP) separator, created by

https://doi.org/10.1021/acsomega.4c07070
ACS Omega 2025, 10, 3228−3261

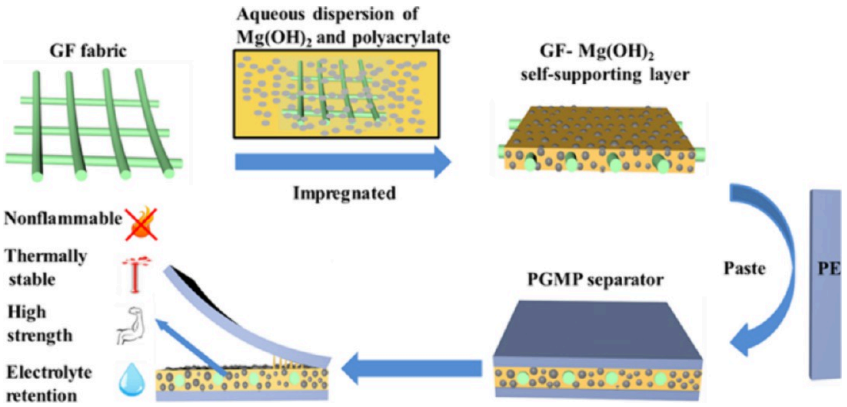

Figure 6. Action mechanism of the PGMP separator.[97] Reprinted with permission from ref 97. Copyright 2022 Wiley-VCH.

integrating glass fiber fabric and $Mg(OH)_2$ with a polyethylene (PE) microporous film, significantly outperforms the commercial PE separator. As illustrated in Figure 6, the PGMP separator's action mechanism involves superior properties such as high thermal stability up to 350 °C, a tensile strength of 250 MPa, ionic conductivity of 0.93 mS/cm, and electrolyte uptake of 86%. These attributes enhance the overall safety of the cell, enabling it to pass nail penetration, impact, and overcharge tests. Additionally, the PGMP separator provides excellent cycle stability, retaining 85% of its capacity after 500 cycles at a 1.0 C rate. Its simple and cost-effective production process makes it a highly promising option for industrial applications.[97]

3.6. Wettability. In lithium-ion batteries, the wettability of separators is a crucial factor influencing the overall performance and efficiency of the battery system. A separator with good wettability facilitates easy penetration of electrolyte into its porous structure, ensuring sufficient electrolyte retention during battery operation. This is essential for maintaining high ionic conductivity within the battery and maximizing its capacity. When a separator exhibits poor electrolyte wettability, it hinders the efficient impregnation of electrolyte into its pores. As a result, the interface resistance between the separator and electrodes increases, leading to reduced charge and discharge efficiency, as well as compromised cycle performance of the battery. To evaluate the wettability of separators, various methods can be employed. One common approach is to measure the rate of liquid absorption and retention by the separator. This can be done by immersing the separator in the electrolyte and then comparing its mass before and after immersion. The difference in mass indicates the amount of electrolyte absorbed by the separator, reflecting its wettability characteristics.[98] Additionally, the wettability of separators can be assessed by measuring the absorption rate or contact angle of droplets on the membrane surface. A higher absorption rate and a lower contact angle indicate better wettability, signifying improved electrolyte penetration and retention capabilities. Ensuring optimal wettability of separators is essential for maximizing the performance and longevity of lithium-ion batteries. By selecting separators with excellent wettability properties, battery manufacturers can enhance the electrolyte distribution within the battery, minimize interface resistance, and ultimately improve the overall efficiency and reliability of the battery system. It is possible to produce core-shell structured silica-poly(cyclotriphosphazene-*co*-4,4′-sulfonyldiphenol) nanoparticles (SiO_2-PZS) nanoparticles and coat both sides of a PE microporous membrane with them. SiO_2-PZS nanoparticle-coated separators show notable improvements in ionic conductivity and liquid electrolyte wettability when compared to those coated with pure SiO_2 particles. The completed coin cells exhibit improved cycle performance and C-rate capability as a result of these improvements, which are especially apparent at an 8 C discharge rate.[99] Zhu et al.[100] introduced a novel composite separator for lithium-ion batteries, produced via a straightforward papermaking method using heat-resistant polyphenylene sulfide (PPS) fibers and bacterial cellulose (BC) nanofibers, termed BC/PPS. The BC nanofibers were specifically employed to control the pore size of the composite membrane. This hybrid BC/PPS separator exhibited outstanding thermal stability, excellent electrolyte wettability, and high ionic conductivity. Consequently, cells incorporating the BC/PPS separator displayed significantly better rate capability and more stable cycling performance compared to those using a commercial separator. In particular, the 20%BC/PPS separator demonstrated superior affinity for liquid electrolytes, as indicated by enhanced wetting behavior, a lower contact angle, and better capillary absorption. These improvements are attributed to its chemical structure and highly porous nature (Figure 7). These characteristics enable the separator to more effectively manage electrolyte distribution within the cell, thereby enhancing overall battery performance.

Xie et al.[101] conducted a systematic investigation into the factors affecting the wettability of commonly used polyolefin separators. These factors include solvent components, types of lithium salts, and their concentrations. To enhance the wettability of these separators toward electrolytes, various wetting additives were examined, such as Pluronic surfactants and water. The study found that adding a trace amount of water (200 ppm) to the electrolyte composed of 1 M $LiPF_6$ in propylene carbonate (PC) significantly improved electrolyte uptake in polyolefin separators. Performance tests on Li| $LiFePO_4$ cells revealed that the inclusion of this wetting additive led to improvements in discharge capacities, rate capability, and cycling stability. Additionally, contact angle measurements were used to assess changes in wettability. These measurements demonstrated that increasing the lithium salt concentration in the electrolyte influenced the separator's wettability, largely due to changes in electrolyte viscosity. Figure 8 illustrates how the contact angle decreases with higher lithium salt concentrations, indicating better wettability.

Under low-temperature and discharge coupling conditions, lithium-ion batteries face significant performance degradation,

https://doi.org/10.1021/acsomega.4c07070
ACS Omega 2025, 10, 3228−3261

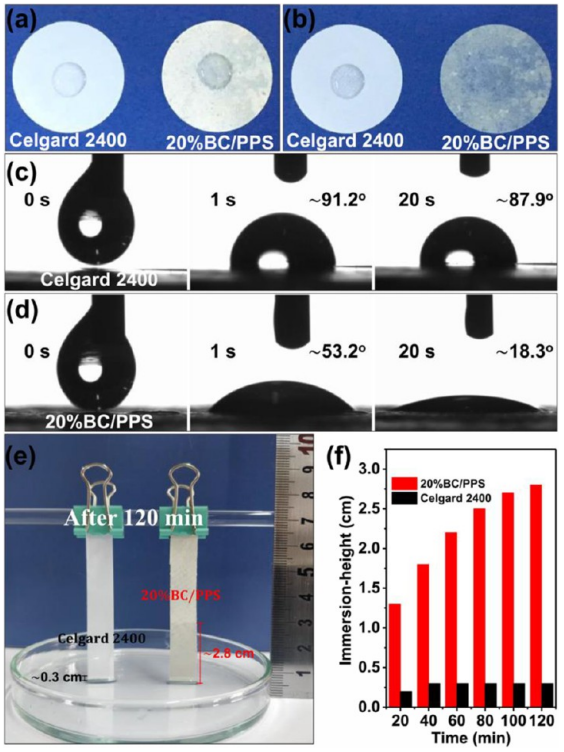

Figure 7. Wettability analyses of separators. Images of liquid electrolyte wetting behavior (a, b). Contact angle variation photographs of electrolyte drop on different separators (c, d). The corresponding photo of electrolyte capillary absorption height after soaking for 120 min (e), and the record of height changed with time (f).[100] Reprinted with permission from ref 100. Copyright 2021 Elsevier.

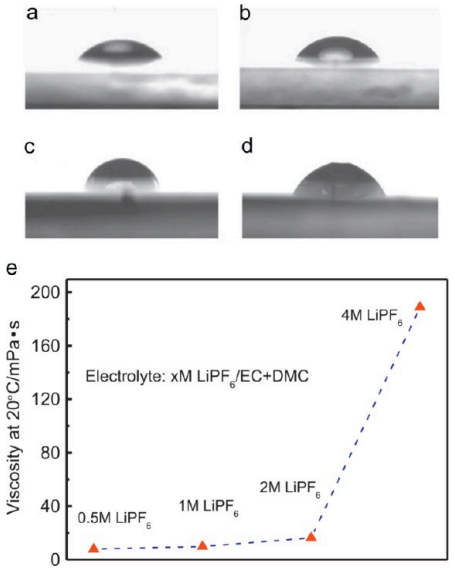

Figure 8. Influence of $LiPF_6$ concentrations on separator wettability toward electrolytes. (a), (b), (c), and (d) show the contact angles on the separator for 0.5 M $LiPF_6$/EC + DMC (1:1), 1 M $LiPF_6$/EC + DMC (1:1), 2 M $LiPF_6$/EC + DMC (1:1), 4 M $LiPF_6$/EC + DMC (1:1) and they are 47.1°, 56.1°, 67.7°, and 58.8°, respectively. (e) Implied viscosity of the electrolytes with different $LiPF_6$ concentrations.[101] Reprinted with permission from ref 101. Copyright 2015 Elsevier.

particularly due to the evolving wettability of the separator. This deterioration affects cycling stability and safety.[102] The separator wettability varies significantly with discharge ambient temperature and current. Microstructure and chemical analysis reveal that electrochemical reaction products deposit on the separator, reducing wettability. Lower temperatures and higher currents increase contact angles, leading to particle agglomeration, sediment formation, and reduced separator-ion compatibility. Experimental results (Figure 9) show that electrolyte uptake indicates better separator wettability than deionized water. Group comparisons reveal varying wettability, with Group 2 performing best. Results suggest that discharge conditions impact wettability, with lower temperatures and larger currents accelerating degradation.

3.7. Electrochemical Stability. In the context of lithium-ion batteries (Li-ion), the electrochemical stability of separators is a critical consideration for ensuring the reliability and safety of battery systems. Li-ion batteries operate within a highly oxidative and reductive environment, particularly during the charge and discharge processes, where lithium ions shuttle between the electrodes. To withstand this extreme redox environment, separators must exhibit robust electrochemical stability. During battery operation, the voltage across the electrodes can vary significantly, with the maximum voltage often reaching up to 4.5 V. This wide voltage range necessitates separators that remain stable and inert within the 0 to 5.0 V range. Maintaining stability within this voltage window is crucial to prevent unwanted reactions between the separator material and the electrolyte or electrodes, which could lead to degradation of battery performance or even safety hazards. Cyclic voltammetry (CV) is a commonly employed technique to assess the electrochemical stability of separators within the operational voltage range of Li-ion batteries. CV involves applying a cyclic voltage waveform to the battery system and measuring the resulting current response. By systematically varying the voltage within the specified range, CV can detect any changes in the electrochemical behavior of the separator material, such as oxidation or reduction reactions.[96] Through CV analysis, researchers can evaluate whether the separator material remains inert and unreactive within the operational voltage window. Any deviations from the expected electrochemical behavior indicate potential reactions between the separator and electrolyte or electrodes, signaling a lack of electrochemical stability. Achieving electrochemical stability in separators is crucial for maintaining the integrity and performance of Li-ion batteries. A stable separator-electrolyte system ensures that the battery operates reliably over multiple charge and discharge cycles without compromising its efficiency or safety. By employing techniques like CV to assess electrochemical stability, researchers and manufacturers can develop separators that meet the demanding requirements of advanced Li-ion battery applications. The use of lithium (Li) metal as an anode in batteries shows promise due to its high theoretical capacity and low reduction potential, but issues like dendrite growth and volume change hinder its practical application. Functional separators, such as those incorporating graphene layers, are seen as a solution to improve safety and electrochemical stability in Li-metal batteries (LMBs). Surface-functionalized graphene separators (SFGS) demonstrate enhanced electrolyte wettability and ionic conductivity, resulting in more stable cycle performance and high Coulombic efficiency.[103] This improvement is attributed to the homogeneous Li-ion flux

https://doi.org/10.1021/acsomega.4c07070
ACS Omega 2025, 10, 3228−3261

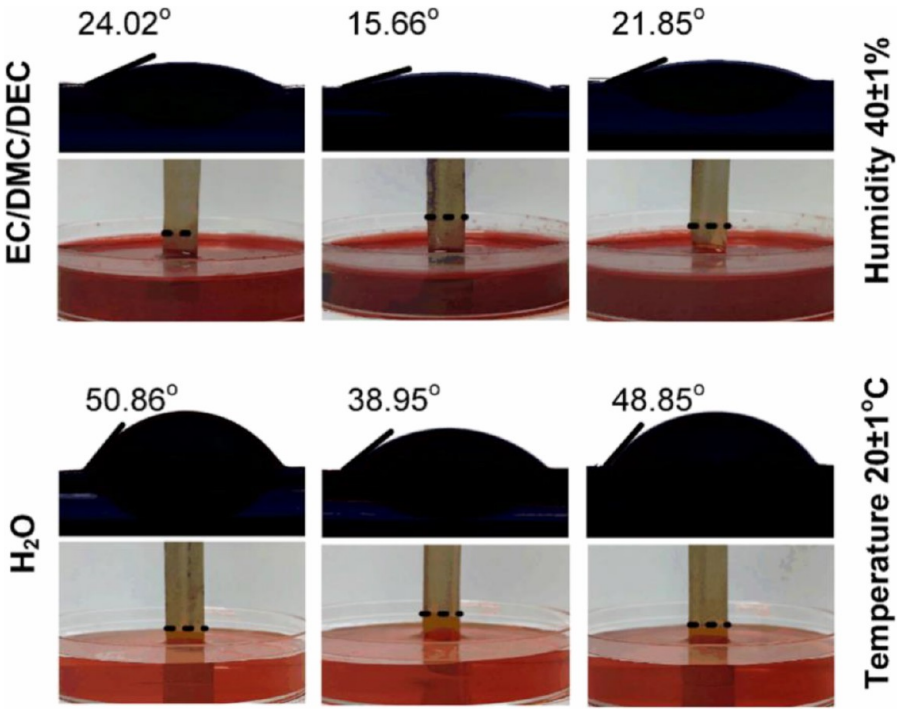

Figure 9. Contact angle and meniscus characteristics after 1 h of soaking in the three groups of lithium-ion batteries subjected to various low-temperature discharge conditions.[102] Reprinted with permission from ref 102. Copyright 2024 Elsevier.

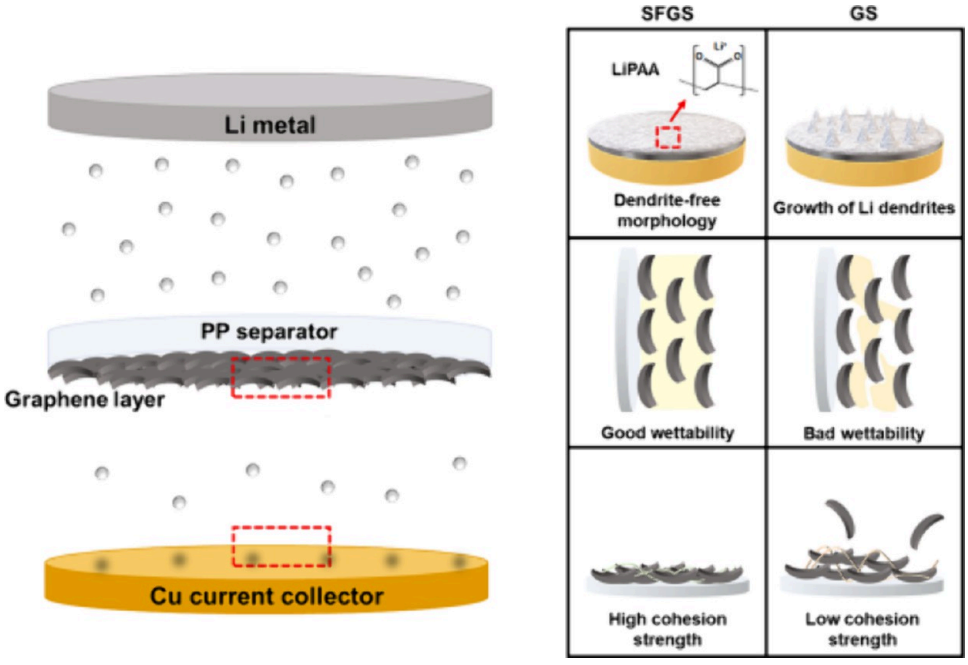

Figure 10. Schematic illustrating the various advantages of the SFGS, compared with the GS.[103] Reprinted with permission from ref 103. Copyright 2023 Elsevier.

induced by the improved wettability, along with the formation of a flexible solid electrolyte interface (SEI) layer facilitated by LiPAA. In contrast, graphene separators (GS) without surface functionalization exhibit poor wetting ability and nonuniform Li-ion flux, limiting their electrochemical stability (Figure 10). Overall, surface-functionalized separators offer a promising approach to address challenges associated with Li-metal anodes and advance the development of high-performance LMBs.

A novel bimetallic $LaNiO_3$ functional material[104] has been developed to serve as a highly efficient polysulfide shuttling stopper, significantly enhancing the electrochemical stability of Li-S batteries. By varying the calcination temperature during synthesis, different $LaNiO_3$ samples with distinct physical and chemical properties were obtained. The $LaNiO_3$ functionalized separators incorporate three key functionalities in one: effective chemisorption of polysulfides (Figure 11a), high electrical conductivity (Figure 11b), and excellent catalytic

https://doi.org/10.1021/acsomega.4c07070
ACS Omega 2025, 10, 3228−3261

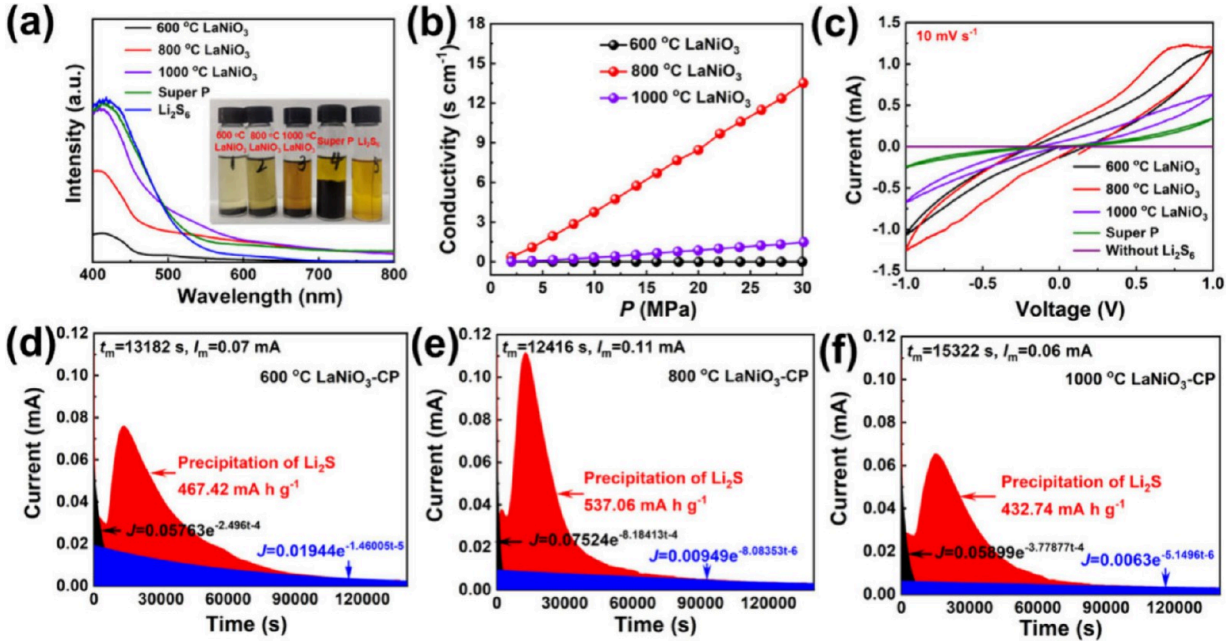

Figure 11. (a) UV-visible spectra of the Li_2S_6 solution after polysulfide adsorption tests (the inset is the photo of the Li_2S_6 solutions after polysulfide adsorption tests). (b) The electrical conductivity of the different materials measured by the four-probe method. (c) CV curves of symmetric cells with 600 °C $LaNiO_3$, 800 °C $LaNiO_3$, 1000 °C $LaNiO_3$, and super P electrodes. Li_2S precipitation experiments with (d) 600 °C $LaNiO_3$, (e) 800 °C $LaNiO_3$, and (f) 1000 °C $LaNiO_3$.[104] Reprinted with permission from ref 104. Copyright 2023 Elsevier.

properties. These properties work together to prevent the detrimental shuttle effect of polysulfides in Li-S batteries, thereby improving the batteries' overall performance and longevity. The 800 °C $LaNiO_3$ electrode shows the highest redox current and Li_2S precipitation capacity, indicating superior polysulfide conversion kinetics and catalytic activity compared to electrodes calcined at 600 and 1000 °C, due to its high electrical conductivity.

3.8. Thermal Behavior and Shutdown. The thermal behavior of separators in lithium-ion batteries is a critical aspect that directly impacts the safety and reliability of battery systems. Maintaining stability at high temperatures is paramount to prevent internal short circuits and thermal runaway, which can lead to catastrophic failures. During battery assembly, separators must withstand mechanical stresses such as bending and tilting without compromising their structural integrity. Any deformation of the separator that results in electrode contact can trigger an internal short circuit. Additionally, the separator should not shrink during battery operation, especially at elevated temperatures, to prevent electrode contact and maintain effective ion transport pathways. To assess thermal stability, criteria such as thermal shrinkage are commonly evaluated. A thermal shrinkage of less than 5% in both machine direction (MD) and transverse direction (TD) after heating for 60 min at 90 °C, under vacuum conditions, is often considered acceptable. This ensures that the separator retains its dimensional stability and integrity even under thermal stress.[105] In the event of abnormal battery conditions leading to temperature rise, the separator must be capable of cutting off the current loop to prevent thermal runaway. This shutdown function is crucial for preventing further escalation of temperature and mitigating safety risks. The shutdown protection temperature, determined through thermodynamic analysis and experimental methods such as thermal battery and simulated battery tests, plays a pivotal role in preventing thermal runaway. For instance, in rechargeable batteries with PE-PP bilayer separators, the shutdown and melting temperatures are specified as 130 and 165 °C, respectively. These temperatures are carefully chosen to ensure that the separator effectively interrupts the current flow before reaching critical temperatures where thermal runaway may occur. Maintaining the mechanical integrity of the separator during the shutdown process is essential to prevent direct electrode contact and subsequent chemical reactions that could exacerbate thermal runaway.[84] Therefore, ensuring the thermal stability and shutdown capability of separators in lithium-ion batteries is essential for preventing safety hazards and maintaining reliable battery performance, particularly under extreme operating conditions. By adhering to stringent thermal criteria and incorporating robust shutdown mechanisms, battery manufacturers can enhance the safety and longevity of lithium-ion battery systems. Figure 12 displays digital photographs and SEM images of glass fiber fabric mats, revealing their large-scale availability and high mechanical flexibility (Figures 12a and 12b). Statistical analysis indicates a diameter range of 5.7−6.9 μm, with an average of approximately 6 μm. The porous structure observed in Figure 12c facilitates lithium ion permeability, meeting separator requirements, with pore sizes ranging from 50 × 50 μm to 100 × 100 μm. Notably, Figure 12d demonstrates the glass fiber fabrics' resistance to damage or firing, contrasting with polymer separators prone to shrinkage under high temperatures. In summary, the flexibility, porous structure, and stability of glass fiber fabrics offer potential for enhancing the safety of lithium-ion batteries as separators.[106]

A thermal shutdown separator was developed for lithium-ion batteries by coating low-density polyethylene microspheres (PM) onto a polypropylene (PP) membrane. This separator maintains normal function at room temperature but rapidly melts and blocks ion flow at elevated temperatures (110−120 °C), effectively stopping battery reactions and preventing thermal runaway.[107] Thermal analysis (Figure 13) shows that

https://doi.org/10.1021/acsomega.4c07070
ACS Omega 2025, 10, 3228−3261

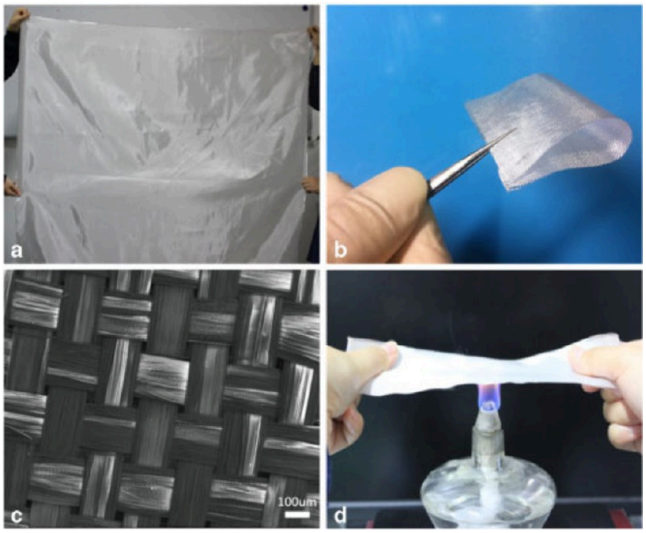

Figure 12. (a) Photograph of glass fiber fabrics. (b) Photograph of glass fiber fabrics with flexibility. (c) SEM image of glass fiber fabrics. (d) Photograph of glass fiber fabrics fired by alcohol lamp. 91 × 66 mm (300 × 300 DPI).[106] Reprinted with permission from ref 106. Copyright 2015 Springer.

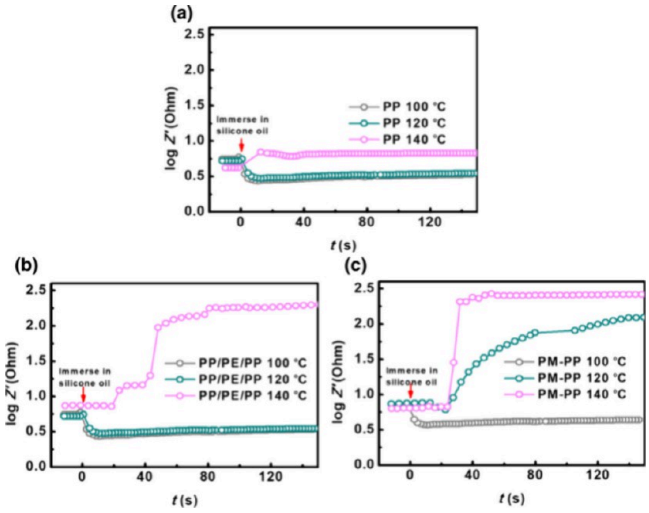

Figure 13. Log $Z'-t$ plots of the SS/separator/SS coin cells using (a) the PP separator, (b) the commercial PP/PE/PP separator, and (c) the PM/PP separator.[107] Reprinted with permission from ref 107. Copyright 2019 Elsevier.

while the PP separator and a PP/PE/PP separator exhibit some changes in impedance with increasing temperature, indicating reduced porosity and structural changes, the PM/PP separator shows a rapid rise in impedance starting at 120 °C, completing within 5 s at 140 °C. This rapid response ensures effective thermal shutdown, preventing thermal runaway and enhancing the safety of LIBs under high-temperature conditions.

A poly(ethylene-*co*-vinyl acetate) (EVA)/polyimide (PI)/EVA (PIE) trilayer separator was developed for sodium-ion batteries (SIBs), featuring excellent thermal stability and a shutdown function.[108] The porous EVA layers are dip-coated on an electrospun-PI support, creating a separator that resists thermal shrinkage up to 200 °C and rapidly shuts down around 100 °C. The PIE separator shows higher ionic conductivity and better electrolyte uptake compared to commercial separators, leading to superior cycling performance in SIBs. The thermal shutdown function of the PIE separator activates at approximately 90 °C and maintains mechanical integrity up to 190 °C, preventing thermal runaway across a wide temperature range (Figure 14).

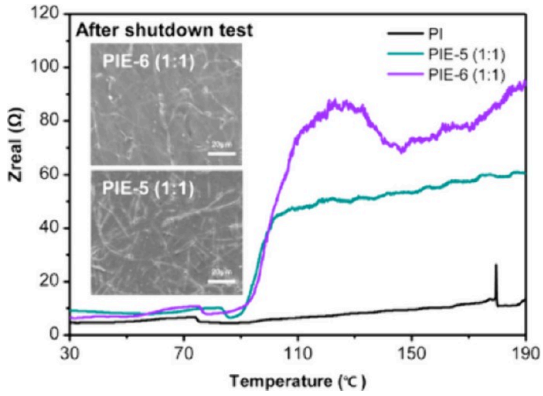

Figure 14. Shutdown test of the PI and PIE separators (Insets: SEM images of PIE-5 (1:1) and PIE-6 (1:1) after shutdown test).[108] Reprinted with permission from ref 108. Copyright 2020 Elsevier.

Zheng et al.[109] optimized a flame-retardant electrospun core-shell fibrous membrane (ECSFM) for battery separators using simulation. The optimal ECSFM, with a polyvinylidene fluoride (PVDF) shell and triphenyl phosphate (TPP) core, had superior thermal shutdown at 177 °C and rupture at 227 °C. Batch preparation was achieved with a 20.33-fold increase in output. The optimized ECSFM effectively prevented thermal runaway, unlike the unoptimized version, demonstrating improved safety and performance for battery applications.

3.9. Cost. The cost of separators in lithium-ion batteries constitutes a significant portion of the total production expenses, currently amounting to over 20% of the overall cost. This cost encompasses various factors, including expenses related to production equipment, energy consumption during manufacturing, and the raw materials used in separator fabrication. Therefore, finding ways to develop a low-cost production process for separators is crucial for reducing the overall cost of rechargeable batteries. Efforts to lower the cost of separators must consider multiple aspects, including optimizing production efficiency, minimizing energy consumption, and sourcing cost-effective materials. Implementing cost-saving measures in separator manufacturing can have a substantial impact on the affordability and accessibility of lithium-ion batteries, thus promoting their widespread adoption across diverse applications. It is important to note that the characteristics of separators are interconnected and influence one another. For instance, reducing the thickness of the separator can potentially enhance the energy and power density of the battery by reducing internal resistance and increasing the effective electrode area. However, this reduction in thickness may compromise the mechanical strength of the separator, affecting its durability and reliability during battery operation.[110,111] In practical applications, manufacturers must carefully balance the various features and characteristics of separators against performance, safety, and cost considerations. Trade-offs may be necessary to optimize battery performance while ensuring that the final product remains affordable and competitive in the market. This involves carefully evaluating the impact of design choices, material selection, and

https://doi.org/10.1021/acsomega.4c07070
ACS Omega 2025, 10, 3228−3261

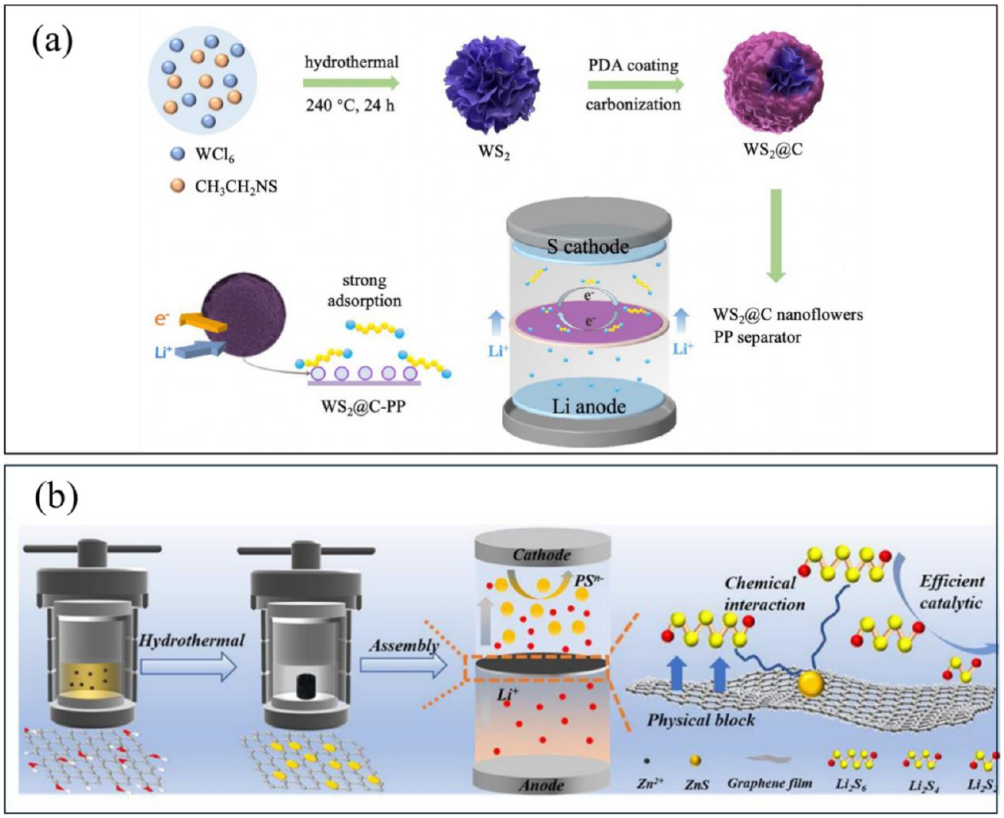

Figure 15. (a) Schematic illustration of the fabrication of WS_2@C composite and its working mechanism in Li-S battery[114] Reprinted with permission from ref 114. Copyright 2022 Springer. (b) Schematic illustration of the synthesis process of ZnS-RGA composites and its synergistic effect of efficient PS blockage and PS conversion catalysis in the Li-S battery.[116] Reprinted with permission from ref 116. Copyright 2022 Elsevier.

production processes on the overall cost-effectiveness of rechargeable batteries. While meeting the basic requirements is essential for separator performance, advanced battery systems often demand multifunctional separators that go beyond these criteria. These separators not only facilitate ion transport and ensure stability but also address specific challenges like polysulfide migration in Li-S batteries.

4. MULTIFUNCTIONAL SEPARATORS

Multifunctional separators are essential in lithium-sulfur (Li-S) batteries to mitigate the polysulfide shuttle effect, enhance electrochemical efficiency, and improve charge storage capacity. They achieve this by preventing polysulfide diffusion, ensuring uniform lithium-ion deposition, and incorporating features like physical adsorption and catalytic conversion.[112] For instance, a TiB_2 separator combined with graphene has been developed to effectively immobilize sulfur and prevent polysulfide shuttling, thereby enhancing sulfur reutilization.[113] Similarly, traditional polypropylene separators were enhanced with WS_2@C nanoflower composites (Figure 15a), which effectively adsorb and catalyze the conversion of lithium polysulfides, leading to improved cycling stability and rate performance, achieving a discharge capacity of 1475 mAh g^{-1} at 0.1 C.[114] Expanding on these innovations, Liang et al.[115] introduced a gradient-structured nanofiber membrane composed of pure gelatin and Super P-MoO_2/MoS_2-gelatin, where the gelatin layer homogenizes lithium flux and the latter effectively adsorbs polysulfides while boosting conversion efficiency. Another advancement involved a modified separator composed of zinc sulfide quantum dots and reduced graphene aerogel (ZnS-RGA), (Figure 15b) designed to immobilize lithium polysulfides and facilitate the sulfur redox reaction, with a three-dimensional porous architecture impeding LiPS migration.[116] Recent research on polyoxometalates (POMs) has led to a novel POM-based supramolecular compound by combining 18-crown-6 (CR6) with $K_3PW_{12}O_{40}$ (KPW) and integrating it with graphene oxide (GO), enhancing Li^+ transport and catalyzing polysulfide transformation, achieving a specific capacity of 1073.3 mAh g^{-1} at 1.0 C with 81.5% retention after 250 cycles.[117] Chen et al. further contributed by designing a multifunctional separator utilizing polyaniline (PANI) encapsulated amorphous vanadium pentoxide (V_2O_5) nanowires, resulting in enhanced polysulfide adsorption, catalytic activity, and ionic conductivity, while PANI improves electrical conductivity and flexibility, effectively suppressing polysulfide shuttling and enhancing cycling stability.[118] Additionaly, a covalent triazine framework/multiwall carbon nanotube (CTF/MWCNT) hybrid was introduced, combining strong polysulfide anchoring from CTF with high electrical conductivity from MWCNT, significantly enhancing sulfur utilization with a specific capacity of 982 mAh g^{-1} at 2 C and demonstrating excellent cycling stability with only 0.045% capacity loss per cycle at 1 C over 1000 cycles. This collective progress underscores the critical role of multifunctional separators in advancing the performance of Li-S batteries.[119] As multifunctional separators continue to evolve, further exploring materials that enhance conductivity and polysulfide retention remains crucial.

https://doi.org/10.1021/acsomega.4c07070
ACS Omega 2025, 10, 3228−3261

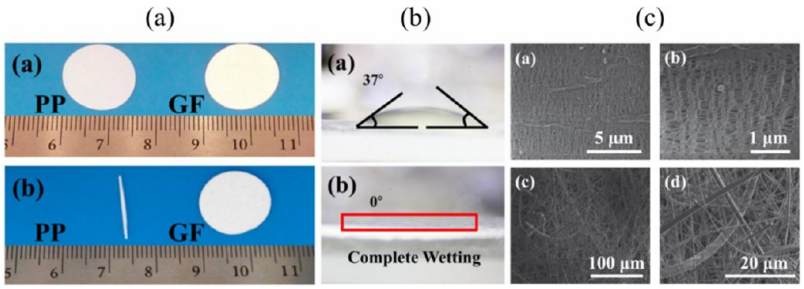

Figure 16. (a) Photographs of PP and GF separators before (top) and after (below) thermal treatment at 150 °C for 2h. (b) Contact angle photographs of PP (top) and GF (below) separators using liquid electrolyte. (c) SEM images of PP (top) and GF (below) separators with different resolutions.[140] Reprinted with permission from ref 140. Copyright 2016 Elsevier.

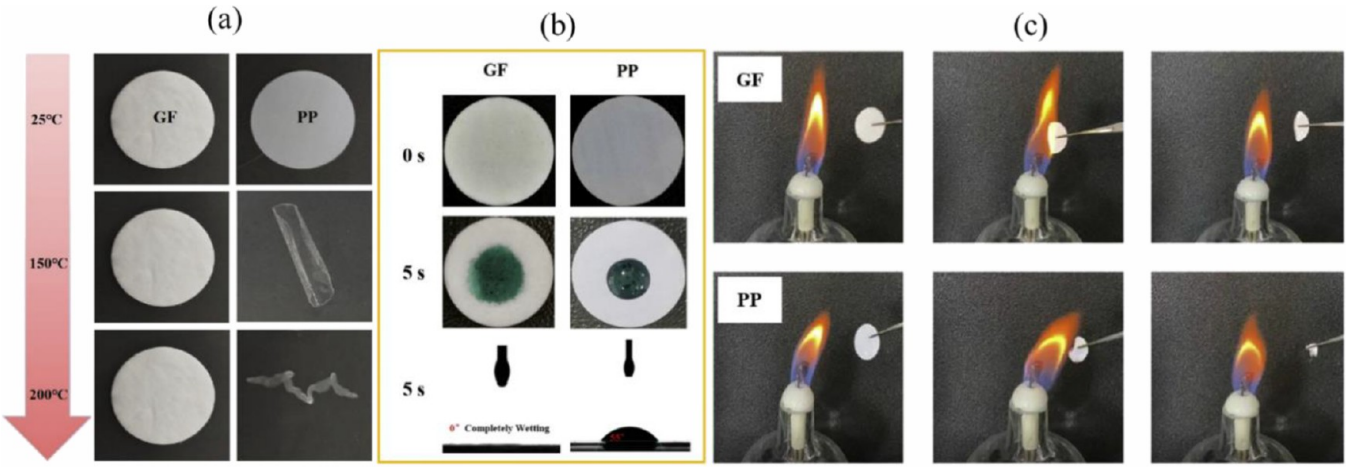

Figure 17. (a) Photographs of GF and Celgard 2400 (PP) separator heated at 25 °C, 150 °C, and 200 °C in a vacuum oven. (b) Contact angle characterization of GF and Celgard 2400 (PP) separator. (c) Flame resistant behavior of GF and Celgard 2400 (PP) separator.[141] Reprinted with permission from ref 141. Copyright 2020 Elsevier.

5. PROPERTIES OF GLASS FIBER SEPARATORS

Glass fiber (GF) is an inorganic, nonmetallic material with excellent properties like high aspect ratio, low thermal conductivity, strong corrosion resistance, stable chemical performance, and electrical insulation. It is used in insulation,[120] fire prevention,[121,122] heat insulation[123−125] and sound insulation,[126−128] adsorption,[129,130] and as a polymer precursor,[131−133] finding applications in plastics, rubber, chemicals, and aerospace. The commonly used polyolefin microporous membrane, like polypropylene (PP), has limitations such as low porosity, poor wettability to electrolyte, and instability at high temperatures.[134,135] On the other hand, glass fiber (GF) membranes offer better properties like electronic insulation, high thermal (550 °C) and chemical stability, cost-effectiveness, and good affinity to electrolyte, making them promising for Li-S batteries.[136] Additionally, the hydroxyl groups in GF facilitate the deposition of functional nanostructures like metal-organic framework (MOF), and the structure of GF accommodates functional materials well. Recent studies show GF-based separators in batteries, including Li-S, hold great potential for efficiency.[137−139]

PP separator shrinks significantly when exposed to high temperature due to its poor thermal stability, stemming from the low melting point of PP (Figure 16(a)). In contrast, GF separator maintains its dimensions, attributed to its borosilicate structure's intrinsic thermal resistance, enhancing battery safety under high charge/discharge rates or elevated temperatures.[140] A separator needs good electrolyte wettability for faster electrolyte filling and efficient retention during battery operation. PP separator has a contact angle of 37°, indicating poor wetting by the electrolyte, while GF separator shows complete wetting with a 0° contact angle, owing to its interconnected microporous structure and lyophilic nature, ensuring superior electrolyte wettability (Figure 16(b)). The highly porous structure of the GF separator increases intake of soluble polysulfide intermediates, slows down their diffusion to the Li anode, improving active material utilization, and protecting the Li anode surface from diffused polysulfides. This leads to better electrochemical performance. Additionally, the high porosity facilitates electrolyte permeation and ion transport, enabling efficient diffusion of lithium ions (Li^+) between the cathode and anode during charge and discharge cycles. FE-SEM analysis (Figure 16(c)) reveals that the PP separator has uniform slit-like pores, designed to prevent short circuits from dendritic lithium growth. In contrast, the GF separator consists of randomly arranged fibers, creating a highly porous structure with pores in the macroscopic range. The GF separator exhibits significantly higher porosity (66%) compared to the PP separator (41%), which enhances its ionic conductivity, facilitating rapid ionic transportation in the electrolyte. Before cycling, the metallic lithium anode surface appeared smooth. However, after cycling with a PP separator, significant corrosion damage and cracks were observed on the lithium anode surface due to side reactions with soluble lithium polysulfides. On the other hand, after cycling with a GF separator, the surface of the lithium anode stayed compara-

https://doi.org/10.1021/acsomega.4c07070
ACS Omega 2025, 10, 3228−3261

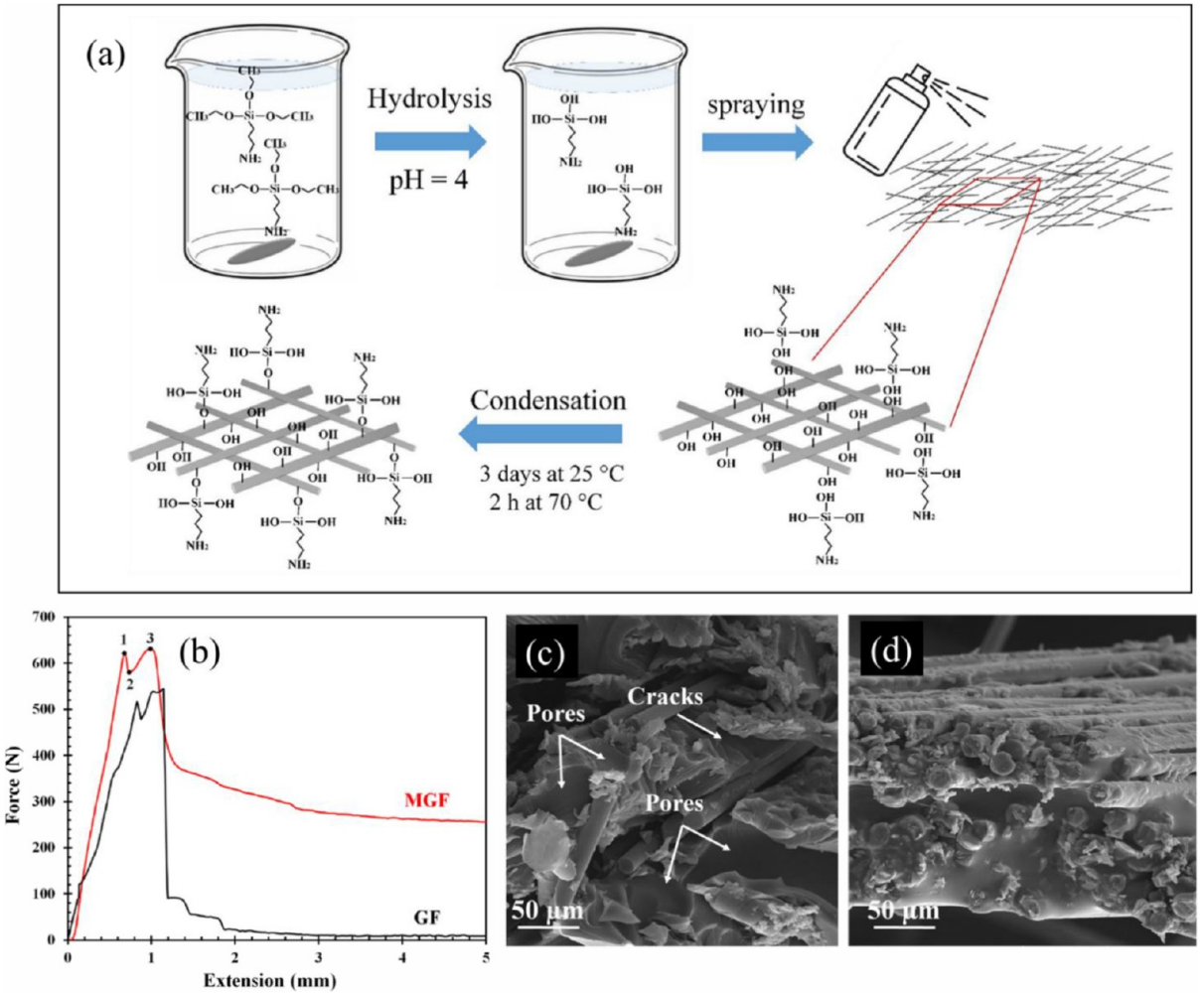

Figure 18. (a) The schematic modification of GFs with APTES. (b) The tensile stress-strain test results of GF and MGF epoxy composites. (c,d) FESEM images of surface fracture of (c) GF and (d) MGF in epoxy composites.[150] Reprinted with permission from ref 150. Copyright 2023 Nature Portfolio.

tively smooth and less damaged, suggesting that the GF separator can inhibit polysulfide diffusion to the lithium anode, leading to better cycling performance.

The thermal shrinkage behavior of GF and Celgard 2400 membranes was evaluated by heating them to 25 °C, 150 °C, and 200 °C for 30 min (Figure 17a). Celgard 2400 wrinkled significantly at 150 °C and melted further at 200 °C. In contrast, no obvious morphology change was seen for GF membrane at 200 °C, indicating excellent battery safety with GF separators. This nonflammable property is crucial for preventing safety hazards during thermal runaway. The wettability of separators significantly affects electrolyte uptake and ion conductivity. Two separators (GF and Celgard 2400) were evaluated using a spreading test (Figure 17b). GF membranes immediately absorbed the electrolyte and laterally diffused it within about 5 s. In contrast, Celgard 2400 maintained its shape and had an inferior contact angle of 55° even after several hours, indicating poor wettability. The fast soaking process prevented capturing the contact angle for GF separator, demonstrating its excellent wettability. In Figure 17c, Celgard 2400 melts and catches fire quickly when exposed to fire due to its combustible polyolefin components. In contrast, GF separator demonstrate excellent flame resistance and no shrinkage when exposed to fire.[141]

Glass fibers have good mechanical properties, providing good support for electrodes and preventing deformation and short circuits in Li-S batteries. Their chemical inertness ensures compatibility with various electrolytes, preventing degradation and enhancing battery longevity. Additionally, glass fibers are cost-effective and readily available, making them suitable for large-scale Li-S battery production; however, it is worth to mention that glass fibers have limitations as battery separators, such as poor retention of soluble polysulfides leading to capacity fading, susceptibility to pore clogging which impedes ion transport, and fragility that complicates handling and manufacturing. Additionally, their limited thickness variations can restrict battery design flexibility. Glass fibers are modified in order to get around these restrictions; this is covered in more detail in the section that follows.

6. MODIFICATION TECHNIQUES FOR GLASS FIBER SEPARATORS

There are numerous studies on the modification of glass fiber membranes used in lithium-oxygen batteries,[142] surface-enhanced Raman scattering (SERS) detection,[143] oil/water separation,[100] biological detection[144] and microfluidics.[145] GF's brittleness and poor wear resistance limit its direct use. To overcome these issues, physical and chemical modification

https://doi.org/10.1021/acsomega.4c07070
ACS Omega 2025, 10, 3228−3261

methods are employed to enhance its compatibility and binding ability with polymer matrices, expanding its application range. GF's main component, amorphous silicon dioxide, forms a highly inert three-dimensional network, necessitating surface functionalization to produce modified GF (MGF).[146−148] Modification techniques can significantly impact the mechanical properties of glass fibers, such as tensile strength, modulus of elasticity, flexibility, and puncture resistance, which are crucial for their use in Li-S battery separators. Enhancements through surface functionalization or coating deposition can improve tensile strength by enhancing adhesion between fibers and polymer binders. Techniques like heat treatment can increase stiffness, resulting in a higher modulus of elasticity. Adjustments to surface morphology can affect flexibility, making fibers more resilient to bending and reducing fracture risks. Reinforcing the surface or bulk properties can enhance puncture resistance, preventing damage and improving durability and safety of the separators. The influence of modified glass fibers on the electrochemical performance and stability of LSBs is crucial for battery efficiency, cycling stability, and lifespan. Modifications can enhance the electrical conductivity of glass fibers, improving electron transfer and overall electrochemical performance. They can also improve polysulfide trapping, reducing capacity fading and enhancing cycling stability. Modifications that enhance ion transport properties facilitate better lithium ion distribution, reducing polarization and improving rate capability. Additionally, surface coatings and reinforcements can increase chemical and long-term stability, prolonging separator lifespan. Ensuring compatibility with electrolyte and electrode materials is essential to prevent performance and safety issues.[149]

6.1. Surface Functionalization. Surface functionalization involves the introduction of functional groups onto the surface of glass fibers to alter their chemical properties and enhance their interaction with electrolyte components and active materials in the battery. This can be achieved through techniques such as silanization,[150] where silane coupling agents are used to graft functional groups (e.g., hydroxyl, amino, or thiol groups) onto the surface of glass fibers, imparting specific chemical functionalities and improving adhesion to polymer binders or active materials. Shariatmadar et al. modified the GF surface using 3-aminopropyl triethoxysilane (APTES) and then used it as a strong fiber-reinforced polymer (FRP) in an epoxy matrix (Figure 18a). Silanization notably improved the mechanical performance of the FRP, as shown by tensile strength measurements and FE-SEM cross-sectional images, which indicated better interfacial bonding between the epoxy matrix and GF. In the tensile strength measurements (Figure 18b), the curves show that plastic deformation comes after elastic deformation. The curves were used to determine the upper yield point (designated as 1 in Figure 18b, red), lower yield point (2), ultimate tensile strength (number 3), and elongation. Comparing the GF specimen to the MGF specimen, lesser elongation and tensile strength were found due to the greater quantity of pores and cracks in GF. For modified glass fiber (MGF), the maximum force recorded was 625 N, while for GF, it was approximately 550 N. The GF curves in the plastic region displayed oscillations. According to the test, the MGF sample had better tensile strength and mechanical behavior than the GF sample. When GF is magnified to a 1000× magnification in SEM images (Figure 18c), it is clear that pores and cracks have formed on its surface (Figure 18c, left). These features may be the first location of fracture and failure. There are no signs of cavities or cracks on the surface of the modified glass fiber (MGF) fracture specimens. This further demonstrated the MGF sample's superior mechanical behavior. After being grafted on MGF, the amino groups of APTES can chemically react with the epoxide groups of epoxy resin to create a matrix that is extremely compatible and prevents the formation of cracks and voids.[150]

Li et al.[151] attempted to selectively separate dyes from binary solutions by modifying glass fiber membranes with APTMS via chemical bonding (Figure 19a). In particular, glass fiber

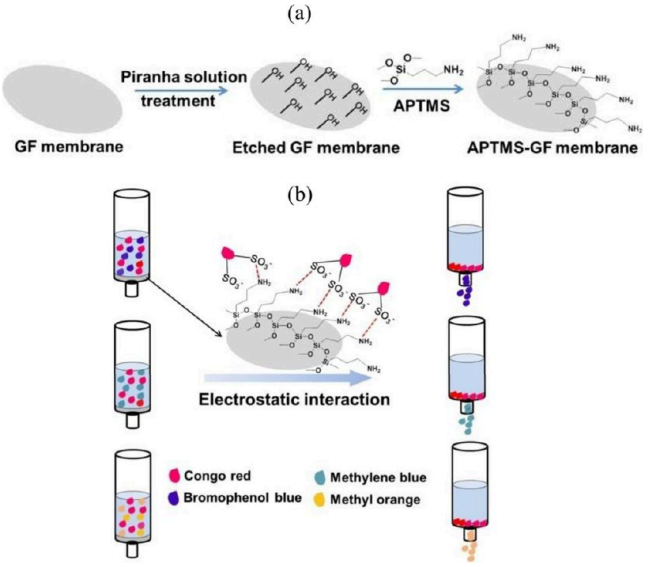

Figure 19. (a) Fabrication of the APTMS-GF composite membrane. (b) Schematic of the proposed separation mechanism on the APTMSGF composite membrane.[151] Reprinted with permission from ref 151. Copyright 2018 Wiley-VCH on behalf of Chemistry Europe.

membranes might have their adsorptive selectivity and adsorptive capacity enhanced after being modified in a single step with common silanes. The abundant amide groups on the membrane surface aim to join with SO_3 groups of dye molecules via electrostatic contact after functionalization with APTMS (Figure 19b).

Surface modification with polymers involves coating or grafting polymer chains onto the surface of glass fibers to modify their properties. Polymer coatings can improve mechanical flexibility, enhance chemical stability, or introduce specific functionalities such as hydrophilicity/hydrophobicity or ion selectivity. Polymer coatings can be applied using techniques such as dip coating, spin coating, or polymerization reactions on the surface of glass fibers. A technique was presented that uses adhesion-promoting coatings to chemically modify the fiber-matrix interface in a reusable manner, hence improving the mechanical properties of glass fiber reinforced thermoplastic polymers. After activation, the reactive intermediates created can insert via insertion processes (Called C-H insertion cross-linking or CHic) into any nearby carbon-hydrogen bond to eventually build a network of cross-linked polymers. In the process, the developing network also connects to nearby organic molecules on the surfaces that need to be changed at the same time. In this manner, the system that promotes adhesion creates a network of polymers that are

https://doi.org/10.1021/acsomega.4c07070
ACS Omega 2025, 10, 3228−3261

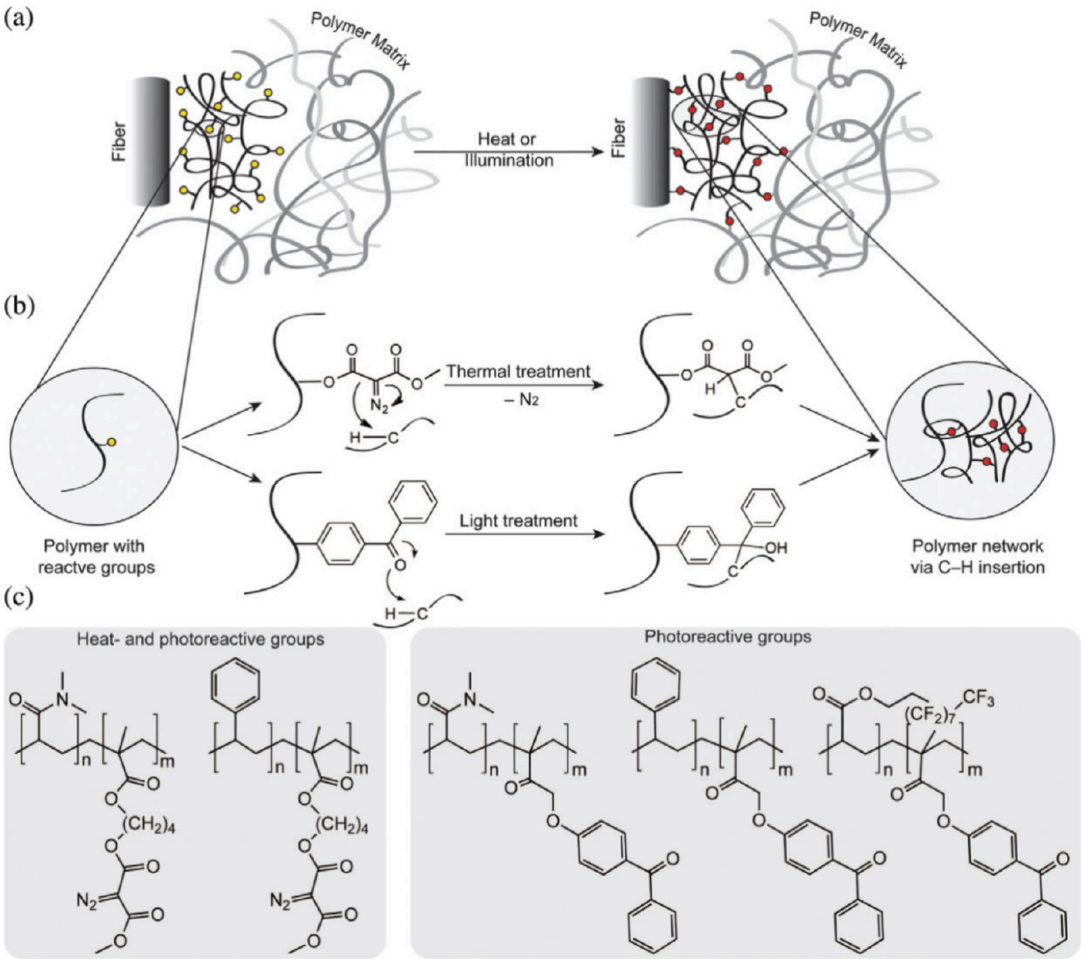

Figure 20. (a) Schematic depiction of the chemical modification of the fiber-matrix interface with adhesion promoter. (b) Illustration of the CHic mechanism due to activation of the cross-linker unit incorporated into the polymer. (c) Polymer systems selected as adhesion promoters containing diazacarbonyl (left) and benzophenone groups (right).[152] Reprinted with permission from ref 152 Copyright 2019 Wiley.

covalently attached to the polymer matrix and fiber surface (Figure 20), guaranteeing the adherence of the two elements. This method's surface reactions work well with a variety of matrix systems.[152]

6.2. Chemical Coating Deposition. These techniques involve the deposition of thin film coatings onto the surface of glass fibers to modify their properties. Various coating materials, such as polymers, metal oxides, or conductive carbon-based materials, can be deposited onto the glass fiber surface using methods such as chemical vapor deposition (CVD), atomic layer deposition (ALD), or solution-based coating techniques. These coatings can improve mechanical strength, enhance chemical stability, facilitate ion transport, or provide active sites for chemical reactions within the battery. The chemical vapor deposition (CVD) technique was employed to coat Li_2O-ZrO_2-BaO-SiO_2 glass fibers with Nb_2O_5, using $NbCl_5$ as a precursor. Different coating methods were tested. The optimal method involved heat treatment and subsequent water hydrolysis, producing a uniform Nb_2O_5 coating without cracks. A homogeneous layer of coating is formed along the longitudinal section of the glass fiber (Figures 21a and 21b).[153]

Carbon films were deposited on silica glass fibers using methane via thermal CVD.[154] The study found that at 950 °C, increasing coating thickness increases disorder in the carbon film, while at a fixed thickness of 1200 nm, increasing the

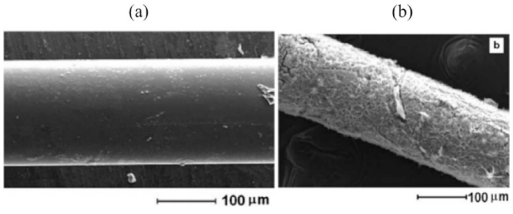

Figure 21. (a) Micrograph of the side view of uncoated glass fiber. (b) Glass fiber heat treated at 300 °C for 2 h, coated with $NbCl_5$ and hydrolyzed for 24 h.[153] Reprinted with permission from ref 153. Copyright 2012 Taylor and Francis.

deposition temperature from 925 to 1025 °C increases order and nanograin size in the film (Figure 22).

Tzounis et al.[155] developed a novel method for creating hierarchical single-wall carbon nanotube-coated glass fibers (GF-CNT) to enable self-sensing structural health monitoring of epoxy laminate composites. The CNT-modified glass fibers were produced using a scalable wet-chemical blade coating process. Figure 23 illustrates the fabrication steps for creating the hierarchical multiscale GF-CNT structure. Scanning Electron Microscopy (SEM) analysis (Figure 23e) confirmed that the glass fibers were uniformly coated with a nanolayer of CNTs. Electrical characterization of the GF-CNT fibers revealed strong orthotropic resistivity, meaning the electrical

https://doi.org/10.1021/acsomega.4c07070
ACS Omega 2025, 10, 3228−3261

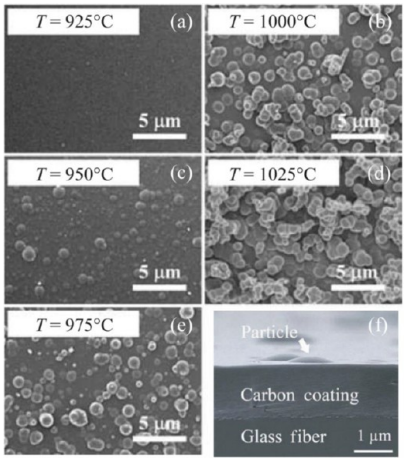

Figure 22. (a–e) FESEM surface morphology of the carbon film deposited on the silica glass fiber with the deposition temperature, *T*, from 925 to 1025 °C, where the coating thickness is about 1200 nm.[154] (f) FESEM photograph of the cross section of the carbon film deposited on silica glass fiber. Reprinted with permission from ref 154. Copyright 2009 Taylor and Francis.

resistance varied with direction. The damage sensing capability of these fibers was validated through mode I Double Cantilever Beam tests, where the electrical resistance increased proportionally to the growth of delamination in the composite. This change in resistance was used to detect and monitor structural damage. The experimental results were in good agreement with a predictive analytical model, confirming the effectiveness of the GF-CNT fibers for real-time damage detection in epoxy laminate composites.

Electrophoretic Deposition (EPD) was utilized to coat glass fibers with graphene nanoplatelets (GNPs) to improve the mechanical properties of fiber-reinforced polymers. GNPs were dispersed in ethanol with Sodium Lauryl Sulfate and then deposited onto the glass fibers using a 100 V DC voltage for 30 min. Since glass fiber is nonconductive and amorphous, it was positioned near the cathode (-ve) to facilitate the deposition of the graphene nanoplatelets. Figure 24 (left) provides a detailed analysis of the deposition process. After deposition, the coated fibers were heated at 60 °C for 60 min in a hot air oven to stabilize the coating. Figure 24 (right) systematically presents the GNP coating process. The quality and presence of the graphene coating were confirmed through Scanning Electron Microscopy (SEM), X-ray Diffraction (XRD), and Raman spectroscopy. Mechanical tests, including tensile, flexural, and interfacial shear stress tests, showed significant improvements in the mechanical properties of the coated fibers. Notably, the interfacial strength increased to 78.42 MPa. These results demonstrate that EPD is an effective method for achieving a homogeneous nanoparticle coating on glass fibers, leading to enhanced mechanical properties of fiber-reinforced polymers.[156]

Glass fibers, commonly used for reinforcing cement-based products, suffer from poor alkali resistance. Wang et al.[157] applied MnO_2-based nanoparticle coatings to alkali-resistant glass fibers (ARGF) using oleic acid and potassium

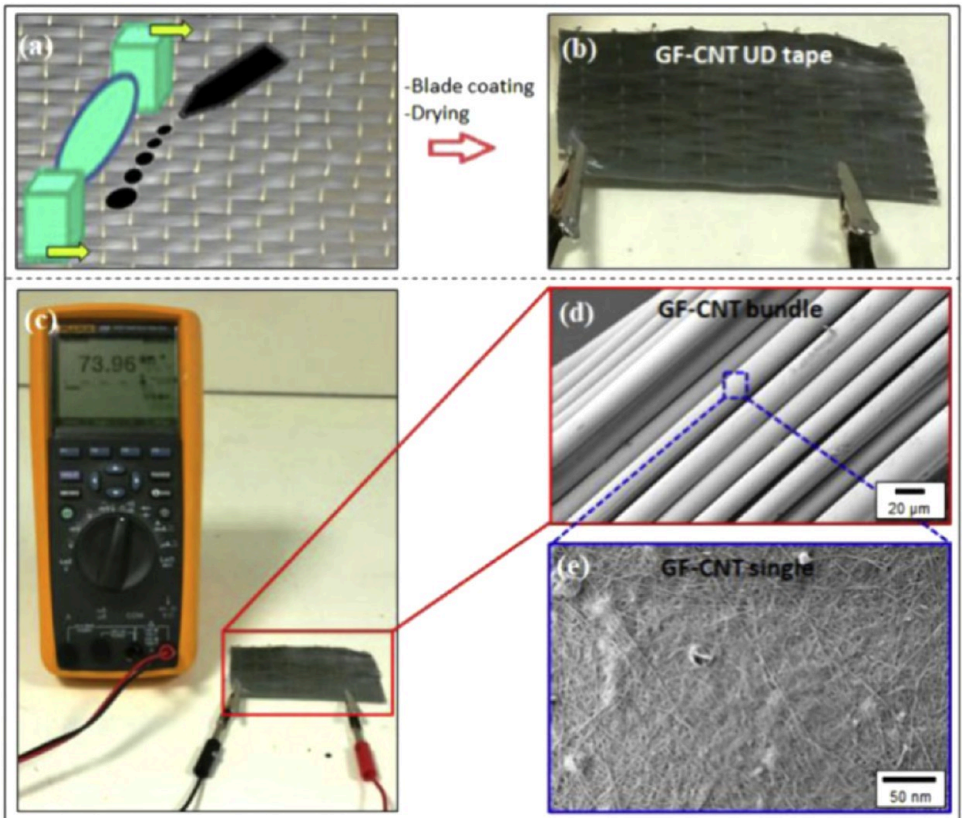

Figure 23. (a) Schematic illustration of the blade coating method followed to fabricate the GF-CNT. (b) Digital photo of the obtained GF-CNT UD tape. (c) Digital photo showing the resistance value of the GF-CNT UD conductive tape measured by a digital multimeter. (d, e) SEM images of GF-CNT bundle at low magnification and single GF-CNT filament at high magnification, showing the SWCNT dense network covering the fiber surface.[155] Reprinted with permission from ref 155. Copyright 2019 Elsevier.

https://doi.org/10.1021/acsomega.4c07070
ACS Omega 2025, 10, 3228−3261

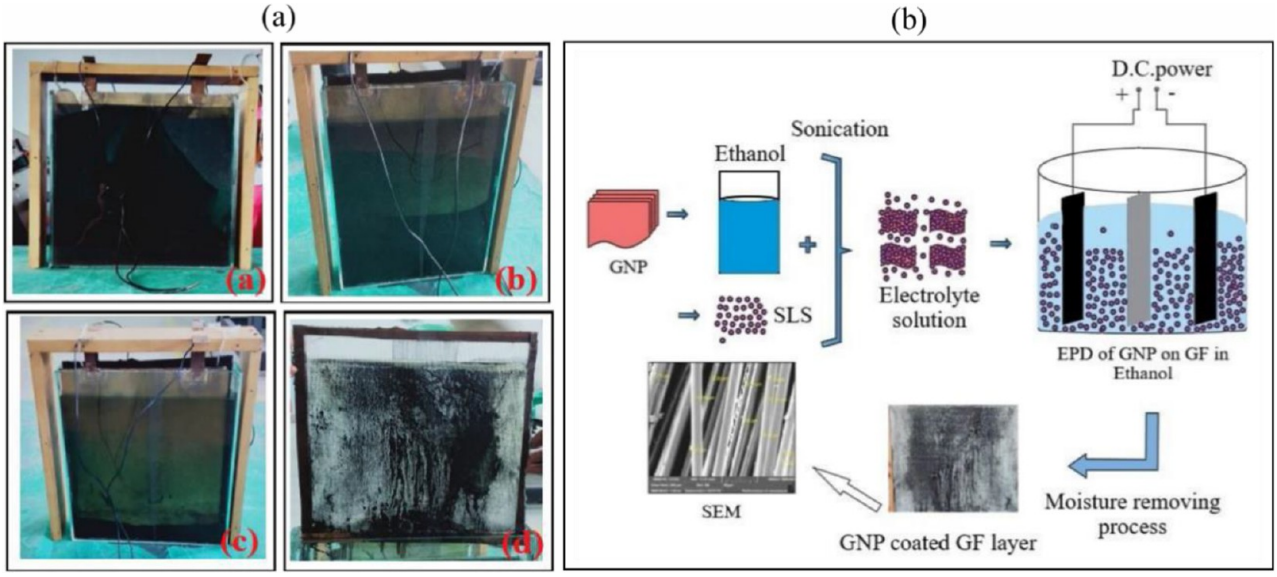

Figure 24. (left) EPD process flow (a) before providing 100 V DC power, (b) 20 min after supply provided, (c) 30 min after supply provided, and (d) after deposition. (right) Schematic representation of the GNP coating through EPD technique.[156] Reprinted with permission from ref 156. Copyright 2021 Elsevier.

permanganate. The surface property of ARGF-Mn is influenced by the duration of surface modification. Using an optimal OA:PP ratio, it was found that increasing the modification time from 12 to 24 h enhanced surface roughness due to nanoparticle formation. However, extending the time to 30 h reduced roughness due to densification of the nanoparticle layer. SEM analysis determined the optimal modification time as 24 h (Figure 25). This approach ensures

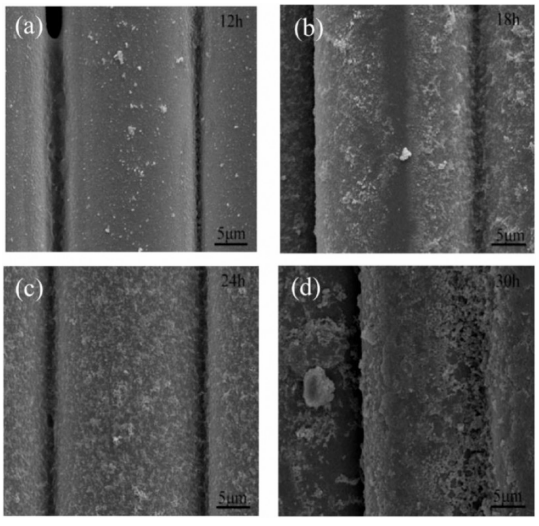

Figure 25. SEM images of alkali-resistant glass fibers modified with OA:PP ratio of 10 for (a) 12, (b) 18, (c) 24, and (d) 30 h, respectively.[157] Reprinted with permission from ref 157. Copyright 2023 MDPI.

a uniform nanoparticle coating on the alkali-resistant glass fibers. This enhancement makes modified ARGFs suitable for broader use in alkaline cement-based applications.

6.3. Vacuum Filtration. Modifying commercial glass fiber separators via vacuum filtration enhances filtration efficiency, increases flow rates, and provides excellent chemical and thermal resistance. These filters offer superior mechanical strength, versatility, better particle retention, cost-effectiveness, minimal clogging, and easy integration into existing systems, making them ideal for a wide range of applications. The modification of commercial glass fiber separators using carbon-derived materials shows significant potential in protecting Zn metal anodes due to their mechanical and electrical properties.[106,158,159] Graphite fluoride nanoflakes (GFNs) are incorporated into commercial glass fiber separators using vacuum filtration to create GFNs-PVDF@GF, enhancing the performance of zinc metal anodes. The strong zinc affinity and high electronegativity of GFNs help to homogenize Zn^{2+} transport and suppress SO_4^{2-} flux, reducing zinc dendrite growth and byproduct formation. The GFNs are vacuum-filtered with PVDF into the glass fiber pores, resulting in a separator with uniform pore size and a flat surface. This configuration optimizes ion transmission and ensures well-distributed Zn^{2+} deposition.[160] To create GFNs-PVDF@GF separators, GFNs are exfoliated from graphite fluoride, resulting in nanoflakes of irregular size and thickness. These nanoflakes are then mixed with PVDF in *N*-methyl-2-pyrrolidone (NMP) and vacuum-filtered into the pores of the glass fibers (Figure 26). This method ensures a homogeneous coating, enhancing the separator's overall performance and longevity. SEM and TEM images show GFNs as nanosheets with a disordered atomic structure, differing from graphite fluoride. XPS confirms F and C elements in GFNs. GFNs fill gaps and adhere uniformly to glass fibers, resulting in separators with uniform pores and flat surfaces. This modification optimizes ion transmission and smooths the glass fiber surface, ensuring even Zn^{2+} deposition.

6.4. Functional Nanoparticle Incorporation. Nanoparticles such as metal oxides (e.g., titanium dioxide, aluminum oxide), conductive carbon materials (e.g., carbon nanotubes, graphene), or redox-active materials (e.g., metal sulfides, metal-organic frameworks) can be dispersed or immobilized[161] onto the surface of glass fibers using techniques such as solution mixing, electrospinning, or in situ growth methods. These nanoparticles can improve mechanical strength, increase surface area, enhance polysulfide adsorption, or provide

https://doi.org/10.1021/acsomega.4c07070
ACS Omega 2025, 10, 3228−3261

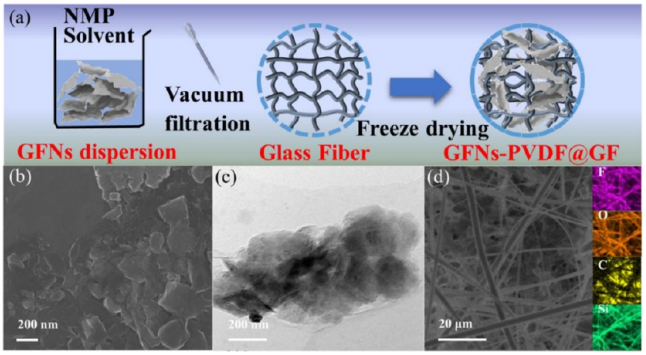

Figure 26. (a) Schematic illustration of the preparation of GFNs-PVDF@GF separator. (b) SEM image and (c) TEM image of GFNs. (d) SEM images of the GFNs-PVDF@GF separator and corresponding elemental mapping.[160] Reprinted with permission from ref 160. Copyright 2023 Elsevier.

catalytic activity for electrochemical reactions, thereby improving battery performance and cycling stability. An analysis was conducted on the applicability of graphene nanoplatelets (GNPs) as a coating on glass fiber textiles for strain monitoring purposes.[162] The impact of functionalization on the coating's morphology and the material's electrical behavior was investigated using both functionalized and nonfunctionalized GNPs. When NH_2-functionalized GNPs were utilized, as opposed to nonfunctionalized GNPs, the nanoparticles adhered to the fiber's surface and significantly increased the efficacy of the electrical network that was formed along the fibers, resulting in an electrical conductivity of about 10^2 S/m. The sensitivity values that were obtained under tensile stresses ranged from around 840 to 16400.

6.5. Spray Method. Huang et al. developed a modified separator aimed at stabilizing aqueous zinc-ion batteries (AZIBs) by directly applying a Ketjen black (KB) conductive carbon layer onto the cathode side of a commercial glass fiber separator.[163] The addition of this conductive carbon layer proved beneficial in their kinetic studies, where it effectively reduced charge transfer resistance and enhanced the diffusion coefficient of H^+ and Zn^{2+} ions within the MnO_2 cathode. These findings underscored the practicality and feasibility of separator modification as a strategy for designing high-energy aqueous zinc-ion secondary batteries. The fabrication process and structure of the KB separator are detailed in Figure 27a. A simple and scalable spray printing method was employed to deposit the KB carbon layer onto the separator. This method facilitated precise control over the thickness of the carbon layer without causing penetration to the opposite side or uneven scraping. Subsequent heat treatment further improved the adhesion of KB to the separator material. Field Emission Scanning Electron Microscopy (FESEM) images (Figure 27b) revealed the commercial glass fiber (GF/A) separator with its characteristic microsized uneven fibers and porous structure. In contrast, the KB separator (Figures 27c and 27d) displayed even distribution of KB carbon particles on the surface fibers and uniformly dispersed pores. These features contribute significantly to enhancing ion transport properties within the battery system. Figure 27e illustrates MnO_2 electrodeposition on carbon paper, with the carbon paper becoming covered in brown MnO_2 postdeposition. FESEM images (Figures 27f–h) reveal that the smooth carbon fibers were fully covered with

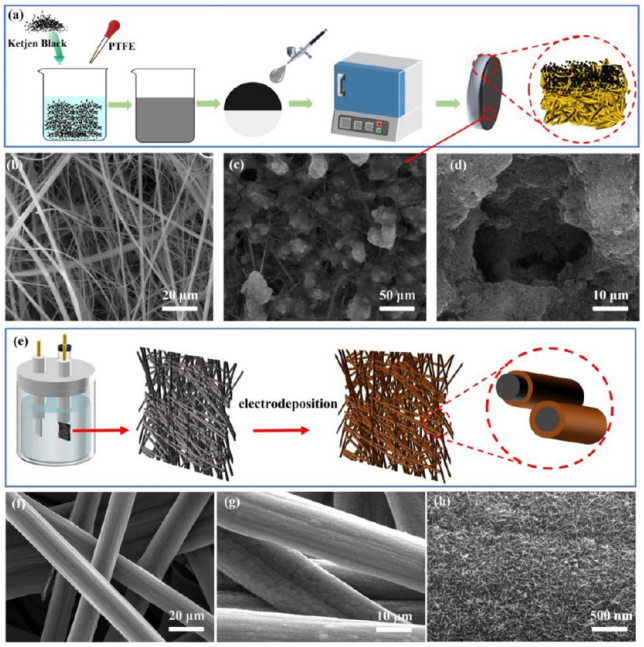

Figure 27. (a) Schematic diagram of the preparation processes and structure of KB separator. (c) FESEM image of the GF/A separator. (c) and (d) FESEM image of the Ketjen black composite glass fiber separator. (e) Schematic illustration of the electrochemical deposition process of MnO_2 on carbon paper. (f) FESEM image of the original carbon paper. (g) and (h) FESEM image of the MnO_2.[163] Reprinted with permission from ref 163. Copyright 2023 Elsevier.

vertically aligned MnO_2 nanosheets, enhancing ion diffusion and increasing the electrode-electrolyte contact area.

6.6. Dip-Coating. Dip-coating involves immersing a substrate (in this case, a glass fiber separator) into a solution (SiO_2 gel nanoparticles in deionized water), then lifting it out and allowing it to dry. This process can be repeated multiple times to ensure adequate coating and penetration of the solution into the substrate.[164] A polyurethane/SiO_2 gel nanoparticles/glass fiber (PU/SiO_2/GF) nanocomposite separator was developed specifically for aprotic Li-O_2 batteries. In this design, the outer polyurethane (PU) coating serves dual functions as an air-impermeable and waterproof barrier, crucial for battery stability. Meanwhile, the SiO_2 gel nanoparticles embedded within the glass fiber (GF) structure act as both a supportive framework and a conductor for Li^+ ions. Comparisons between Li-O_2 batteries using the PU/SiO_2/GF nanocomposite separator and traditional GF separators revealed significant improvements in cycling performance, demonstrating effective prevention of Li corrosion and dendrite formation.[165] The morphological evolution of the GF separator into the PU/SiO_2/GF nanocomposite separator was characterized using Scanning Electron Microscopy (SEM). Initially, the GF separator exhibited large pores (Figure 28a). After immersion in a SiO_2 suspension, these pores became densely packed with SiO_2 gel nanoparticles, filling the void spaces (Figure 28b). Subsequently, coating both sides of the SiO_2/GF structure with PU solution resulted in a smooth, pore-free PU/SiO_2/GF nanocomposite separator (Figure 28c). X-ray Diffraction (XRD) patterns showed changes in the amorphous structure of the separators, indicating the incorporation of SiO_2 nanoparticles and PU coating altered the characteristic peaks (Figure 28d). These structural modifications highlight how the PU/SiO_2/GF nanocomposite

https://doi.org/10.1021/acsomega.4c07070
ACS Omega 2025, 10, 3228−3261

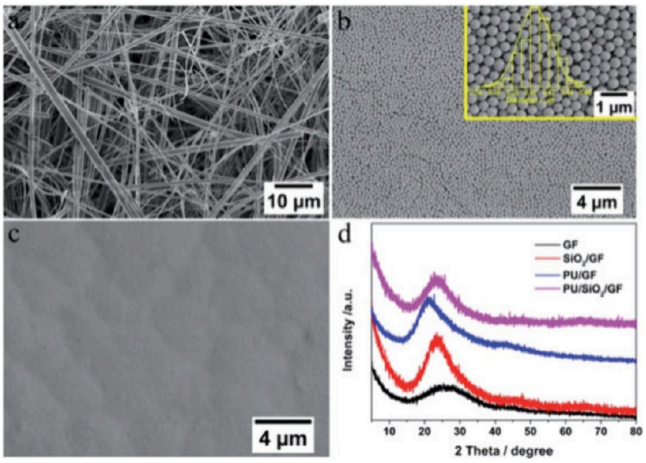

Figure 28. SEM images of (a) the GF, (b) SiO_2/GF, and (c) PU/SiO_2/GF separators, as well as (d) XRD patterns of the GF, SiO_2/GF, PU/GF, and PU/SiO_2/GF separators.[165] Reprinted with permission from ref 165. Copyright 2018 Royal Society of Chemistry.

separator enhances battery performance by improving stability, conductivity, and overall longevity in Li-O_2 battery applications.

The melamine formaldehyde resin (MFR)-coated glass microfiber membrane composite separator (Figure 29a) exhibits enhanced tensile strength, improved porous structure, and impressive thermo-stability without shrinkage at 150 °C. Figures 29b and 29c compare contact angle images and the photographs of liquid electrolyte wettability of separators. As seen in Figure 29d, the Celgard 2400 separator shows a noticeable shrinkage (about 30%) after being stored at 150 °C for 1 h, as well as a color shift from white to transparent; in contrast, the GMF-15 shows no discernible shrinkage following storage at 150 °C. It shows favorable wettability, electrochemical stability, and improved cycling performance in $LiCoO_2$/graphite cells and safety in $LiFePO_4$/Li cells at 120 °C, making it a promising candidate for high-performance lithium-ion batteries.[166]

6.7. Impregnation. The method described for glass fiber modification is known as impregnation. Impregnation involves filling a porous substrate (in this case, a 3D glass fiber cloth) with a solution or mixture (like poly(ethylene oxide), LiTFSI, and ionic liquids) to create a composite material. This method ensures that the glass fiber cloth is evenly distributed within the polymer matrix, forming a robust network structure. Zhang et al. developed solid polymer electrolytes (PEO@GFC-x% ILs) by incorporating poly(ethylene oxide) (PEO), LiTFSI (lithium bis(trifluoromethanesulfonyl)imide), and ionic liquids (ILs) into a 3D glass fiber cloth framework (Figure 30). This innovative structure was designed to enhance several critical properties including thermal stability, mechanical strength, and ionic conductivity. The 3D glass fiber cloth framework provides a robust structural support for the polymer electrolyte, improving its mechanical integrity. The incorporation of PEO and ILs enhances the ionic conductivity of the electrolyte, facilitating efficient ion transport within the battery system. Batteries utilizing this electrolyte configuration demonstrated stable performance and maintained high specific capacities over 100 charge-discharge cycles.[167]

Alkali metal batteries, such as lithium (Li) and sodium (Na) batteries, encounter challenges such as dendrite growth and instability at the solid-electrolyte interphase (SEI). To address these issues, researchers have developed a glass fiber separator infused with polytetrafluoroethylene nanospheres (PTFE-NSs), which effectively regulate the flux of Li^+ and Na^+ ions, ensuring uniform deposition during charging cycles. COMSOL simulations have demonstrated that the negatively charged

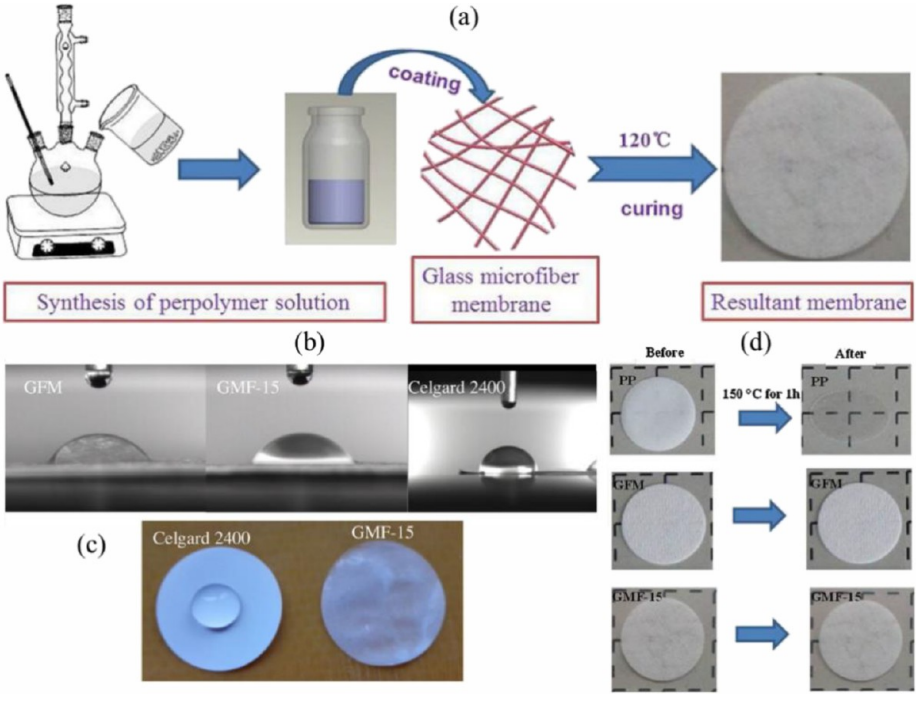

Figure 29. (a) A schematic illustration of composite separator fabrication process. (b) Contact angle images of GFM, GMF-15 and PP separators. (c) The photographs of liquid electrolyte wettability of two different separators. (d) The thermal shrinkage images before and after storing at 150 °C for 1 h.[166] Reprinted with permission from ref 166. Copyright 2015 Elsevier.

https://doi.org/10.1021/acsomega.4c07070
ACS Omega 2025, 10, 3228−3261

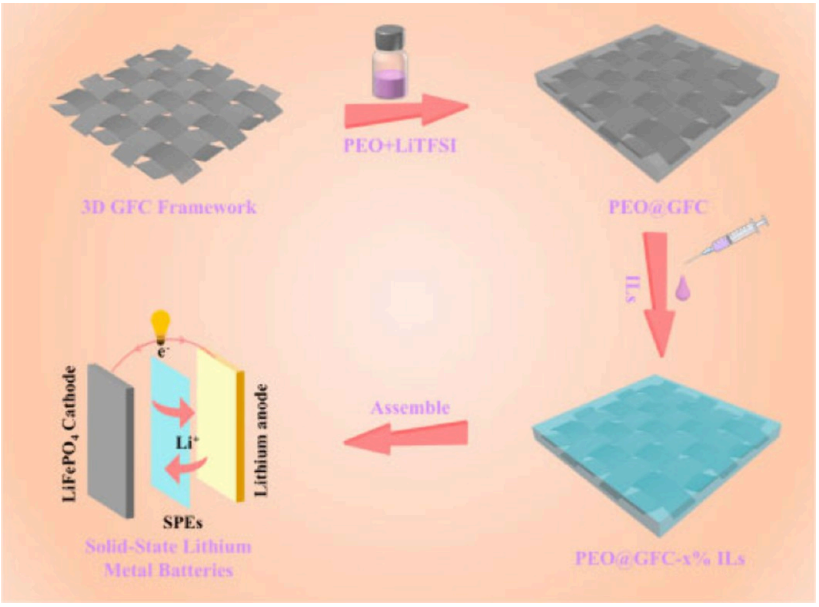

Figure 30. Schematic illustration for preparation of solid polymer electrolytes (SPEs) and solid-state lithium metal batteries (SSLMBs).[167] Reprinted with permission from ref 167. Copyright 2020 Elsevier.

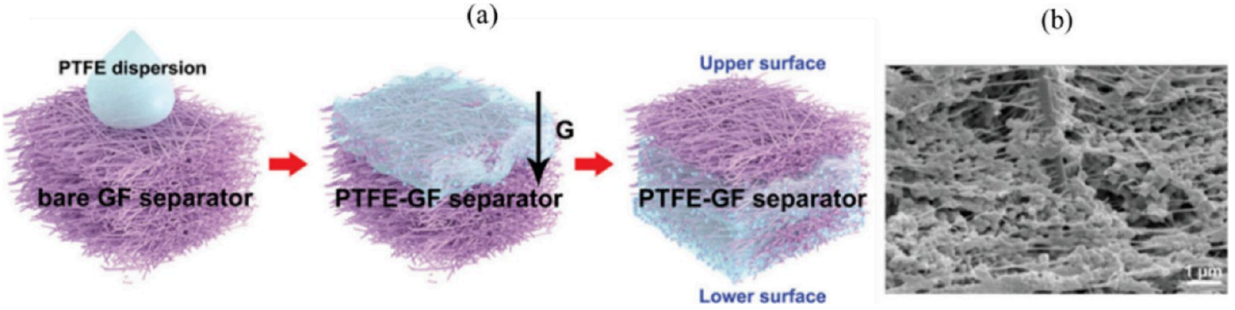

Figure 31. (a) Schematic illustration of the preparation of PTFE-GF separators. (b) High-magnification cross-sectional SEM images of PTFE-GF separators.[158] Reprinted with permission from ref 158. Copyright 2023 Wiley.

PTFE-NSs enhance the local electric field near the anode, thereby facilitating more efficient transfer of cations.[158] Figure 31 illustrates the process of modifying a glass fiber (GF) separator by drop-casting a PTFE suspension onto it. During solvent evaporation, high-density polytetrafluoroethylene nanospheres condense on one side of the separator, forming a layer that plays a crucial role in improving battery performance. This innovative approach not only addresses dendrite formation and SEI stability issues but also enhances the overall efficiency and safety of alkali metal batteries by promoting homogeneous ion transport and deposition.

6.8. In-Situ Polymerization. In-situ polymerization is a method used to modify glass fibers by polymerizing monomers directly within or around the glass fibers. This technique integrates the polymerization process directly with glass fibers, resulting in a composite material with enhanced properties. Specifically, a glass fiber-enhanced PBA gel polymer electrolyte (GF-PBA) was developed, showcasing exceptional thermal and electrochemical stability, rigidity, flexibility, and high ionic conductivity. Through an in situ polymerization method, the GF-PBA electrolyte was incorporated into a half battery configuration, significantly improving the electrolyte-electrode contact. The interaction between the glass fiber and Li^+ ions enhances the dissociation of lithium salts, thereby boosting ionic conductivity and ion transference within the electrolyte.[168] The glass fiber membrane-supported gel polymer electrolyte (GF-GPE) is prepared by immersing the glass fiber membrane in butyl acrylate monomer and subsequently inducing polymerization (Figure 32a). Initially appearing white and fragile, the glass fiber membrane transforms into a flexible and translucent material upon conversion into GF-GPE (Figure 32b). This transformation indicates that the PBA gel polymer has penetrated the pores of the glass fiber membrane, forming an interpenetrating network. Morphological analysis (Figures 32c and 32d) further illustrates that the pores of the glass fiber membrane are completely filled with the gel polymer electrolyte, ensuring a continuous pathway for Li^+ ion transport.

6.9. The Doctor Blade Casting Method. This technique involves preparing slurries containing desired materials (carbon, carbon nanotube, conductive carbon, and polyvinylidene fluoride) in a solvent (like *N*-methyl-2-pyrrolidone (NMP)) and then coating the GF membranes with these slurries using a doctor blade. The process begins with coating separators under vacuum to create carbon-modified GF membrane separators. These separators, enhanced with porous carbon derived from biomass, significantly improve the performance of Li-S batteries. They exhibit higher initial capacity and lower charge transfer resistance compared to uncoated separators, indicating effective inhibition of poly-

https://doi.org/10.1021/acsomega.4c07070
ACS Omega 2025, 10, 3228−3261

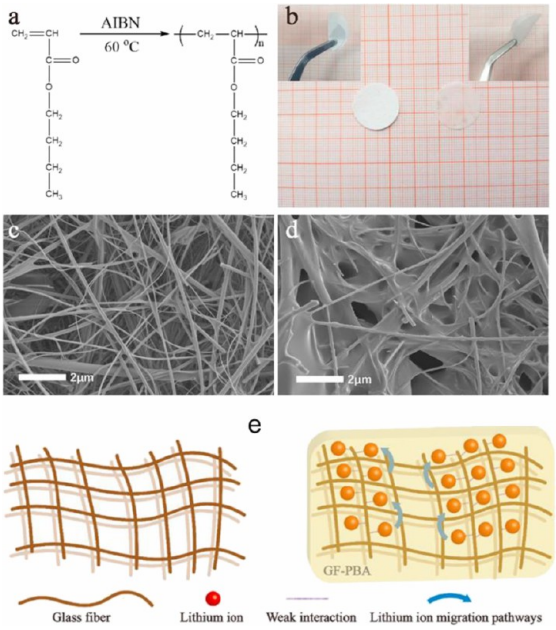

Figure 32. (a) Polymerization mechanism of BA monomers. (b) The digital images of pristine glass fiber membrane and GF-PBA polymer electrolyte. SEM images of (c) pristine glass fiber membrane and (d) GF-PBA. (e) Schematic of lithium ion dissociation and conduction mechanism.[168] Reprinted with permission from ref 168. Copyright 2020 Elsevier.

sulfide shuttling.[169] Figures 33a and 33b depict photographic images of Oak Tree fruit shells, which serve as the biomass source. Figures 33c and 33d show FESEM images of pyrolyzed carbon (PC) and KOH activated porous carbon (AC) samples. PC appears uniform without pores, resembling solid graphitic carbon, while AC displays a rough surface with nanoscale channel-like pores, enhancing surface area and polysulfide capturing capability. Figures 33e and 33f illustrate cross-sectional views of PC and AC coated GF separators. AC coatings exhibit uniform thickness throughout, unlike PC coatings, which may vary due to PC's larger particle size and lack of activation. This structural difference influences the separators' performance in Li-S batteries, highlighting the importance of carbon activation for optimizing polysulfide immobilization and battery efficiency.

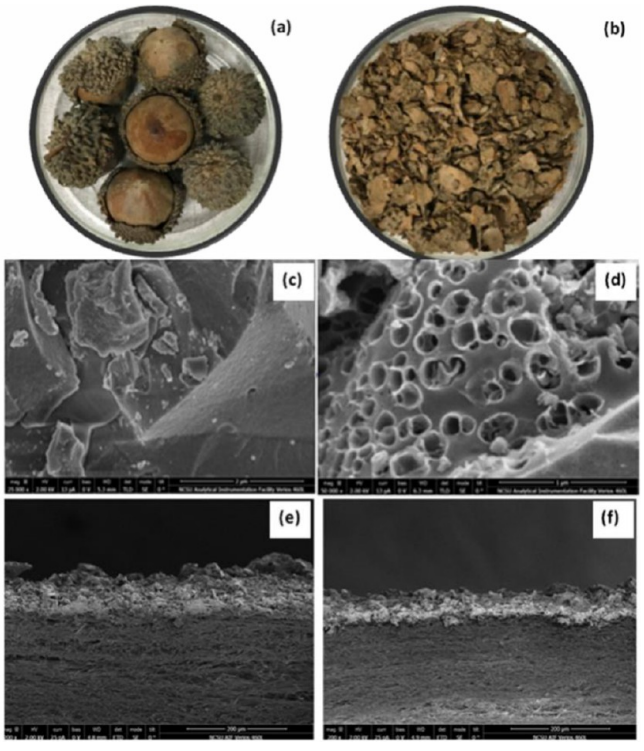

Figure 33. Photographic images of (a) Oak tree fruit cells and (b) crushed fruit cells. FESEM images of (c) pyrolyzed carbon and (d) activated carbon. FESEM images of the cross-sectional view of (e) pyrolyzed carbon and (f) activated carbon coated GF separators.[169] Reprinted with permission from ref 169. Copyright 2017 Elsevier.

The glass platelets are successfully integrated into the glass fiber nonwoven in a single tape-casting step, influenced by the viscosity of the slurry, platelet dimensions, and fiber interspaces.[155] Figure 34a and 34b show the separator and a demonstration of its flexibility. An illustration of the platelet integration process is shown in Figure 34c. Larger platelets than fiber interspaces hinder integration. The process involves three stages: no specific alignment in the slurry, horizontal alignment by the doctor-blade, and pushing into the nonwoven.[159]

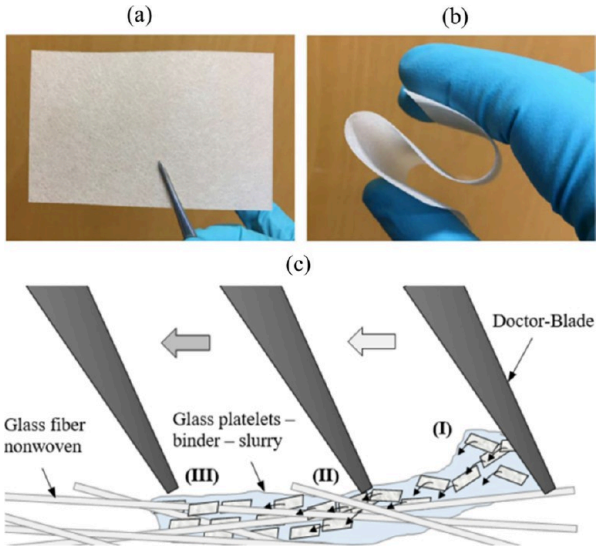

Figure 34. Pictures of a glass fiber nonwoven/glass platelet composite separator: (a) top view; (b) demonstration of the separator's flexibility. (c) Illustration of the integration process of micrometer-sized glass platelets in a glass fiber nonwoven by tape casting.[159] Reprinted with permission from ref 159. Copyright 2018 MDPI.

Although glass fiber separators offer advantages like thermal stability and superior electrolyte wettability, further modifications are crucial to effectively suppress polysulfide shuttling and optimize their performance in Li-S batteries.

7. MODIFIED GF AS SEPARATORS IN LSBS

Modified glass fiber separators reduce shuttle effects in LSBs by acting as effective physical barriers, chemically adsorbing polysulfides, enhancing ionic conductivity, catalytically converting polysulfides, and maintaining structural integrity. These modifications help confine polysulfides to the cathode region, improving battery efficiency and lifespan. Studying polysulfide interactions is essential for understanding the mechanisms underlying polysulfide shuttling and degradation in lithium-

https://doi.org/10.1021/acsomega.4c07070
ACS Omega 2025, 10, 3228−3261

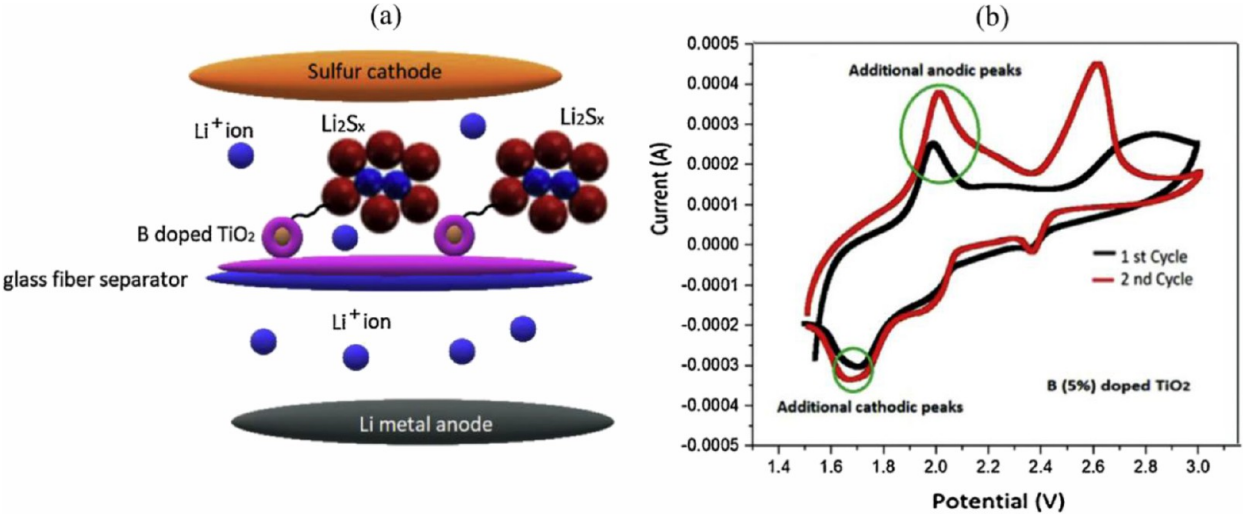

Figure 35. (a) Schematic illustrations of Li-S batteries with B doped TiO_2 coated separator. (b) First two CV curves of the cell with B (5%) doped TiO_2 coating swept at 0.1 mV s^{-1}.[17] Reprinted with permission from ref 17. Copyright 2020 Elsevier.

sulfur (Li-S) batteries. Various analytical techniques are employed to investigate the adsorption, diffusion, transformation, and reactivity of polysulfide species within the battery system. These techniques provide valuable insights into the factors influencing polysulfide behavior and guide the development of strategies to mitigate polysulfide-related issues. CV analysis reveals the electrochemical activity and redox potentials of polysulfide species during charge/discharge cycles. Eroglu et al.[17] introduced a simple method to address the shuttle effect and capacity degradation in lithium-sulfur (Li-S) batteries using B-doped TiO_2 nanopowder-coated separators. The incorporation of boron (B) dopant into the TiO_2 structure enhances chemisorption with polysulfide species, crucial for mitigating capacity fading (Figure 35a). In CV curves (Figure 35b), two cathodic peaks indicate the formation of long-chain lithium polysulfide (Li_2S_n, $4 < n < 8$) and short-chain lithium sulfide (Li_2S_2 or Li_2S), with additional peaks suggesting gradual electrochemical activation of the separator over cycles. Anodic peaks observed around 2.60 V indicate the conversion of insoluble lithium sulfides into soluble polysulfides and elemental sulfur (S8). This suggests a chemical transformation where lithium ions react with sulfides to form higher-order polysulfides, which are soluble and can shuttle within the battery system. Additionally, peaks appearing at 1.69 V correspond to the process of lithium ions deintercalating from titanium dioxide (TiO_2). This voltage range signifies the removal of lithium ions from the crystal lattice of TiO_2, allowing them to migrate out into the electrolyte. Conversely, peaks observed at 1.93 and 2 V indicate the reverse process, where lithium ions are intercalated back into TiO_2. This phase involves the insertion of lithium ions into the crystal structure of TiO_2, effectively storing energy within the material. The discrete reduction and oxidation peaks that corresponded to the insertion and extraction reactions of lithium ions into the TiO_2 are described by the reactions[170−172] as follows:

$$TiO_2 + xLi^+ + xe^- \leftrightarrow Li_xTiO_2 \quad (1)$$

$$TiO_2 + Li_2S_n \leftrightarrow Li_2S_nTiO_2 \quad (2 \le n \le 8) \quad (2)$$

The sharper and higher current peaks in later cycles suggest increased surface area for lithium ion insertion/extraction, enhancing the trapping of lithium polysulfides.

Ponnada et al.[173] introduced flexible glass fiber separators coated with Cu/MOF and Fe/MOF through a solvothermal method, aiming to address challenges in lithium-sulfur (Li-S) batteries. These coatings utilize Lewis acid-base interactions to effectively anchor polysulfides and mitigate polysulfide crossover. In their study, cyclic voltammetry (CV) of Li-S cells equipped with these modified separators illustrates distinct redox peak intensities (Figure 36). The CV analysis reveals

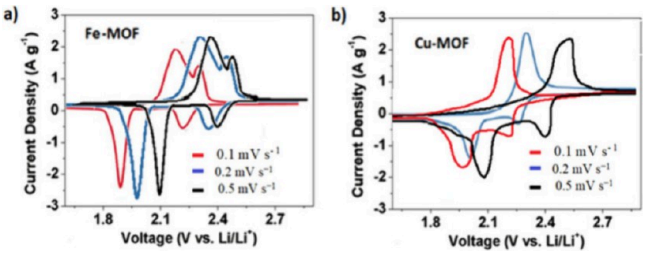

Figure 36. CV curves of the cell with (a) Fe/MOF coatings and (b) Cu/MOF swept at different scan rates.[173] Reprinted with permission from ref 173. Copyright 2023 Elsevier.

that cells employing Fe/MOF-coated separators exhibit higher peak intensities compared to Cu/MOF-coated ones, indicating faster reaction rates facilitated by the efficiency of iron dopants in the MOF structure. Anodic peaks observed around 2.42 and 2.37 V signify the transformation of insoluble lithium sulfides into soluble polysulfides, with broader peaks observed for both Cu/MOF and Fe/MOF coatings. Cathodic peaks appearing at 2.40 and 2.35 V indicate the conversion of polysulfides into long-chain lithium polysulfides, with further reduction to Li_2S_2 and Li_2S occurring at 2.19 and 2.12 V, respectively. Fe/MOF-coated separators demonstrate more positive reduction and negative oxidation peaks across different scan rates compared to Cu/MOF, highlighting their superior redox kinetics. The reversible electrochemical processes observed in the CV curves indicate robust performance of the Fe/MOF-coated separators, characterized by distinct and well-defined redox peaks, which

https://doi.org/10.1021/acsomega.4c07070
ACS Omega 2025, 10, 3228−3261

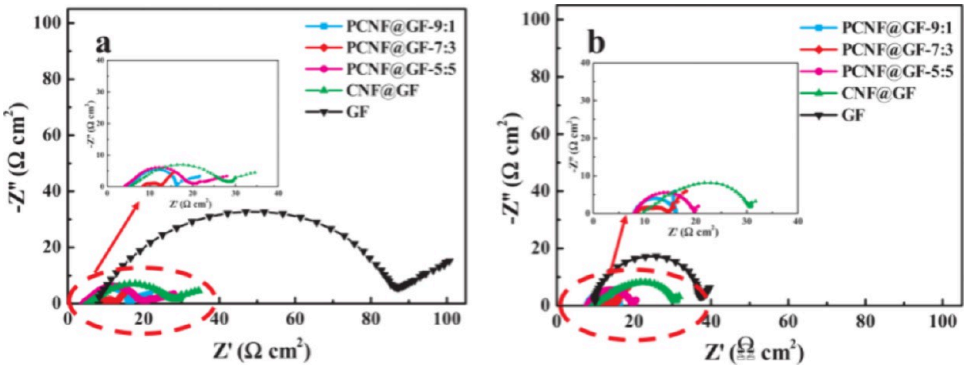

Figure 37. Electrochemical impedance spectra (EIS) of the cells with GF, CNF@GF, PCNGF@GF-9:1, PCNGF@GF-7:3, and PCNGF@GF-5:5 (a) before and (b) after 200 cycles at the rate of 0.2 C.[174] Reprinted with permission from ref 174. Copyright 2018 Elsevier.

are crucial for enhancing the efficiency and stability of Li-S battery systems.

Carbonized nanofibers were produced by first electrospinning polymer solutions containing PAN, PAN/PMMA in varying ratios, followed by thermal treatment. These nanofibers were subsequently coated onto glass fiber (GF) separators.[174] The electrochemical impedance spectroscopy (EIS) spectrum (Figure 37) obtained from batteries using these modified separators reveals distinct features: (1) A sloping line observed at lower frequencies indicates the diffusion characteristics of lithium ions within the electrode material. This slope reflects how readily lithium ions move through the electrode structure, influenced by factors such as pore size and connectivity within the carbonized nanofiber-coated separator; (2) A semicircle appearing in the high frequency zone represents the charge transfer resistance at the electrode-electrolyte interface. This resistance arises from the transfer of electrons during the electrochemical reactions involved in battery operation.[175,176] The presence of these two characteristic features in the EIS spectrum indicates that the carbonized nanofiber-coated GF separators effectively influence both lithium ion diffusion and charge transfer processes in the battery. This modification strategy aims to enhance the overall performance and efficiency of lithium-ion batteries by optimizing ion transport and reducing internal resistance. The diameter of the semicircle shows the buildup of unchecked polysulfides and symbolizes the charge transfer resistance (R_{ct}). Electrochemical impedance spectra (EIS) analysis shows that the PCNF@GF cells have lower charge transfer resistance (R_{ct}) compared to CNF@GF and GF separator cells, due to their porous nanofiber structure. Before cycling, PCNF@GF cells exhibit smaller R_{ct} values, which decrease further after cycling due to chemical activation and improved wetting between the electrode and electrolyte. The PCNF@GF-7:3 cell maintains stable R_{ct} values even after 200 cycles, indicating efficient polysulfide management and enhanced charge and Li ion transport.

The UiO-67-GF separator is a novel composite designed to address critical challenges in LSBs, specifically the issues of LiPS shuttle and lithium dendrite formation. This separator combines Ce-UiO-67, a MOF, with a glass fiber (GF) membrane (Figure 38(a–f)). The Ce-UiO-67 crystals are uniformly dispersed throughout the GF membrane, featuring a regular octahedral structure with large pores and a three-dimensional network. The unique porous architecture of Ce-UiO-67, coupled with its catalytic metal centers, enhances the separator's capability to immobilize LiPS species and suppress dendrite growth. This structural feature is crucial for improving the overall performance and stability of Li-S batteries. The composite separator, approximately 520 μm thick, exhibits even distribution of Ce, O, and C elements, confirming successful integration of the MOF crystals into the GF matrix.[177] Figure 38(g,h) illustrates the Li stripping/plating behaviors with GF and UiO-67-GF separators. The original GF separator, with its large pores, allows free Li ion transport, leading to nonuniform Li deposition and dendrite growth, resulting in low efficiency and poor cycling performance. In contrast, the UiO-67-GF separator, with its MOF grains and O-containing groups, ensures fast and uniform Li diffusion and deposition, effectively inhibiting dendrites and stabilizing Li plating/stripping performance.

Li et al.[178] developed a novel composite separator for lithium-sulfur (Li-S) batteries using Ti_3C_2[179] nanosheets coated on a glass fiber (GF) membrane. This separator was fabricated through a vacuum filtration process.

The conductive Ti_3C_2 nanosheet serves as a strong LiPS reservoir, while the commercial GF membrane is used as the separator due to its high porosity and electrolyte uptake (Figure 39, top). Using an H-type glass cell, the diffusion of LiPSs was directly observed. When using a pure GF separator, Li_2S_7 diffused from the left to the right chamber within 4 h, turning the right chamber yellow. However, with a Ti_3C_2 nanosheet-covered GF separator, the right chamber remained colorless for 24 h, indicating significantly less diffusion of Li_2S_7 (Figure 39, middle). UV-visible spectroscopy is a widely used technique for quantifying the concentration of soluble polysulfide species in the electrolyte. By measuring the absorbance of light at specific wavelengths, UV-visible spectroscopy can detect polysulfides (e.g., Li_2S_x) formed during battery operation. Changes in absorbance over time provide information about polysulfide dissolution, diffusion, and reactivity in Li-S batteries. UV-vis absorption spectra showed that with a Ti_3C_2 nanosheet-covered GF separator, only 10.9% of Li_2S_7 diffused to the right chamber after 24 h, compared to 86.5% with a pure GF separator. This demonstrates that the Ti_3C_2 nanosheet effectively suppresses LiPS diffusion, enhancing sulfur utilization (Figure 39, bottom).

By applying a carbon coating to the glass fiber separator (CGF), Zhu et al. were able to achieve a high capacity, extended cycle life, and rapid charge rate. Among the greatest findings to far are the exceptional cycling performance with a high capacity of 956 $mAhg^{-1}$ after 200 cycles and the superb high-rate responsiveness up to 4 C that were attained (Figure 40).[180]

https://doi.org/10.1021/acsomega.4c07070
ACS Omega 2025, 10, 3228−3261

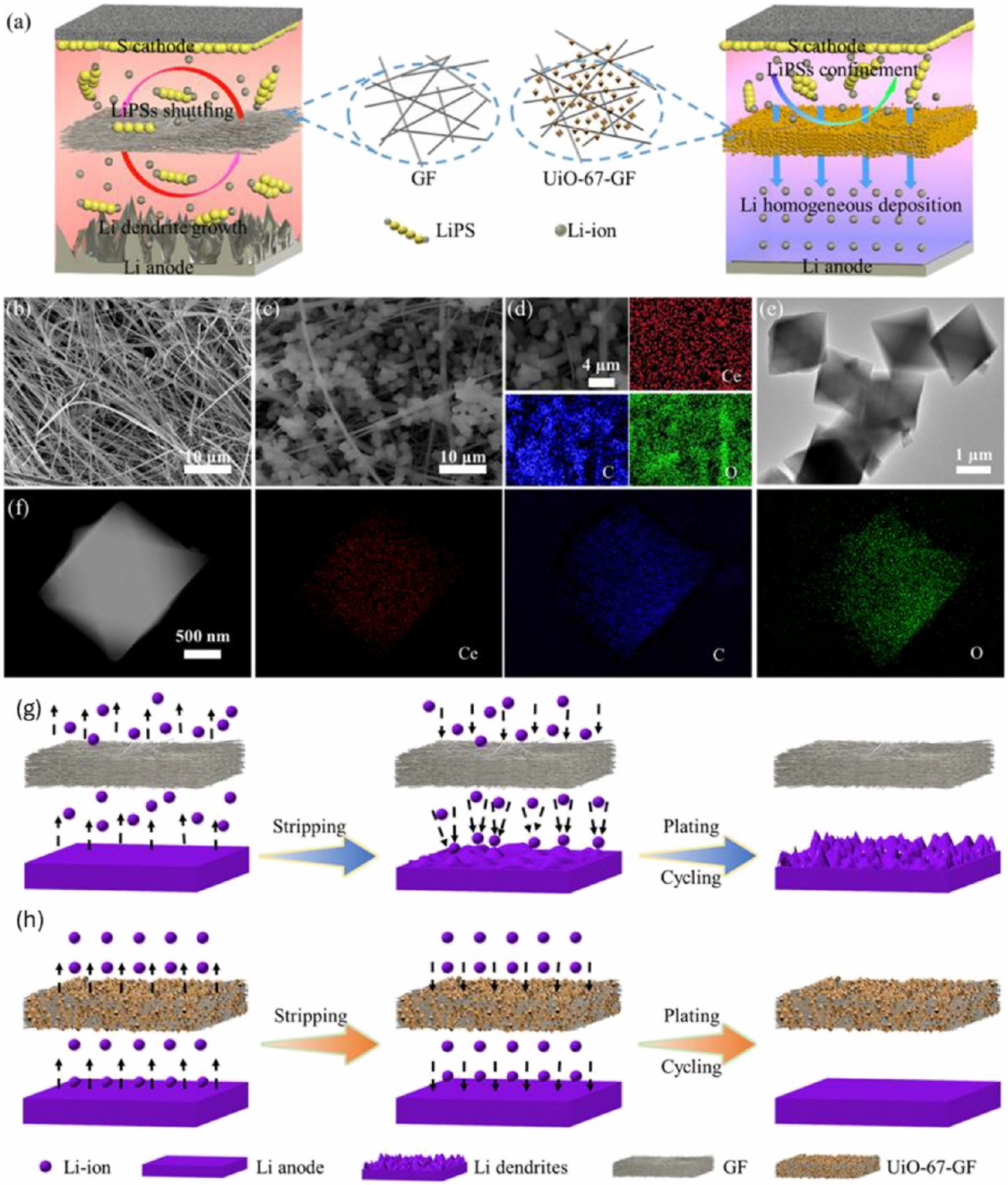

Figure 38. (a) Schematic representation of the synthetic strategy for the UiO-67-GF separator. SEM images of (b) GF and (c) UiO-67-GF separator. (d) Elemental mappings of UiO-67-GF. (e) TEM image and (f) elemental mappings of Ce-UiO-67 crystals. (g,h) Schematic illustrations of the electrochemical behaviors of Li anodes with (g) GF and (h) UiO-67-GF separators.[177] Reprinted with permission from ref 177. Copyright 2022 Elsevier.

Table 2 presents a comparison of the capacity decay rates per cycle for various modified glass fiber (GF) separators. This detailed analysis highlights the performance and stability differences among the modified GF separators. By evaluating the capacity decay rates, the table provides insights into the effectiveness of each modification in enhancing the longevity and efficiency of lithium-sulfur batteries.

8. SUMMARY AND OUTLOOK

Lithium-sulfur (Li-S) batteries hold immense potential for next-generation energy storage due to their high theoretical capacity and energy density. However, challenges such as polysulfide shuttling and slow reaction kinetics continue to hinder their practical application. GF separators have emerged as promising candidates due to their superior thermal stability, electrolyte wettability, and potential for functional modification. This review has highlighted recent advancements in leveraging GF separators to address the issues associated with Li-S batteries. Modification strategies, such as applying functional coatings and integrating advanced materials, have significantly improved the electrochemical performance of Li-S batteries by reducing polysulfide migration and enhancing cycling stability. These innovations demonstrate that modifying GF separators, without complicating sulfur cathode

https://doi.org/10.1021/acsomega.4c07070
ACS Omega 2025, 10, 3228−3261

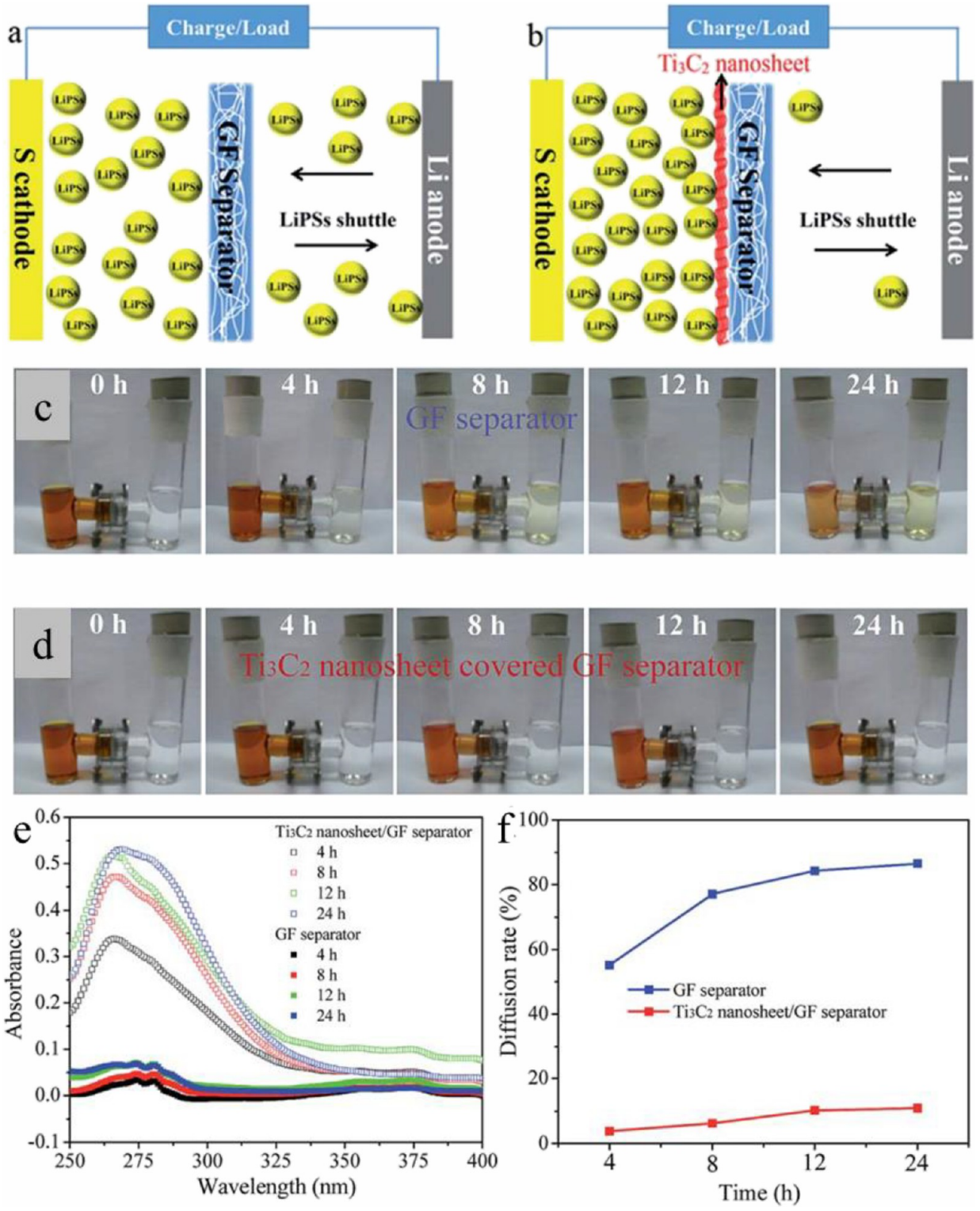

Figure 39. (a,b) Schematic of the electrode configuration using the GF membrane as the separator: (a) without and (b) with a few-layered Ti_3C_2 nanosheet. (c,d) Optical images of the diffusion of Li_2S_7: (c) H-type cell with the GF separator; (d) H-type cell with the Ti_3C_2 nanosheet covered GF composite separator. (e) Time-dependent UV-vis absorption spectra of Li_2S_7/THF in the right chamber of the H-type cell equipped with the GF separator and Ti_3C_2 nanosheet covered GF composite separator. (f) The corresponding diffusion rates calculated based on the time dependent UV-vis absorption spectra.[178] Reprinted with permission from ref 178. Copyright 2016 The Royal Society of Chemistry.

fabrication, offers a simple and effective solution to the persistent challenges in Li-S battery technology.

Looking ahead, further advancements in multifunctional GF separator technologies will be crucial to ensure their essential role in advancing Li-S batteries toward commercial viability. Future research should focus on optimizing key separator properties such as thickness, mechanical strength, porosity, surface area, and catalytic activity by developing novel

https://doi.org/10.1021/acsomega.4c07070
ACS Omega 2025, 10, 3228−3261

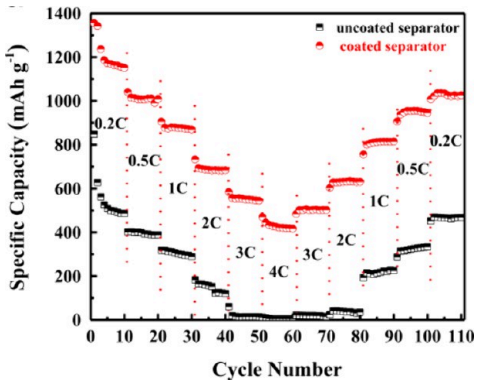

Figure 40. (a) Rate cyclability of Li-S cells with pristine GF (PGF) and carbon coated glass fiber (CGF) up to 4 C.[180] Reprinted with permission from ref 180. Copyright 2016 Elsevier.

Table 2. Comparison of the Capacity Decay Rate (per Cycle) of the Modified GF Separators

GF Modification	Thickness (mm) of Layer on GF	Decay per Cycle (%)
Bare GF[181]	260[a]	0.27
UiO-67[90]	19	0.04
Cu-MOF[16]	18	0.08
Fe-MOF[16]	22	0.06
Ketjen Black and mesoporous TiO_2 (KB/MTiO$_2$)[182]	10	0.11
B doped TiO_2[17]	46	0.11
Ti_3C_2[183]		0.13
Activated porous carbon on glass fiber (ACGF)[169]		0.25
Porous carbon nanofibers (PCFN)[174]	25	0.31

[a]No layer on GF.

materials and scalable production methods. These efforts will be pivotal in bridging the gap between laboratory-scale innovations and commercial applications, ultimately unlocking the full potential of Li-S batteries for energy storage.

AUTHOR INFORMATION

Corresponding Authors

Razieh Fazaeli − *Department of Chemical Engineering, Waterloo Institute for Nanotechnology (WIN), Waterloo, ON N2L 3G1, Canada; Department of Chemistry, Shahreza Branch, Islamic Azad University, Shahreza 86145-311, Iran;* orcid.org/0000-0003-3452-0066; Email: raziehfazaeli@yahoo.com, fazaeli@iaush.ac.ir

Yuning Li − *Department of Chemical Engineering, Waterloo Institute for Nanotechnology (WIN), Waterloo, ON N2L 3G1, Canada;* orcid.org/0000-0003-3679-8133; Email: Yuning.li@uwaterloo.ca

Authors

Hamid Aliyan − *Department of Chemistry, Shahreza Branch, Islamic Azad University, Shahreza 86145-311, Iran*

Zhe Huang − *Department of Chemical Engineering, Waterloo Institute for Nanotechnology (WIN), Waterloo, ON N2L 3G1, Canada*

Yonglin Wang − *Department of Chemical Engineering, Waterloo Institute for Nanotechnology (WIN), Waterloo, ON N2L 3G1, Canada*

Complete contact information is available at: https://pubs.acs.org/10.1021/acsomega.4c07070

Notes

The authors declare no competing financial interest.

ACKNOWLEDGMENTS

The authors thank the Natural Sciences and Engineering Research Council of Canada (NSERC) for the financial support provided through the Discovery Grants (RGPIN-2022-03835) and Alliance Grants (ALLRP 581429-23).

REFERENCES

(1) Rosenman, A.; Markevich, E.; Salitra, G.; Aurbach, D.; Garsuch, A.; Chesneau, F. F. Review on Li-Sulfur Battery Systems: an Integral Perspective. *Adv. Energy Mater.* **2015**, *5*, No. 1500212.

(2) Manthiram, A.; Fu, Y.; Chung, S.-H.; Zu, C.; Su, Y.-S. Rechargeable Lithium−Sulfur Batteries. *Chem. Rev.* **2014**, *114* (23), 11751−11787.

(3) Zheng, S.; Khan, N.; Worku, B. E.; Wang, B. Review and prospect on low-temperature lithium-sulfur battery. *Chem. Eng. J.* **2024**, *484*, No. 149610.

(4) Feng, S.; Fu, Z.-H.; Chen, X.; Zhang, Q. A review on theoretical models for lithium−sulfur battery cathodes. *InfoMat* **2022**, *4* (3), No. e12304.

(5) Jang, J.; Oh, J.; Jeong, H.; Kang, W.; Jo, C. A Review of Functional Separators for Lithium Metal Battery Applications. *Materials* **2020**, *13* (20), 4625.

(6) Huang, Z.; Gao, X.; Wang, Y.; Li, Y. Mitigating first charge overpotential of Li2S-based lithium-sulfur batteries by leveraging PVDF reaction with the LiOH/Li2O layer. *J. Power Sources* **2023**, *582*, No. 233530.

(7) Fazaeli, R.; Yan, L.; Li, Y. 3D hierarchical nanosheet Ni−Fe/CFP as a novel cathode for lithium−sulfur batteries. *J. Iran. Chem. Soc.* **2020**, *17* (3), 545−553.

(8) Wen, C.; Zheng, X.; Li, X.; Yuan, M.; Li, H.; Sun, G. Rational design of 3D hierarchical MXene@AlF3/Ni(OH)2 nanohybrid for high-performance lithium-sulfur batteries. *Chem. Eng. J.* **2021**, *409*, No. 128102.

(9) Zhang, Z.; Kong, L.-L.; Liu, S.; Li, G.-R.; Gao, X.-P. A High-Efficiency Sulfur/Carbon Composite Based on 3D Graphene Nanosheet@Carbon Nanotube Matrix as Cathode for Lithium−Sulfur Battery. *Adv. Energy Mater.* **2017**, *7* (11), No. 1602543.

(10) Bhauriyal, P.; Heine, T. Catalysing the performance of Li−sulfur batteries with two-dimensional conductive metal organic frameworks. *J. Mater. Chem. A* **2022**, *10* (23), 12400−12408.

(11) Yan, L.; Gao, X.; Wahid-Pedro, F.; Quinn, J. T. E.; Meng, Y.; Li, Y. A novel epoxy resin-based cathode binder for low cost, long cycling life, and high-energy lithium−sulfur batteries. *J. Mater. Chem. A* **2018**, *6* (29), 14315−14323.

(12) Ma, Z.; Zuo, Z.; Li, Y. Zinc Complex-Based Multifunctional Reactive Lithium Polysulfide Trapper Approaching Its Theoretical Efficiency. *ACS Appl. Mater. Interfaces* **2021**, *13* (20), 23936−23944.

(13) Ma, Z.; et al. Lithiated carboxylated nitrile butadiene rubber with strong polysulfide immobilization ability as a binder for improving lithium-sulfur battery performance. *J. Power Sources* **2022**, *542*, No. 231771.

(14) Gao, Z.; et al. Promises, Challenges, and Recent Progress of Inorganic Solid-State Electrolytes for All-Solid-State Lithium Batteries. *Adv. Mater.* **2018**, *30* (17), No. 1705702.

(15) Watanabe, H.; et al. Discharge Behavior within Lithium−Sulfur Batteries Using Li−Glyme Solvate Ionic Liquids. *J. Phys. Chem. C* **2023**, *127* (14), 6645−6654.

(16) Yuan, C.; et al. Boosting the Rate Performance of Li−S Batteries via Highly Dispersed Cobalt Nanoparticles Embedded into Nitrogen-Doped Hierarchical Porous Carbon. *CCS Chem.* **2022**, *4* (8), 2829−2841.

https://doi.org/10.1021/acsomega.4c07070
ACS Omega 2025, 10, 3228−3261

(17) Eroglu, O.; Kiai, M. S.; Kizil, H. Glass fiber separator coated by boron doped anatase TiO2 for high-rate Li−S battery. *Mater. Res. Bull.* **2020**, *129*, No. 110917.
(18) Lee, H.; Yanilmaz, M.; Toprakci, O.; Fu, K.; Zhang, X. A review of recent developments in membrane separators for rechargeable lithium-ion batteries. *Energy Environ. Sci.* **2014**, *7* (12), 3857−3886.
(19) Zhu, Y.; Xiao, S.; Shi, Y.; Yang, Y.; Hou, Y.; Wu, Y. A Composite Gel Polymer Electrolyte with High Performance Based on Poly(Vinylidene Fluoride) and Polyborate for Lithium Ion Batteries. *Adv. Energy Mater.* **2014**, *4* (1), No. 1300647.
(20) "Membranes | Free Full-Text | Membranes in Lithium Ion Batteries". Accessed: July 23, 2024. [Online]. Available: https://www.mdpi.com/2077-0375/2/3/367.
(21) Boaretto, N.; et al. Lithium solid-state batteries: State-of-the-art and challenges for materials, interfaces and processing. *J. Power Sources* **2021**, *502*, No. 229919.
(22) Song, S. W.; et al. Hierarchically porous hydrogel electrolyte prepared from interpenetrating polymer networks for flexible Zn-Air batteries. *Energy Storage Mater.* **2023**, *60*, No. 102802.
(23) "Thick Electrode Design for Facile Electron and Ion Transport: Architectures, Advanced Characterization, and Modeling | Accounts of Materials Research". Accessed: September 21, 2024. [Online]. Available: https://pubs.acs.org/doi/10.1021/accountsmr.1c00281.
(24) Joardder, M. U. H.; Kumar, C.; Brown, R. J.; Karim, M. A. A micro-level investigation of the solid displacement method for porosity determination of dried food. *J. Food Eng.* **2015**, *166*, 156−164.
(25) Park, S.; Kang, M.-C.; Oinam, Y.; Amoozegar, A.; Pyo, S. Measurement of skeletal density and porosity of construction materials using a new proposed vacuum pycnometer. *Measurement* **2022**, *196*, No. 111209.
(26) Kato, Y.; et al. Porosity and size analysis of porous microparticles by centrifugal sedimentation with and without density gradient. *Powder Technol.* **2022**, *407*, No. 117663.
(27) Salado, M.; Lizundia, E. Advances, challenges, and environmental impacts in metal−air battery electrolytes. *Mater. Today Energy* **2022**, *28*, No. 101064.
(28) Park, S.; et al. Capillarity ion concentration polarization as spontaneous desalting mechanism. *Nat. Commun.* **2016**, *7* (1), 11223.
(29) Cao, J. K.; Zhou, D. F.; Zhang, Y. B. Improvements in the surface tension measurement using the capillary rise method and its application to water under external magnetic fields. *J. Mol. Liq.* **2023**, *382*, No. 121988.
(30) Cerepi, A.; Humbert, L.; Burlot, R. Dynamics of capillary flow and transport properties in porous media by time-controlled porosimetry. *Colloids Surf. Physicochem. Eng. Asp.* **2002**, *206* (1), 425−444.
(31) Lu, J.; Wang, K.; Qu, M.-L. Experimental determination on the capillary water absorption coefficient of porous building materials: A comparison between the intermittent and continuous absorption tests. *J. Build. Eng.* **2020**, *28*, No. 101091.
(32) "Dynamic Contact Angle - an overview | ScienceDirect Topics". Accessed: August 30, 2024. [Online]. Available: https://www.sciencedirect.com/topics/engineering/dynamic-contact-angle.
(33) Libois, Q.; Lévesque-Desrosiers, F.; Lambert-Girard, S.; Thibault, S.; Domine, F. Optical porosimetry of weakly absorbing porous materials. *Opt. Express* **2019**, *27* (16), 22983−22993.
(34) Maslov, K.; Zhang, H. F.; Hu, S.; Wang, L. V. Optical-resolution photoacoustic microscopy for *in vivo* imaging of single capillaries. *Opt. Lett.* **2008**, *33* (9), 929−931.
(35) Salvadori, A.; Grazioli, D.; Magri, M.; Geers, M. G. D.; Danilov, D.; Notten, P. H. L. On the role of saturation in modeling ionic transport in the electrolyte of (Lithium ion) batteries. *J. Power Sources* **2015**, *294*, 696−710.
(36) Yiotis, A.; Karadimitriou, N. K.; Zarikos, I.; Steeb, H. Pore-scale effects during the transition from capillary- to viscosity-dominated flow dynamics within microfluidic porous-like domains. *Sci. Rep.* **2021**, *11*, 3891.
(37) Niu, D.; Gao, H. Thermal Conductivity of Ordered Porous Structures Coupling Gas and Solid Phases: A Molecular Dynamics Study. *Materials* **2021**, *14* (9), 2221.
(38) Zhuang, L.; Kim, K. Y.; Diaz, M.; Yeom, S. Evaluation of water saturation effect on mechanical properties and hydraulic fracturing behavior of granite. *Int. J. Rock Mech. Min. Sci.* **2020**, *130*, No. 104321.
(39) Luo, J.; Su, Q.; Zhai, X.; Zou, Y.; Yu, Q. An improved gravimetric method with anti-solvent addition to measure the solubility of d-allulose in water. *J. Food Eng.* **2023**, *355*, No. 111582.
(40) Ge, X.; et al. Laboratory NMR Study to Quantify the Water Saturation of Partially Saturated Porous Rocks. *Lithosphere* **2023**, *2023*, No. 1214083.
(41) Sheikhi, S.; Burukhin, A.; Cheremisin, A. A novel approach to measuring fluid saturation using X-ray computed tomography. *Korean J. Chem. Eng.* **2023**, *40* (11), 2708−2715.
(42) O'Carroll, D. M.; Abriola, L. M.; Polityka, C. A.; Bradford, S. A.; Demond, A. H. Prediction of two-phase capillary pressure−saturation relationships in fractional wettability systems. *J. Contam. Hydrol.* **2005**, *77* (4), 247−270.
(43) Reinaudi, G.; Lahaye, T.; Wang, Z.; Guéry-Odelin, D. Strong saturation absorption imaging of dense clouds of ultracold atoms. *Opt. Lett.* **2007**, *32* (21), 3143−3145.
(44) Hou, S.; Gao, T.; Li, X.; Wang, C. *Operando* probing ion and electron transport in porous electrodes. *Nano Energy* **2020**, *67*, No. 104254.
(45) Borah, R.; Hughson, F. R.; Johnston, J.; Nann, T. On battery materials and methods. *Mater. Today Adv.* **2020**, *6*, No. 100046.
(46) Yan, X. Q.; Zhou, C. Y.; Fang, Y. G.; Lin, L. S. Experiment Study on Determination of Surface Area of Finegrained Soils by Mercury Intrusion Porosimetry. *IOP Conf. Ser. Earth Environ. Sci.* **2017**, *100* (1), No. 012003.
(47) Liu, Q.-S.; et al. Effective transport network driven by tortuosity gradient enables high-electrochem-active solid-state batteries. *Natl. Sci. Rev.* **2023**, *10* (3), No. nwac272.
(48) Chen, Z.; Zhao, Y. Tortuosity estimation and microstructure optimization of non-uniform porous heterogeneous electrodes. *J. Power Sources* **2024**, *596*, No. 234095.
(49) Fu, J.; Thomas, H. R.; Li, C. Tortuosity of porous media: Image analysis and physical simulation. *Earth-Sci. Rev.* **2021**, *212*, No. 103439.
(50) Tick, G. R.; Mccoll, C. M.; Yolcubal, I.; Brusseau, M. L. Gas-phase Diffusive Tracer Test for the In-Situ Measurement of Tortuosity in the Vadose Zone. *Water. Air. Soil Pollut.* **2007**, *184* (1−4), 355−362.
(51) Kashyap, V.; et al. Accuracy of vascular tortuosity measures using computational modelling. *Sci. Rep.* **2022**, *12* (1), 865.
(52) Nhunduru, R. A. E.; Jahanbakhsh, A.; Shahrokhi, O.; Wlodarczyk, K. L.; Garcia, S.; Maroto-Valer, M. M. The Impact of Wettability on Dynamic Fluid Connectivity and Flow Transport Kinetics in Porous Media. *Water Resour. Res.* **2022**, *58* (6), No. e2021WR030729.
(53) Ye, Z.; et al. Evaluation of Connectivity Characteristics on the Permeability of Two-Dimensional Fracture Networks Using Geological Entropy. *Water Resour. Res.* **2021**, *57* (10), No. e2020WR029289.
(54) Armatas, G. S. Determination of the effects of the pore size distribution and pore connectivity distribution on the pore tortuosity and diffusive transport in model porous networks. *Chem. Eng. Sci.* **2006**, *61* (14), 4662−4675.
(55) Gharbi, O.; Blunt, M. J. The impact of wettability and connectivity on relative permeability in carbonates: A pore network modeling analysis. *Water Resour. Res.* **2012**, *48* (12), W12513.
(56) Al-Maharma, A. Y.; Patil, S. P.; Markert, B. Effects of porosity on the mechanical properties of additively manufactured components: a critical review. *Mater. Res. Express* **2020**, *7* (12), No. 122001.
(57) Osman, A. I.; et al. Coordination-driven innovations in low-energy catalytic processes: Advancing sustainability in chemical production. *Coord. Chem. Rev.* **2024**, *514*, No. 215900.

https://doi.org/10.1021/acsomega.4c07070
ACS Omega 2025, 10, 3228−3261

(58) Tavagh-Mohammadi, B.; Masihi, M.; Ganjeh-Ghazvini, M. Point-to-point connectivity prediction in porous media using percolation theory. *Phys. Stat. Mech. Its Appl.* **2016**, *460*, 304−313.
(59) Afsharpoor, A.; Javadpour, F. Pore Connectivity Between Organic and Inorganic Matter in Shale: Network Modeling of Mercury Capillary Pressure. *Transp. Porous Media* **2018**, *125* (3), 503−519.
(60) Wildenschild, D.; Sheppard, A. P. X-ray imaging and analysis techniques for quantifying pore-scale structure and processes in subsurface porous medium systems. *Adv. Water Resour.* **2013**, *51*, 217−246.
(61) "Fluid Flow Concentration on Preferential Paths in Heterogeneous Porous Media: Application of Graph Theory - Tang - 2021 - Journal of Geophysical Research: Solid Earth - Wiley Online Library". Accessed: August 30, 2024. [Online]. Available: https://agupubs-onlinelibrary-wiley-com.proxy.lib.uwaterloo.ca/doi/full/10.1029/2021JB023164.
(62) Saputra, B. D.; Fauzi, U. Analysis of the Effect of Coordination Number on Permeability of the Three-Dimensional (3D) Rock Model Using the Lattice Boltzmann Method (LBM). *J. Phys. Conf. Ser.* **2024**, *2734* (1), No. 012053.
(63) Chen, S.-C.; Lee, E. K. C.; Chang, Y.-I. Effect of the coordination number of the pore-network on the transport and deposition of particles in porous media. *Sep. Purif. Technol.* **2003**, *30* (1), 11−26.
(64) He, J.; Blumenfeld, R.; Zhu, H. Mechanical Behaviors of Sandy Sediments Bearing Pore-Filling Methane Hydrate under Different Intermediate Principal Stress. *Int. J. Geomech.* **2021**, *21* (5), No. 04021043.
(65) Xiong, Q.; Baychev, T. G.; Jivkov, A. P. Review of pore network modelling of porous media: Experimental characterisations, network constructions and applications to reactive transport. *J. Contam. Hydrol.* **2016**, *192*, 101−117.
(66) Yin, Y.; Qu, Z.; Prodanović, M.; Landry, C. J. Identifying the dominant transport mechanism in single nanoscale pores and 3D nanoporous media. *Fundam. Res.* **2023**, *3* (3), 409−421.
(67) Sherman, T.; Bianchi Janetti, E.; Guédon, G. R.; Porta, G.; Bolster, D. Upscaling transport of a sorbing solute in disordered non periodic porous domains. *Adv. Water Resour.* **2020**, *139*, No. 103574.
(68) Beu, T. A. Molecular dynamics simulations of ion transport through carbon nanotubes. III. Influence of the nanotube radius, solute concentration, and applied electric fields on the transport properties. *J. Chem. Phys.* **2011**, *135* (4), No. 044516.
(69) Tsai, Y.-C.; Chiu, C.-C. Solute Diffusivity and Local Free Volume in Cross-Linked Polymer Network: Implication of Optimizing the Conductivity of Polymer Electrolyte. *Polymers* **2022**, *14* (10), 2061.
(70) Hao, Z.; et al. On-Chip Ni−Zn Microbattery Based on Hierarchical Ordered Porous Ni@Ni(OH)2 Microelectrode with Ultrafast Ion and Electron Transport Kinetics. *Adv. Funct. Mater.* **2019**, *29* (16), No. 1808470.
(71) Coppens, M.-O.; Ye, G. Nature-Inspired Optimization of Transport in Porous Media. In *Diffusive Spreading in Nature, Technology and Society*; Bunde, A., Caro, J., Chmelik, C., Kärger, J., Vogl, G., Eds.; Springer International Publishing: Cham, Switzerland, 2023; pp 215−245. DOI: 10.1007/978-3-031-05946-9_11.
(72) Sun, H.; Koch, M. Fractal generation of surface area of porous media. *Stoch. Hydrol. Hydraul.* **1998**, *12* (2), 83−96.
(73) Adler, P. M. Transports in fractal porous media. *J. Hydrol.* **1996**, *187* (1), 195−213.
(74) Lee, H.; Yanilmaz, M.; Toprakci, O.; Fu, K.; Zhang, X. A review of recent developments in membrane separators for rechargeable lithium-ion batteries. *Energy Environ. Sci.* **2014**, *7* (12), 3857−3886.
(75) Abraham, K. M. Directions in secondary lithium battery research and development. *Electrochim. Acta* **1993**, *38* (9), 1233−1248.
(76) Kim, J.; Choi, S. W.; Jo, S.; Lee, W.; Kim, B. Characterization and Properties of P(VdF-HFP)Based Fibrous Polymer Electrolyte Membrane Prepared by Electrospinning. *J. Electrochem. Soc. - J. Electrochem. Soc.* **2005**, *152*, A295.
(77) Lee, Y.; Ryou, M. H.; Seo, M.; Choi, J. W.; Lee, Y. M. Effect of polydopamine surface coating on polyethylene separators as a function of their porosity for high-power Li-ion batteries. *Electrochim. Acta* **2013**, *113*, 433−438.
(78) Wang, Y.; Li, Q. M.; Xing, Y. Porosity variation of lithium-ion battery separators under uniaxial tension. *Int. J. Mech. Sci.* **2020**, *174*, No. 105496.
(79) Zhang, H.; et al. Nanofibrillated Cellulose (NFC) as a Pore Size Mediator in the Preparation of Thermally Resistant Separators for Lithium Ion Batteries. *ACS Sustain. Chem. Eng.* **2018**, *6*, 4838.
(80) Gigova, A. Investigation of the porous structure of battery separators using various porometric methods. *J. Power Sources* **2006**, *158* (2), 1054−1061.
(81) Sousa, R. E.; et al. Influence of the porosity degree of poly(vinylidene fluoride-*co*-hexafluoropropylene) separators in the performance of Li-ion batteries. *J. Power Sources* **2014**, *263*, 29−36.
(82) Rajagopalan Kannan, D. R.; Terala, P. K.; Moss, P. L.; Weatherspoon, M. H. Analysis of the Separator Thickness and Porosity on the Performance of Lithium-Ion Batteries. *Int. J. Electrochem.* **2018**, *2018* (1), 1925708.
(83) Zhao, M.; Wang, J.; Chong, C.; Yu, X.; Wang, L.; Shi, Z. An electrospun lignin/polyacrylonitrile nonwoven composite separator with high porosity and thermal stability for lithium-ion batteries. *RSC Adv.* **2015**, *5* (122), 101115−101120.
(84) Zhang, S. S. A review on the separators of liquid electrolyte Li-ion batteries. *J. Power Sources* **2007**, *164* (1), 351−364.
(85) McCormack, P.; Luo, H.; Geise, G.; Koenig, G. Conductivity, permeability, and stability properties of chemically tailored poly-(phenylene oxide) membranes for Li+ conductive non-aqueous redox flow battery separators. *J. Power Sources* **2020**, *460*, No. 228107.
(86) Jiang, Y.; et al. A high-throughput screening permeability separator with high catalytic conversion kinetics for Li−S batteries. *J. Mater. Chem. A* **2022**, *10* (41), 22080−22092.
(87) Zheng, X.; et al. Functionalization of Graphene and Dielectric Property Relationships in PVDF/graphene Nanosheets Composites. *Int. J. Electrochem. Sci.* **2018**, *13* (1), 1−13.
(88) Zhu, G.-L.; et al. Dependence of Li-Ion Battery Energy Density on Separator Thickness. *J. Electrochem. Soc.* **2021**, *168*, 110545.
(89) Xiang, Y.; et al. Advanced Separators for Lithium-Ion and Lithium−Sulfur Batteries: A Review of Recent Progress. *ChemSusChem* **2016**, *9* (21), 3023−3039.
(90) Tian, R.; et al. Quantifying the factors limiting rate performance in battery electrodes. *Nat. Commun.* **2019**, *10* (1), 1933.
(91) Samarasingha, P. B.; Lee, M.-T.; Valvo, M. Reactive surface coating of metallic lithium and its role in rechargeable lithium metal batteries. *Electrochim. Acta* **2021**, *397*, No. 139270.
(92) Verma, C.; Quraishi, M. A.; Ebenso, E. E. Corrosive electrolytes. *Int. J. Corros. Scale Inhib.* **2020**, *9* (4), 1261−1276.
(93) Huang, X. Separator technologies for lithium-ion batteries. *J. Solid State Electrochem.* **2011**, *15* (4), 649−662.
(94) Chae, S. H.; Kang, S.-H.; Cheong, H.-W.; Han, Y. S.; Yoon, D.-H. Thermal batteries with ceramic felt separators − Part 1: Wetting, loading behavior and chemical stability. *Ceram. Int.* **2017**, *43* (5), 4015−4022.
(95) Plaimer, M.; et al. Evaluating the trade-off between mechanical and electrochemical performance of separators for lithium-ion batteries: Methodology and application. *J. Power Sources* **2016**, *306*, 702−710.
(96) Costa, C. M.; Rodrigues, H. M.; Gören, A.; Machado, A. V.; Silva, M. M.; Lanceros-Méndez, S. Preparation of Poly(vinylidene fluoride) Lithium-Ion Battery Separators and Their Compatibilization with Ionic Liquid − A Green Solvent Approach. *ChemistrySelect* **2017**, *2* (19), 5394−5402.
(97) "A Nonflammable and Thermally Stable Polyethylene/Glass Fiber−Magnesium Hydroxide/Polyethylene Composite Separator with ...." Accessed: July 23, 2024. [Online]. Available: http://ouci.dntb.gov.ua/en/works/logMxEQl/.

https://doi.org/10.1021/acsomega.4c07070
ACS Omega 2025, 10, 3228−3261

(98) Zhang, H.; Wang, X.; Liang, Y. Preparation and characterization of a Lithium-ion battery separator from cellulose nanofibers. *Heliyon* **2015**, *1* (2), No. e00032.
(99) "Enhanced wettability and electrochemical performance of separators for lithium-ion batteries by coating core-shell structured silica-poly(cyclotriphosphazene-co-4,4●-sulfonyldiphenol) particles - NASA/ADS". Accessed: July 23, 2024. [Online]. Available: https://ui.adsabs.harvard.edu/abs/2019JPS···43626839F/abstract.
(100) Zhou, X.; He, C. Tailoring the surface chemistry and morphology of glass fiber membranes for robust oil/water separation using poly(dimethylsiloxanes) as hydrophobic molecular binders. *J. Mater. Chem. A* **2018**, *6* (2), 607−615.
(101) Xie, Y.; et al. Enhancement on the wettability of lithium battery separator toward nonaqueous electrolytes. *J. Membr. Sci.* **2016**, *503*, 25.
(102) Wang, S.; Ma, Z.; Zhao, W.; Guo, Z.; Zhao, H.; Ren, L. Deterioration mechanism of the wettability of a lithium-ion battery separator induced by low-temperature discharge. *Appl. Energy* **2024**, *364*, No. 123136.
(103) "Towards high performance Li metal batteries: Surface functionalized graphene separator with improved electrochemical ki...." Accessed: July 23, 2024. [Online]. Available: http://ouci.dntb.gov.ua/en/works/9Zw61QO7/.
(104) Wang, W.; et al. Three-in-one LaNiO3 functionalized separator boosting electrochemical stability and redox kinetics for high-performance Li-S battery. *J. Energy Chem.* **2023**, *82*, 581−591.
(105) Chen, W.; et al. Water-Based Organic-Inorganic Hybrid Coating for a High-Performance Separator. *ACS Sustain. Chem. Eng.* **2016**, *4* (7), 3794−3802.
(106) Luo, X.; Pan, W.; Liu, H.; Gong, J.; Wu, H. Glass fiber fabric mat as the separator for lithium-ion battery with high safety performance. *Ionics* **2015**, *21* (11), 3135−3139.
(107) Zhang, C.; et al. A polyethylene microsphere-coated separator with rapid thermal shutdown function for lithium-ion batteries. *J. Energy Chem.* **2020**, *44*, 33−40.
(108) Kim, S.; et al. Poly(ethylene-co-vinyl acetate)/polyimide/poly(ethylene-co-vinyl acetate) tri-layer porous separator with high conductivity and tailored thermal shutdown function for application in sodium-ion batteries. *J. Power Sources* **2021**, *482*, No. 228907.
(109) "Coaxial electrospun core-shell lithium-ion battery separator with flame retardant and thermal shutdown functions | Semantic Scholar". Accessed: July 23, 2024. [Online]. Available: https://www.semanticscholar.org/paper/Coaxial-electrospun-core-shell-lithium-ion-battery-Zheng-Zeng/b64969d4e3c77307de1c00ddcf5b3d34a5815cc9.
(110) "Membranes | Free Full-Text | Recent Advances in Poly(vinylidene fluoride) and Its Copolymers for Lithium-Ion Battery Separators". Accessed: July 23, 2024. [Online]. Available: https://www.mdpi.com/2077-0375/8/3/45.
(111) Costa, C. M.; Silva, M. M.; Lanceros-Méndez, S. Battery separators based on vinylidene fluoride (VDF) polymers and copolymers for lithium ion battery applications. *RSC Adv.* **2013**, *3* (29), 11404−11417.
(112) Chan, T.-C.; Chung, S.-H. Stability Enhancement of Lithium−Sulfur Batteries Using Electrospun Separator/Electrolyte Membranes. *ACS Sustain. Chem. Eng.* **2024**, *12*, 14230.
(113) Jin, L.; et al. Metallically conductive TiB2 as a multi-functional separator modifier for improved lithium sulfur batteries. *J. Power Sources* **2020**, *448*, No. 227336.
(114) Xie, F.; et al. A Multi-Functional Separator for Li-S Batteries: WS2@C Nanoflowers Catalyze the Rapid Recycling of Lithium Polysulfides by Polar Attraction. *ChemElectroChem.* **2022**, *9* (15), No. e202200474.
(115) Liang, X.; et al. Super P and MoO2/MoS2 co-doped gradient nanofiber membrane as multi-functional separator for lithium−sulfur batteries. *Rare Met.* **2024**, *43* (9), 4263−4273.
(116) Liu, Z.; Hu, Z.; Jiang, X.; Zhang, Y.; Wang, X.; Zhang, S. Multi-functional ZnS quantum Dots/Graphene aerogel modified separator for high performance lithium-sulfur batteries. *Electrochim. Acta* **2022**, *422*, No. 140496.
(117) Jiang, X.; et al. Fabrication of A Multi-functional Separator Incorporating Crown ether- Polyoxometalate Supramolecular Compound for Lithium-Sulfur Batteries. *Chem. − Eur. J.* **2024**, *30* (58), No. e202402706.
(118) Chen, K.; et al. Polyaniline Encapsulated Amorphous V2O5 Nanowire-Modified Multi-Functional Separators for Lithium−Sulfur Batteries. *Small Methods* **2021**, *5* (3), No. 2001056.
(119) Shi, Q. X.; et al. CTF/MWCNT hybrid multi-functional separator as high-efficiency polysulfide tamer for high-performance Li−S battery. *Electrochim. Acta* **2021**, *367*, No. 137418.
(120) Li, C.-D.; Chen, Z.-F.; Saeed, M.-U. Characterization of hybrid glass wool suspensions and optimization of microstructure and tensile strength of the associated wet-laid mats by various blendings and numbers of beating revolutions. *Mater. Struct.* **2016**, *49* (5), 1861−1869.
(121) Ferry, L.; Lopez-Cuesta, J. M.; Chivas, C.; Hoy, G. M. W.; Dvir, H. Incorporation of a grafted brominated monomer in glass fiber reinforced polypropylene to improve the fire resistance. *Polym. Degrad. Stab.* **2001**, *74* (3), 449.
(122) Li, L.; Li, B.; Tang, F. Influence of maleic anhydride-grafted EPDM and flame retardant on interfacial interaction of glass fiber reinforced PA-66. *Eur. Polym. J.* **2007**, *43* (6), 2604−2611.
(123) Kallel, H.; Doumouro, J.; Krachmalnicoff, V.; De Wilde, Y.; Joulain, K. Thermal emission from a single glass fiber. *J. Quant. Spectrosc. Radiat. Transfer* **2019**, *236*, No. 106598.
(124) Di, X.; Gao, Y.; Bao, C.; Hu, Y.; Xie, Z. Optimization of glass fiber based core materials for vacuum insulation panels with laminated aluminum foils as envelopes. *Vacuum* **2013**, *97*, 55−59.
(125) Yang, L.; Sáez, E. R.; Nagel, U.; Thomason, J. L. Can thermally degraded glass fibre be regenerated for closed-loop recycling of thermosetting composites? *Compos. Part Appl. Sci. Manuf.* **2015**, *72*, 167−174.
(126) Wu, C.; et al. Preparation and characterization of ultralight glass fiber wool/phenolic resin aerogels with a spring-like structure. *Compos. Sci. Technol.* **2019**, *179*, 125−133.
(127) "Effect of cross-sectional morphology and composite structure of glass fiber felts on their corresponding acoustic properties | Fibers and Polymers". Accessed: July 23, 2024. [Online]. Available: https://link.springer.com/article/10.1007/s12221-016-5519-7.
(128) Wang, F.; Chen, Z.; Wu, C.; Yang, Y.; Zhang, D.; Li, S. Analysis of acoustic performance of glass fiber felts after water absorption and their estimation results by artificial neural network. *J. Text. Inst.* **2020**, *111* (7), 1008−1016.
(129) Todorova, K.; Kolev, V.; Nacheva, G.; Ivanov, I. G. Isolation of Plasmid DNA by Adsorption on Glass Fibers. *Biotechnol. Biotechnol. Equip.* **2002**, *16* (1), 145.
(130) Wang, C.; Zhang, Y.; Tan, H.; Du, X. Non-calcined ZrO2 sol-coated hollow glass fibre membrane: Preparation, microstructure, and dye separation. *Ceram. Int.* **2021**, *47* (9), 12906−12915.
(131) Gao, H. T.; Liu, X. H.; Zhang, S. J.; Qi, J. L. Synergistic effect of glass fibre and Al powder on the mechanical properties of glass-ceramics. *Ceram. Int.* **2018**, *44* (13), 15167−15175.
(132) Parveen, S.; Pichandi, S.; Goswami, P.; Rana, S. Novel glass fibre reinforced hierarchical composites with improved interfacial, mechanical and dynamic mechanical properties developed using cellulose microcrystals. *Mater. Des.* **2020**, *188*, No. 108448.
(133) Mazrouei-Sebdani, Z.; et al. Multiple assembly strategies for silica aerogel-fiber combinations − A review. *Mater. Des.* **2022**, *223*, No. 111228.
(134) Chung, S.-H.; Manthiram, A. Bifunctional Separator with a Light-Weight Carbon-Coating for Dynamically and Statically Stable Lithium-Sulfur Batteries. *Adv. Funct. Mater.* **2014**, *24* (33), 5299−5306.
(135) Chung, S.-H.; Manthiram, A. A polyethylene glycol-supported microporous carbon coating as a polysulfide trap for utilizing pure sulfur cathodes in lithium-sulfur batteries. *Adv. Mater. Deerfield Beach Fla* **2014**, *26* (43), 7352−7357.

https://doi.org/10.1021/acsomega.4c07070
ACS Omega 2025, 10, 3228−3261

(136) Chung, S.-H.; Han, P.; Singhal, R.; Kalra, V.; Manthiram, A. Electrochemically Stable Rechargeable Lithium−Sulfur Batteries with a Microporous Carbon Nanofiber Filter for Polysulfide. *Adv. Energy Mater.* **2015**, *5* (18), No. 1500738.
(137) Ai, W.; et al. Dual confinement of polysulfides in boron-doped porous carbon sphere/graphene hybrid for advanced Li-S batteries. *Nano Res.* **2018**, *11* (9), 4562−4573.
(138) "Insight into the Effect of Boron Doping on Sulfur/Carbon Cathode in Lithium−Sulfur Batteries". Accessed: July 23, 2024. [Online]. Available: http://ouci.dntb.gov.ua/en/works/9QeOJG69/.
(139) "Manipulating the redox kinetics of Lisbnd S chemistry by porous hollow cobalt-B, N codoped-graphitic carbon polyhedrons for high performance lithium-sulfur batteries - NASA/ADS". Accessed: July 23, 2024. [Online]. Available: https://ui.adsabs.harvard.edu/abs/2019Carbo.149..564L/abstract.
(140) Zhu, J.; et al. Understanding glass fiber membrane used as a novel separator for lithium-sulfur batteries. *J. Membr. Sci.* **2016**, *504*, 89−96.
(141) Zhao, Z.; et al. Aluminum silicate fiber membrane: A cost-effective substitute for fiber glass separator in Li−O2 battery. *Mater. Today Energy* **2020**, *17*, No. 100485.
(142) Woo, H.-S.; Kim, J.-H.; Moon, Y.-B.; Kim, W. K.; Ryu, K. H.; Kim, D.-W. A dual membrane composed of composite polymer membrane and glass fiber membrane for rechargeable lithium-oxygen batteries. *J. Membr. Sci.* **2018**, *550*, 340−347.
(143) Zhao, Y.; et al. Dense AuNP/MoS2 hybrid fabrication on fiber membranes for molecule separation and SERS detection. *RSC Adv.* **2017**, *7* (58), 36516−36524.
(144) Song, K.-S.; Nimse, S. B.; Sonawane, M. D.; Lin, Y.; Zhou, Z.; Kim, T. A glass fibre membrane platform for ultra-sensitive detection of cardiac troponin T. *Analyst* **2017**, *142* (20), 3816−3821.
(145) Fang, X.; Wei, S.; Kong, J. Paper-based microfluidics with high resolution, cut on a glass fiber membrane for bioassays. *Lab. Chip* **2014**, *14* (5), 911−915.
(146) Siddiqui, U.; Khalid, H.; Ghafoor, S.; Javaid, A.; Asif, A.; Khan, A. S. Analyses on mechanical and physical performances of nano-apatite grafted glass fibers based dental composites. *Mater. Chem. Phys.* **2021**, *263*, No. 124188.
(147) Cova, F.; Benedetto, A.; Chiodini, N.; Lorenzi, R.; Vedda, A.; Ouspenski, V. Influence of the fiber drawing process on mechanical and vibrational properties of sol-gel silica glass. *Journal of Non-Crystalline Solids* **2021**, *555*, No. 120534.
(148) Yang, W.; et al. Synthesis of phosphorus-containing silane coupling agent for surface modification of glass fibers: Effective reinforcement and flame retardancy in poly(1,4-butylene terephthalate). *Chem. Eng. J.* **2017**, *321*, 257−267.
(149) "Adsorption of volatile benzene series compounds by surface-modified glass fibers: kinetics, thermodynamic adsorption efficiencies, and mechanisms", CoLab. Accessed: July 23, 2024. [Online]. Available: https://colab.ws/articles/10.1007%2Fs11356-020-12227-4.
(150) Shariatmadar, M.; et al. Strengthening the mechanical characteristics and cathodic delamination resistance of fiber-reinforced polymer through chemical surface modification of glass fibers. *Sci. Rep.* **2023**, *13* (1), 13418.
(151) Li, J.-L.; et al. Facile Surface Modification of Glass-Fiber Membrane with Silylating Reagent through Chemical Bonding for the Selective Separation and Recycling of Diverse Dyes from Aqueous Solutions. *ChemistrySelect* **2018**, *3* (45), 12734−12741.
(152) Abdul Hamid, Z. M.; Florea, M.; Fliegener, S.; Schober, M.; Hohe, J.; Rühe, J. "Chemical modification of fiber-matrix interfaces of glass fiber reinforced thermoplastics and methods for interface characterization", 2019. Accessed: July 23, 2024. [Online]. Available: https://publica.fraunhofer.de/handle/publica/254701.
(153) da Silveira, C. B.; de Oliveira, A. F.; de Campos, S. D.; de Campos, E. A.; Fraporti, A. D. Nb2O5 coating of glass fibres applied by chemical vapour deposition. *Surf. Eng.* **2012**, *28* (1), 68−72.
(154) Chen, S.; Shiue, S.; Yang, T.; Cheng, K.; Chen, P.; Lin, H. The individual effect of coating thicknesses and deposition temperatures on Raman spectra of carbon films deposited on silica glass fibers by thermal chemical vapor deposition. *J. Chin. Inst. Eng.* **2009**, *32* (5), 711−715.
(155) Tzounis, L.; et al. Highly conductive ultra-sensitive SWCNT-coated glass fiber reinforcements for laminate composites structural health monitoring. *Compos. Part B Eng.* **2019**, *169*, 37−44.
(156) Nisha, M. S.; Ravali, K. V.; Senthil Kumar, P.; Faruk Khan, P.; Vinay, P.; Jairam, K. Efficient electrophoretic deposition of an intensification process to enhance the mechanical properties of glass fibre reinforced polymer. *Chem. Eng. Process. - Process Intensif.* **2021**, *160*, No. 108298.
(157) "Materials | Free Full-Text | Enhancement of Alkali Resistance of Glass Fibers via In Situ Modification of Manganese-Based Nanomaterials". Accessed: July 23, 2024. [Online]. Available: https://www.mdpi.com/1996-1944/16/16/5663.
(158) Liu, Y.; et al. Ion Flux Regulation through PTFE Nanospheres Impregnated in Glass Fiber Separators for Long-Lived Lithium and Sodium Metal Batteries. *Adv. Energy Mater.* **2023**, *13* (24), No. 2204420.
(159) Schadeck, U.; Kyrgyzbaev, K.; Zettl, H.; Gerdes, T.; Moos, R. Flexible, Heat-Resistant, and Flame-Retardant Glass Fiber Nonwoven/Glass Platelet Composite Separator for Lithium-Ion Batteries. *Energies* **2018**, *11* (4), 999.
(160) "Design on modified glass fiber separator by graphite fluoride nanoflakes for Zn metal anodes with highly reversibility", CoLab. Accessed: July 23, 2024. [Online]. Available: https://colab.ws/articles/10.1016%2Fj.jpowsour.2023.233323.
(161) Zheng, F.; et al. A Highly Sensitive CRISPR-Empowered Surface Plasmon Resonance Sensor for Diagnosis of Inherited Diseases with Femtomolar-Level Real-Time Quantification. *Adv. Sci.* **2022**, *9* (14), No. 2105231.
(162) Moriche, R.; Jiménez-Suárez, A.; Sánchez, M.; Prolongo, S. G.; Ureña, A. Graphene nanoplatelets coated glass fibre fabrics as strain sensors. *Compos. Sci. Technol.* **2017**, *146*, 59−64.
(163) Huang, D.; Zhou, X.; Liu, L.; Li, H.; Lin, G.; Li, J.; Wei, Z. Improved Electrochemical Performance of Aqueous Zinc-Ion Batteries with Modified Glass Fiber Separator by Ketjen Black. *Colloids Surf. Physicochem. Eng. Asp.*. **2023**, *663*, 130991.
(164) Pyo, M.; Jeong, S.; Kim, J. H.; Jeon, M. J.; Lee, E.-J. Hydrophobicity and Membrane Distillation Performance of Glass Fiber Membranes Modified by Dip Coating of Pure PDMS. *J. Environ. Chem. Eng.* **2024**, *12* (3), 112534.
(165) Luo, K.; et al. Enhanced cycling stability of Li−O2 batteries by using a polyurethane/SiO2/glass fiber nanocomposite separator. *J. Mater. Chem. A* **2018**, *6* (17), 7770−7776.
(166) Wang, Q. Robust and thermal-enhanced melamine formaldehyde−modified glassfiber composite separator for high-performance lithium batteries. *Electrochim. Acta* **2015**, *182*, 334−341.
(167) Zhang, Z.; Huang, Y.; Gao, H.; Li, C.; Huang, J.; Liu, P. 3D Glass Fiber Cloth Reinforced Polymer Electrolyte for Solid-State Lithium Metal Batteries. *J. Membr. Sci.* **2021**, *621*, 118940.
(168) Wu, S.; Zheng, H.; Tian, R.; Hei, Z.; Liu, H.; Duan, H. In-situ preparation of gel polymer electrolyte with glass fiber membrane for lithium batteries. *J. Power Sources* **2020**, *472*, No. 228627.
(169) Selvan, R. K.; et al. Biomass-derived porous carbon modified glass fiber separator as polysulfide reservoir for Li-S batteries. *J. Colloid Interface Sci.* **2018**, *513*, 231−239.
(170) Wang, Y.; Chen, T.; Mu, Q. Electrochemical performance of W-doped anatase TiO2 nanoparticles as an electrode material for lithium-ion batteries. *J. Mater. Chem.* **2011**, *21* (16), 6006−6013.
(171) Ali, Z.; et al. Design and evaluation of novel Zn doped mesoporous TiO2 based anode material for advanced lithium ion batteries. *J. Mater. Chem.* **2012**, *22* (34), 17625−17629.
(172) "Mesoporous Anatase TiO_2 with High Surface Area and Controllable Pore Size by F−-Ion Doping: Applications for High-Power Li-Ion Battery Anode", Scilit. Accessed: July 23, 2024. [Online]. Available: https://www.scilit.net/publications/69dc80fc6faef5d9fd5be93229366152.

https://doi.org/10.1021/acsomega.4c07070
ACS Omega 2025, 10, 3228−3261

(173) Ponnada, S.; et al. Sustainable metal-organic framework co-engineered glass fiber separators for safer and longer cycle life of Li-S batteries. *J. Alloys Compd.* **2023**, *941*, No. 168962.
(174) Li, Y.; et al. Glass fiber separator coated by porous carbon nanofiber derived from immiscible PAN/PMMA for high-performance lithium-sulfur batteries. *J. Membr. Sci.* **2018**, *552*, 31−42.
(175) Wang, L.; Liu, J.; Haller, S.; Wang, Y.; Xia, Y. A scalable hybrid separator for a high performance lithium−sulfur battery. *Chem. Commun.* **2015**, *51* (32), 6996−6999.
(176) "Impedance analysis of porous carbon electrodes to predict rate capability of electric double-layer capacitors - NASA/ADS". Accessed: July 23, 2024. [Online]. Available: https://ui.adsabs.harvard.edu/abs/2014JPS...267..411Y/abstract.
(177) Dang, B.; Li, Q.; Luo, Y.; Zhao, R.; Li, J.; Wu, F. Metal-organic framework-based glass fiber separator as an efficacious polysulfide barrier and dendrite suppressor for lithium-sulfur batteries. *J. Alloys Compd.* **2022**, *915*, No. 165375.
(178) Lin, C.; et al. A few-layered Ti3C2 nanosheet/glass fiber composite separator as a lithium polysulphide reservoir for high-performance lithium−sulfur batteries. *J. Mater. Chem. A* **2016**, *4* (16), 5993−5998.
(179) Chen, Z.; et al. CRISPR-Cas13a-powered electrochemical biosensor for the detection of the L452R mutation in clinical samples of SARS-CoV-2 variants. *J. Nanobiotechnology* **2023**, *21* (1), No. 141.
(180) Zhu, J.; et al. A novel separator coated by carbon for achieving exceptional high performance lithium-sulfur batteries. *Nano Energy* **2016**, *20*, 176−184.
(181) Li, J.-G.; Lee, P.-Y.; Ahmed, M. M. M.; Mohamed, M. G.; Kuo, S.-W. Varying the Hydrogen Bonding Strength in Phenolic/PEO-b-PLA Blends Provides Mesoporous Carbons Having Large Accessible Pores Suitable for Energy Storage. *Macromol. Chem. Phys.* **2020**, *221* (10), No. 2000040.
(182) Shan, L.; et al. Entrapment of polysulfides by a Ketjen Black & mesoporous TiO2 modified glass fiber separator for high performance lithium-sulfur batteries. *J. Alloys Compd.* **2019**, *779*, 412−419.
(183) Lin, C.; et al. A few-layered Ti3C2 nanosheet/glass fiber composite separator as a lithium polysulphide reservoir for high-performance lithium−sulfur batteries. *J. Mater. Chem. A* **2016**, *4* (16), 5993−5998.

https://doi.org/10.1021/acsomega.4c07070
ACS Omega 2025, 10, 3228−3261